15th INTERNATIONAL CONFERENCE on COHESIVE SEDIMENT TRANSPORT PROCESSES

13 - 17 OCTOBER 2019 • ISTANBUL / TURKEY

YILDIZ TECHNICAL UNIVERSITY - YILDIZ CAMPUS

ABSTRACT BOOK

www.intercoh2019.org

PREFACE

The INTERCOH 2019 conference, held in Istanbul, Turkey, October 13-17, is a technical specialty conference focused on the physical processes of cohesive sediment in the natural environment. The INTERCOH conference series, initiated by Dr. Reg Parker and Prof. Ashish Mehta, is an international platform where scientists and engineers worldwide can meet and exchange experiences to develop a better understanding of the transport of fine-grained sediments. INTERCOH 2019 is the 15th edition of an international gathering of scientists and engineers facing challenges posed by the presence of cohesive sediments ("mud") in the aquatic environment. Previous editions took place in Florida, USA (1981, 1984, 1988, 1991, 2013), Wallingford, UK (1994), Seoul, Korea (1998), Delft, The Netherlands (2000), Virginia, USA (2003), Saga, Japan (2005), Brest, France (2007), Rio de Janeiro / Paraty, Brazil (2009), Shanghai, China (2011), Leuven, Belgium (2015) and Montevideo, Uruguay (2017). More than sixty scientists attended the INTERCOH 2019 issue. For further information on INTERCOH, visit the website www.intercoh.org

The abstract book is the permanent record of the conference containing the findings of the world's leading scientists and engineers in the area of cohesive sediment transport processes. The contents are a valuable source of up-to-date information on the current activity of research groups across the globe, covering the following topics: Mud rheology and fluid mud; Suspended matter and flocculation; Bed shear, erosion and bed exchange; Sediment characterization; Siltation, Dredging and plumes; Biological and ecological controls; Coastal and estuarine hydrodynamics; Coastal and estuarine morphodynamics; and Wetlands dynamics. The submitted abstracts have been evaluated by members of the Steering Committee. Local Organizing Committee (LOC) was in charge of the editorial duties. Full papers will be published in the journal Ocean Dynamics (Springer) after peer-review, forming a Topical Collection.

This conference would not have been possible without the efforts of many people. Firstly, we thank the chair, Susana Vinzon, the members of the Steering Committee, and Ashish Mehta for trusting us in the organization of the meeting. The conference secretariat was well taken care of by Dekon Congress & Tourism. Finally, we would also like to thank the administration of the Yildiz Technical University for providing the remarkable conference facilities in the Auditorium of the Yildiz Technical University.

Cihan Sahin and Yalcin Yuksel
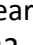Co-Chairs INTERCOH 2019

ORAL
PRESENTATIONS

INTERCOH - Bottom Shear, Erosion and Bed Exchange

O1028 - SEDIMENT TRANSPORT MODELING IN THE RIVER LAGOON SEA SYSTEM ON THE SOUTH EASTERN COASTS OF THE BALTIC SEA
Bottom Shear Erosion and Bed Exchange

Jovita Mezine [1], Christian Ferrarin [2], Petras Zemlys [1], Georg Umgiesser [2] Klaipėda University, Marine Research Institute, Klaipėda-Lithuania [1] Cnr - National Research Council of Italy, Ismar Institute of Marine Sciences, Venice-Italy [2]

Jovita Mezine1, Christian Ferrarin2 and Georg Umgiesser1,2
1 Marine Research Institute, Klaipėda University, Universiteto ave.
17, 92294, Klaipėda, Lithuania
E-mail: jovita.mezine@apc.ku.lt
2 CNR - National Research Council of Italy, ISMAR ⬚ Institute of Marine Sciences, Venice, Castello 2737/f, 30122, Venice

The Curonian lagoon is the largest shallow freshwater lagoon in Europe, with the volume of 6.3 km3 with the average depth of 3.8 m and average annual salinities in the southern part of 0.08 and 2.45 in the northern part. The lagoon is separated from the south-eastern Baltic Sea by a sandy Curonian Spit and has the only one narrow inlet in the north (Klaipeda Strait). The hydrology of the system is strongly related to the discharges of the Nemunas River that enters the lagoon in the middle of the eastern lagoon coasts and brings about 21.8 km3 of water per year with the suspended sediments concentrations (SSC) in the water surface varying from 4 mg l-1 in winter until 20 mg l-1 in flood period. The bottom of the southern part of the lagoon is covered mainly with silty and muddy sediments while in the northern part the sandy bottom sediments are dominant.

The aim of this study was to investigate the sediment dynamics in the lagoon with high river discharge and sediment load through the analysis of in situ data and the application of a sediment transport model. The SHYFEM modeling system was applied for the sediment dynamics analysis in the lagoon for the period 2004-2016. SHYFEM is a finite element 3-D hydrodynamic model that includes a transport and diffusion model and a radiation transfer model of the heat at the water surface and other modules. For the sediment transport simulations the SEDTRANS05 module was used. The integrate approach allowed to identify the patterns of the riverine suspended sediments and map erosion-accumulation zones in the lagoon after long-term simulation of 13-year. The sampling campaigns were organized for the years 2014-2015. The collected data was important for understanding the characteristics of the riverine and lagoon sediments and showed that the suspended organic matter plays a crucial role on the sediment dynamics for this coastal system. After these findings a new formula for the sediment settling velocity was introduced to the sediment transport model.

The numerical experiments carried out to study sediment dynamics gave satisfactory results and the possibility to get holistic view of the river-lagoon-sea system. The sensitivity tests were done to undertand the influence of strong wind events and ice cover effect for the system. The simulation results showed that during storm events a big amount of sediments is washed out of the system, forming erosion zones in the system. Scenarios without ice cover indicated that lagoon would have much higher suspended sediment concentrations in winter season

15th INTERNATIONAL CONFERENCE on COHESIVE SEDIMENT TRANSPORT PROCESSES
13 - 17 OCTOBER 2019 • ISTANBUL / TURKEY
YILDIZ TECHNICAL UNIVERSITY - YILDIZ CAMPUS

INTERCOH - Bottom Shear, Erosion and Bed Exchange

compared with the present situation with ice. The analysis of long-term (13 years) simulation results showed that the lagoon acts as a sediment sink with accumulation zones in the southern and central part of the lagoon. On average about 62% of the riverine sediments is trapped in the lagoon with a marked spatially varying accumulation distribution.

INTERCOH - Bottom Shear, Erosion and Bed Exchange

O1032 - BIOSTABILIZATION OF FINE SEDIMENT IN RIVERS AND RESERVOIRS EXPLORING THE INTERPLAY BETWEEN FLOW SUBSTRATE AND COMMUNITY
Bottom Shear Erosion and Bed Exchange

Kaan Koca [1], Silke Wieprecht [1], Sabine Ulrike Gerbersdorf [1]
University of Stuttgart, Institute for Modelling Hydraulic and Environmental Systems, Department of Hydraulic Engineering and Water Resources Management, Stuttgart-Germany [1]

Understanding how microbial assemblages ("biofilms") influence sediment stability and erodibility is critical for effective sediment management in rivers and reservoirs. Effective sediment management is relevant to many concerns, including sediment-associated pollutant dispersal, geochemical fluxes, changes in community structures and functions, as well as successful river restoration and reservoir maintenance. Numerous studies have previously shown the stabilization effects of biofilms ("biostabilization") in freshwater and coastal ecosystems. Extracellular polymeric substances (EPS) secreted by microorganisms have been increasingly accepted as a major component influencing biostabilization despite the equivocal results. Still, the mechanisms involved in biostabilization are largely unknown due to complex interactions between flow dynamics, biofilm and geomorphology.

We explore biostabilization potential in fine sediments by unraveling the interplay between flow, biofilm growth and microbial community, and surface roughness response. For this purpose, a series of laboratory-controlled experiments were performed with fine sediment under contrasting flow velocities. Biofilm was cultivated over a period of 15 – 90 days in six recirculating flumes using the water and inoculation from reservoirs in Germany. The weekly development of two-dimensional velocity fields and three-dimensional bed topographies were measured using particle image velocimetry (PIV) and underwater laser scanner, respectively. Adhesion capacity was monitored using magnetic particle induction (MagPI), while the critical shear stress for erosion was determined in a straight erosion flume. The weekly extracted biofilm-bound sediment samples were analyzed for EPS contents (proteins and carbohydrates), bacterial cell numbers and chlorophyll-a concentrations. In parallel, community composition was estimated through prokaryotic 16s and eukaryotic 18s ribosomal ribonucleic acid (rRNA) gene-based amplicon sequencing and fluorescent microscopy techniques.

A fifteen-fold increase (up to 12 Pa) in critical shear stress for erosion was detected for biofilm-bound sediment compared to clean sediment. In most cases, a sudden catastrophic failure of the bed was observed. Increase in critical shear stress was associated with increase in root-mean-square slope of the roughness surface (R^2 = 0.93). The biochemical characterization of biofilm-bound sediment indicated positive correlations between EPS, heterotrophic and autotrophic biomass and sediment stability, providing additional proof on sediment-binding potential of the EPS-matrix. Moreover, preliminary evidence based on the amplicon sequencing of prokaryotes and eukaryotes as well as fluorescent microscopy points out the role of filamentous bacteria (with phylum Cyanobacteria and Chloroflexi) on biostabilization, by entrapping sediment particles within a dense filament network. Interestingly, a comparison of microbial community at contrasting flow conditions revealed the

decisive role of flow speed on heterotrophic and autotrophic microbial community abundance and diversity, and thus on characteristics of the secreted EPS-matrix. Consequently, the mechanism behind the biostabilization cannot be attributed to the EPS-matrix only.

Exploring the feedback between biofilm-bound sediment (microbial communities and EPS-matrix), surface roughness, and flow dynamics is still ongoing, which is expected to reveal the key processes responsible for adhesion and stability of biofilm-bound sediment. Overall, it is imperative that microbial stabilization of sediment must be considered in sediment transport models and management strategies developed for engineering applications.

INTERCOH - Bottom Shear, Erosion and Bed Exchange

O1037 - CONTROLS ON BED ERODIBILITY IN MUDDY PARTIALLY MIXED TIDAL ESTUARIES INSIGHTS FROM THE YORK RIVER ESTUARY VIRGINIA USA
Bottom Shear Erosion and Bed Exchange

Carl Friedrichs [1], Cristin Wright [1], Grace Massey [1]
Virginia Institute of Marine Science, Physical Sciences Dept., Gloucester Point-United States [1]

Appropriate parameterization of time-dependent erodibility of muddy seabeds is a significant barrier to improved understanding and accurate modeling of sediment dynamics in estuaries and other coastal regions. In an effort to better understand controls on muddy seabed erodibility, bed erodibility and associated bed sediment properties have been measured by our group on over 100 cores collected on dozens of cruises over the last 13 years in the York Estuary. We have also inferred time-varying erodibility indirectly in the York Estuary over several years by vertically integrating observations of tidally-varying suspended sediment concentration. This paper synthesizes the results of these long-term observations in this partially-mixed estuary, whose seabed is similar to that of many other moderately energetic, muddy tidal estuaries.

Seabed erodibility was measured directly on bed samples from the York Estuary utilizing a dual core Gust erosion microcosm. This device uses a rotating disc with central suction to impose a nearly uniform shear stress on the surface of 10cm diameter sediment cores. After collection of box cores in the York Estuary, sub-cores for use in the microcosm were carefully transported to the Virginia Institute of Marine Science (VIMS) located nearby on the banks of the York. To minimize consolidation effects, erodibility measurements were generally underway in our sediment lab within about 2h of core collection. Erodibility measurements consisted of a sequence of seven steps of approximately 20-min duration, each with a consecutively increasing shear stress (0.01, 0.05, 0.1, 0.2, 0.3, 0.45, and 0.6Pa) applied to the sediment surface. Bed erodibility was also measured indirectly in the York Estuary utilizing Acoustic Doppler Velocimeters (ADVs). Although an ADV cannot control shear stress, a bottom-mounted ADV still documents time-varying bed stress by measuring near-bed turbulent velocity, and ADV backscatter can be calibrated for suspended sediment concentration. Estimating the vertical integral of suspended sediment concentration during periods of accelerating tidal currents then gives an estimate of eroded mass as a continuous function of stress, analogous to the data provided by a Gust microcosm.

Additional field measurements collected to characterize seabed properties included digital x-radiography of sediment cores and sediment analysis of the upper 1cm of the seabed for disaggregated grain size distribution, concentration of resilient mud aggregates, water content, and organic content. Relationships between bed erodibility, other bed properties, and recent bed stress were examined using general linear models (GLMs), generalized additive models (GAMs), and principal component analysis (PCA).

Conclusions include: (1) that large increases/decreases in erodibility are due to major

deposition/erosion of fresh layers of muddy flocs; (2) that gradual decreases in erodibility are associated with further winnowing of seabed flocs, dewatering of muds via consolidation, and armoring of the surface of the bed by increased concentrations of resilient mud aggregates and sand; and (3) that short-term increases in erodibility follow previous periods of enhanced bed stress, such as following spring tides. In contrast to previous findings in other muddy systems: (1) enhanced organic content in muddy sediments in the York Estuary was not correlated with greater resistance to erosion, but instead greater organic content was a tracer indicating an abundance of freshly deposited, easy to erode flocs; and (2) bed fabric indicative of past bioturbation was not correlated with increased erodibility, but was instead was a sign that a longer time had passed since physical deposition and, thus, the sediment was harder to erode.

INTERCOH - Bottom Shear, Erosion and Bed Exchange

O1040 - MULTI FREQUENCY ACOUSTIC BACKSCATTER MEASUREMENTS IN THE RÍO DE LA PLATA
Bottom Shear Erosion and Bed Exchange

Rodrigo Mosquera [1], Francisco Pedocchi [1]
Universidad De La República - Fing, Imfia, Montevideo-Uruguay [1]

Abstract
This work describes new near bed measurements performed in the Rio de la Plata (RP) estuary 3 km in from Montevideo's coast. The riverbed in the area is composed of fine sediments (1 % sand, 77 % silt, 22 % clay). An instrumented mooring structure was specifically designed in our shop and deployed for two periods of three months each. The objective of the deployment was to increase our understanding of the sediment transport mechanisms in the estuary under different wave, currents, salinity, and stratification conditions. The near bed sediment concentration profile was measured with four Multi-frequency Acoustic Backscatter Sensors (ABS). Point measurements at two vertical locations were recorded with two optical backscatter sensors (OBS) as well. The near bed hydrodynamics were directly measured with an Acoustic Doppler Velocimeter (ADV) and an Acoustic Doppler Current Profiler (ADCP). Water salinity was measured using Conductivity, Temperature, Depth sensors (CTD). During storm conditions a 20 cm thick layer of highly concentrated sediment was registered near the bed. The entrainment of sediment from this layer into the water column was clearly observed to occur under the largest waves of the wave train. To our knowledge this is the first recorded dataset of this kind in the Rio de la Plata.

Introduction
The Rio de la Plata (RP) river is born at the confluence of the Uruguay and the Parana rivers, making them not only its primary source of freshwater, but also its main source of fine sediment. The Suspended Sediment Concentration (SSC) at this location frequently exceeds 0.1 kg/m3. The RP has a funnel shape, going from two kilometers wide at 0 km to two hundred kilometers wide at 300 km downstream, where it reaches the Atlantic Ocean. The RP estuary in the coast of Montevideo is less than ten meters deep. Over the Uruguayan coast the tide regime is micro tidal with a tidal amplitude of about 0.5 m. However, on a weekly basis storms in the South Atlantic Ocean generate meteorological tides that propagate northwards over the Argentinean continental shelf, reaching the RP mouth with amplitudes that may reach 2.5 m (Fossati et al. 2014).

Measurements and data
The field observations were made through two deployments: the first was from December 8, 2017 to February 23, 2018; and the second was from May 25 to August 25 of 2018. The deployment site was located 3.0 km South from the coast of Montevideo, and the mean water depth during the deployment was 7.5 m.

For the first deployment a tripod equipped with a downward looking AQUAscat 1000R multi-frequency Acoustic Backscatter Sensors (ABS) and a Vector Acoustic Doppler Velocimeter (ADV) was deployed to measure the first decimeters above the sediment bed. The ABS had four acoustic transducers, with frequencies between 0.5 to 5 MHz, and was set to record 2 min bursts every 30 min, with a sampling frequency of 32 Hz, and with a 1 cm resolution over a vertical distance of over a meter. The ADV was also set to sample 3 min bursts every 30 min,

INTERCOH - Bottom Shear, Erosion and Bed Exchange

with a sampling frequency of 32 Hz. A Seapoint Turbidity Meter (STM) was also deployed 7 cm below the ABS.

For the second deployment additional instrumentation was attached to the tripod. Water temperature and salinity were measured with a Seacat 19 plus V2 Conductivity, Temperature, and Depth sensor (CTD), and turbidity at a second vertical location was measured with OBS3+ Optical Backscatter Sensor (OBS). Sediment samples from the deployment site were taken to the laboratory to calibrate the acoustic and optical sensors.

During the first deployment that took place in summer, water temperature varied between 20 and 26 ºC, and water depth between 6 and 9 m. The largest significant wave height recorded during this deployment was 2.2 m high and the maximum current registered was 1.4 m/s. In this deployment the ABS was positioned 1 m above the bed, and during some of the storms, a sediment layer of 10 to 20 cm was observed to form above the bed (Fig. 1 right panel). Furthermore, entrainment events of sediment from this layer into the water column were observed under individual waves.

During the second deployment that took place in winter, water temperature varied between 10 and 18 ºC, salinity between 0 and 28 psu, and water depth between 6.5 and 9 m. The largest significant wave height recorded during this deployment was 2.0 m high and the maximum current registered was 1.1 m/s. In this deployment the ABS was 0.4 m above the bed, the 10 to 20 cm sediment layer was also observed.
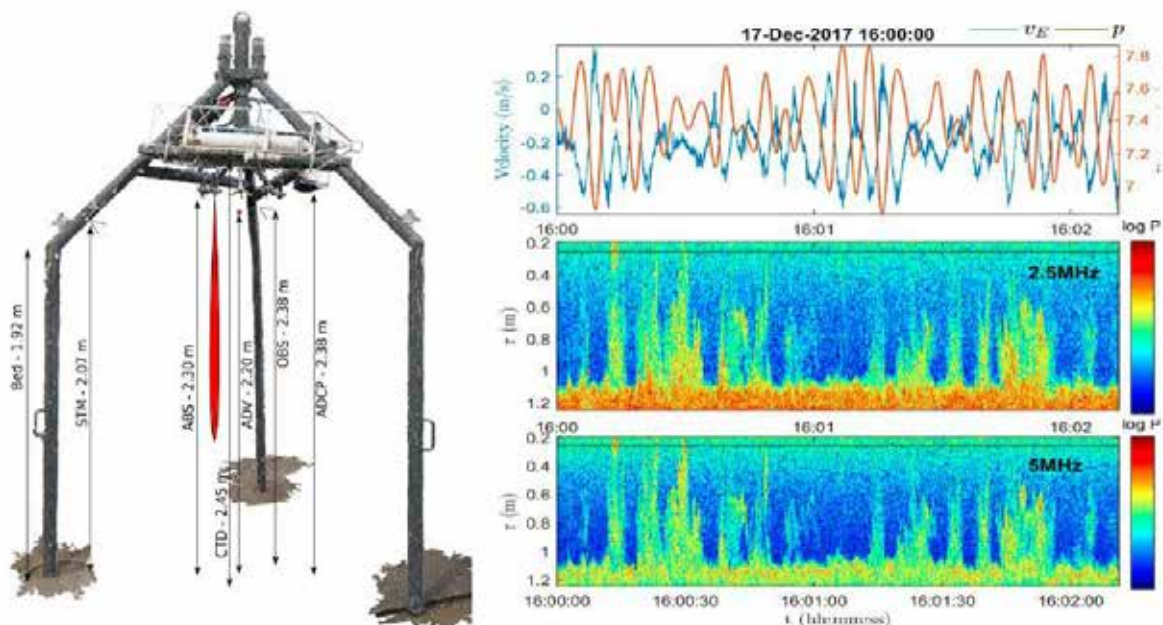

Fig. 1 Left panel, tripod used during the second mooring. Right panel, ADV and ABS data during intense waves in 17 December.

Conclusions

The new measurements in the coast of Montevideo bring significant insight on the cohesive sediment transport processes in the Rio de la Plata estuary. The results show that a highly

concentrated layer, with concentrations of the order of 1 kg/m3 is formed during storms, mostly due to wave action. This highly concentrated layer could then be transported by currents, which during storms can easily surpass 0.5 m/s. The data obtained is still in the process of being analyzed, however it's evident that these preliminary results may have a profound impact on our general understanding of the RP sediment dynamics and its modeling, as well as considerable consequences for the navigation channel design and dredging works.

References

Fossati M., Cayocca F. and Piedra-Cueva I. (2014). Fine sediment dynamics in the Río de la Plata. Advances in Geosciences, 39, 75-80.

INTERCOH - Bottom Shear, Erosion and Bed Exchange

O1050 - DETERMINING EROSION FORMULATION PARAMETERS BY FIELD MEASUREMENTS Bottom Shear Erosion and Bed Exchange

Bram Van Prooijen [1], Qin Zhu [2]

Tu Delft, Hydraulic Engineering, Delft-The Netherlands [1] 2 Guangdong University Of Technology, Institute Of Environmental And Ecological Engineering, Guangdong-China [2]

Introduction

Numerical simulations of muddy systems rely on the definition of the erosion formulation. Since the pioneering work of Ariathurai (1974), the erosion formulation $E = M\left(\tau - \tau_e\right)$ is used, with the erosion rate E, erosion rate coefficient M, bed shear stress τ and critical shear stress for erosion τ_e. As indicated by Sanford&Maa (2001), the different types of erosion (depth-limited, Type I and unlimited, Type II) can be simulated with this equation, using a depth-dependent critical shear stress, $\tau_e(z)$. Despite the simplicity of this equation, it turns out that the different parameters and variables are not easy to determine. In this contribution, we discuss how we determined the bed shear stress, critical shear stress for erosion and the erosion rate coefficient by field observations on tidal flats.

Methods

Field measurements were carried out with ADVs (Nortek Vector) in combination with an OBS. The ADV measures the flow velocities and pressure at high frequency (8Hz). Furthermore, the bed level at the beginning and end of each burst is measured. The OBS is used for turbidity measurements which, after calibration, are translated to sediment concentrations. Measurements have been carried out on different fringing tidal flats in the Netherlands. Here we use the data from Kapellebank, Western Scheldt. Three frames were installed at different heights and distances from the channel (Zhu, 2017). The measurement period included a storm event with significant erosion and a recovery period afterwards.

Bed shear stress

The total bed shear stress is based on the contributions of flow and waves (Soulsby, 1997). We emphasize here that in addition to the tidal flow, the wind-driven flow can be of crucial importance on mudflats with small water depths. Different approaches are used to determine the bed shear stress by flow. We chose the method based on the vertical velocity fluctuations, after filtering out the wave-induced fluctuations. The bed shear stress by waves was based on the definition of the friction coefficient of Soulsby&Clarke (2005) implying smooth turbulent flows. Typical values of total bed shear stress range between 0 and 3 Pa.

Critical bed shear stress

The critical shear stress for erosion was determined by analyzing the timeseries of the bed level variations and bed shear stresses. Almost abrupt changes in bed level were identified during erosion events. Figure 1a shows such an erosion period. It is noted that erosion starts for a smaller critical bed shear stress than it ends with. This already suggests an increase in critical

INTERCOH - Bottom Shear, Erosion and Bed Exchange

bed shear stress for deeper layers. Figure 2a shows the so-obtained bed shear stresses for the different heights within the bed. An increase in critical shear stress for erosion is observed, with values around 0.1Pa near the surface to 1.13Pa at a depth of 12cm. This indicates a significant variation over a limited depth.

Erosion rate parameter

The erosion parameter is determined for the same erosion events as the critical shear stresses for erosion. No indications for Type I erosion were identified. Most erosion events could be classified as Type II erosion. Figure 2b shows the erosion coefficient as function of depth. No significant trend is found for the erosion rate coefficient as function of the eroded depth. A typical value of 0.002 s/m is found, although values up till 0.008 are found, indicating a significant scatter. For comparison, no clear trend with eroded mass was found either by Sanford&Maa (2001), who found values in the range 0.002-0.01 s/m.

Conclusions

The parameters of the erosion rate formulation were determined for a tidal flat in the Western Scheldt. A clear increase in critical shear stress for erosion was found, going deeper into the bed. Such a significant variation over a limited depth has severe consequences for the modelling of such systems. Using a uniform/constant critical shear stress for erosion will initially lead to an underestimation of the erosion rate. Later on, the erosion is overestimated leading to too much erosion of the tidal flat. Bed layers with active layer thicknesses of 1cm or less are required. Furthermore, the history of the bed with its critical shear stress for erosion needs to be accounted for. This would have serious consequences for the computation times.
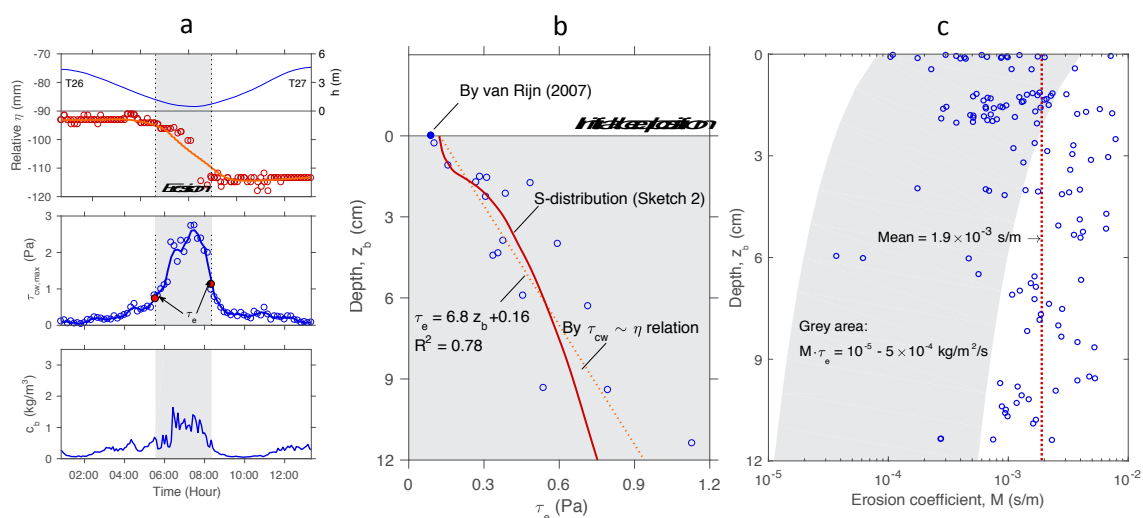

Figure 1: (a) timeseries of the bed level (top), bed shear stress (middle) and concentration (bottom) during an erosion event; (b) critical shear stress for erosion as function of depth; (c) erosion rate coefficient as function of depth.

References

Ariathurai, C.R., 1974. A Finite Element Model for Sediment Transport in Estuaries. PhD thesis,

University of California, Davis, CA.

Sanford, Lawrence P., and Jerome P-Y. Maa. "A unified erosion formulation for fine sediments." *Marine Geology* 179.1-2 (2001): 9-23.

Soulsby, Richard. *Dynamics of marine sands: a manual for practical applications*. Thomas Telford, 1997.

Soulsby, R. L., and S. Clarke. "Bed shear-stress under combined waves and currents on smooth

and rough beds (TR 137)." (2005).

Zhu, Q. "Sediment dynamics on intertidal mudflats: A study based on in situ measurements and

numerical modelling." (2017). PhD thesis TU Delft.
    https://doi.org/10.4233/uuid:5f094e4b-fef9 4216-abbe-3277adc90b28

INTERCOH - Bottom Shear, Erosion and Bed Exchange

O1054 - DISPERSION OF BIO DEPOSITS FROM A DEEP CAGE CULTURE FISH FARM IN THE NORTHERN PERSIAN GULF
Bottom Shear Erosion and Bed Exchange

Mehrnoosh Abbasian [1], Majid Shah-hosseini [2], S. Abbas Haghshenas [1], Aref Farhangmehr [3], Hamid Rezai
[4], Azadeh Razavi Arab [5], Michael John Risk [6]
Institute of Geophysics - University of Tehran, Oceanography, Tehran-Iran [1] Aix-marseille University, Oceanography, Aix-en-provence-France [2] Oceans Research, Coastal Engineering, Tehran-Iran [3] Darya Negar Pars Consulting Engineers, Environmental Engineering, Tehran-Iran [4] Louisiana State University, Oceanography, Baton Rouge-United States [5] Mcmaster University, Oceanography, Durham-Canada [6]

Introduction
With increasing demand for fish in the market, large-scale and intensive finfish mariculture seems inevitable in the Persian Gulf. However, this activity poses a serious threat to the environmental integrity of marine ecosystems of this important body of water. This is why fin-fish Mari culture has faced many oppositions .The negative impact to the benthic community is mainly related to over enrichment of sediments beneath the aquaculture site because of excessive bio-deposits. When the bio deposits reach the bottom, two outcomes are possible; 1) The bottom shear stress, which is determined by bed roughness, current velocity and wave action, may be great enough to re-suspend and disperse the bio deposits., or 2) the bio deposits stay on the bottom, become consolidated and incorporated into the sediments that implies increased organic loading in the sediments both directly below and surrounding the aquaculture site resulting adverse effects on the surrounding benthic organisms. A greater bottom shear stress is required to re-suspend the bio deposits after they have been incorporated into the sediments on the bottom (Sanford and Maa, 2001). Considering the depth conditions appropriate for cage culture, which is usually more than 20 m, the latter outcome is more likely to happen. Here we report observations and modelling of bio-deposit dispersion at a relatively deep water cage culture farm in the Northern Persian Gulf, near Kish Island, where considerable coral reef coverage is present in 15 km surrounding area.

Research Program
This study is part of a research program that is designed to seasonally monitor environmental parameters and sediment transport processes in the vicinity of an operational fin-fish farm. Field observations cover the period of active fish growing in 2018-19. Sediment and hydrodynamic surveys were carried out using arrays of current meters, wave gauges, and sediment traps. Tidal and wind-driven flows as well as wind-wave propagation and sediment dispersion were modeled using Delft-3D software. Model predictions were verified against field measurements. The approximate radius of affected area is compared with the results of bio-indicator monitoring program.

Study of Bio-Indicators
In order to measure the amount of suspended sediment and sedimentation rate a number of ten conical sediment traps were installed around fish cages. The sediment trap consists of a 30 cm long tube with 8 cm opening ending to a cone. The traps were fixed on concrete blocks for better stability. Each installation marked by a buoy for easy recovery. Sediment traps, where recovered after 9 months and trapped sediments sent to laboratory for analysis. Bed

15th INTERNATIONAL CONFERENCE on
COHESIVE SEDIMENT TRANSPORT PROCESSES
13 - 17 OCTOBER 2019 • ISTANBUL / TURKEY
YILDIZ TECHNICAL UNIVERSITY - YILDIZ CAMPUS

INTERCOH - Bottom Shear, Erosion and Bed Exchange

sediments were collected using a Van-veen grab along 4 station around the farms. The surficial sediment layer was carefully recovered and immediately mixed with solution of 10% formalin and 1% Rose Bengal. The samples are then transferred to PET bags and stored in refrigerator for at least 2 weeks (Oron et al., 2014). The bed samples were go through a preparation process before being analyzed for bio-indicator investigations. Benthic foraminifera picked using a binocular microscope, a picking tray and fine brush and archived in gummed microfossil slides. At least 300 individuals picked from each sample. Our preliminary results shows that the abundance and diversity of live foraminifera in the east of cages is far less than other stations and control points (Figure 2). This can be related to shore-parallel (East-West) tidal flows that results to accumulation of pollution is on the eastern side of the cages. That is generally in agreement with results of our model. As the sampling has repeated in different distances from the cages, the radius of affected area can be distinguished from the analysis of alive foraminifera.

Particle Tracking Modelling

To investigate the distribution of biological deposits, flow model and particle tracking module were employed in the open source Delft-3D software. The model were run according to the pure tidal and combined tidal and wind-driven driving forces. The input for particle injection assumed as a concentration with specified release rate and settling velocity of bio-deposits. The model is calibrated to be mainly sensitive to faecal bio deposit concentration. The output of the model are validated against field data, collected using sediment traps. Along with model results, observation of any change in the population and diversity of live benthic foraminifera is essential for evaluation of bio-deposit contamination in the study area. Bio-deposits include wasted fish food and faecal particles of fish. Since the amount of food waste is negligible comparing with consumed fish food (Magill et al., 2006), just fish faecal particles are taken in to account as bio deposits in this study. The results of dispersion modeling are compared with biomarkers monitoring results, as well. The monitoring and modeling results are presented in Figure 2 and fairly good agreement is observed between simulations and observations.
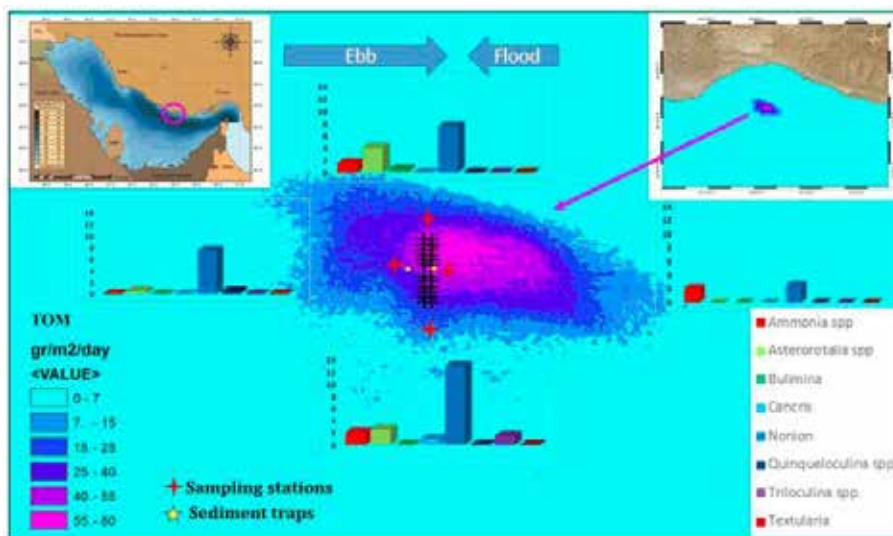

Fig. 2. As shown in the figure most of the accumulation of deposits is on the right side of the cages that the reduction of the number of living organisms also proves the accuracy of this assertion (stars show in red represent to sampling position and in yellow represent to sediment traps places).

References

Magill, S.H., Thetmeyer, H., Cromey, C.J., 2006. Settling velocity of faecal pellets of gilthead sea bream (Sparus aurata L.) and sea bass(Dicentrarchus labrax L.) and sensitivity analysis using measured data in deposition model. Aquaculture 251, 295–305.

Oron, S., Angel, D., Goodman-Tchernov B, Merkado, G., Kiflawi, M., Abramovich, S., (2014). Benthic foraminiferal response to the removal of aquaculture fish cages in the Gulf of Aqaba-Eilat, Red Sea. Mar Micropaleontol,107:8–17

Sanford, L.P. and Maa, J.P.-Y., 2001. A unified erosion formulation for fine sediments. Mar. Geol. 179: 9-23.

INTERCOH - Intertidal & Subtidal Areas

O1060 - NONLINEAR FREQUENCY DOWNSHIFTING OF SPECTRA OF WAVES PROPAGATED OVER THE MUD BANKS
**Bottom Shear Erosion and Bed Exchange**

Sergey Kuznetsov [1], Samiksha Volvaiker [2], Yana Saprykina [1], Sudheesh Kotteppad [3]
Shirshov Institute of Oceanology, Russian Academy of Sciences, Coast & Shelf Laboratory, Moscow-Russia [1] Csir-national Institute of Oceanography, Ocean Engineering (oed), Dona Paula-India [2] Csir-national Institute of Oceanography, Division of Physical Oceanography, Dona Paula-India [3]

Mud banks in a coastal zone are the natural phenomena developing under action of storm waves. Mud banks are formed by interaction of bottom cohesive sediments with waves: waves create these formations, and then by linear and nonlinear manners are transformed over them owing to change of conditions of its propagation - reduction of effective depth, changes of density and viscosity of near bottom layer. Field measurements of waves at Alappuzha, Kerala, India at July 2014 over the mud banks demonstrate the dissipative and nonlinear features of its transformation such as diminishing of significant wave height and relative growing of energy at lower sideband of spectra. To separate the influence of dissipation and nonlinearity we estimate the role of nonlinearity using the bi-spectral analysis of wave chronograms measured at the same place in different times at presence and absence of mud banks. The typical transformation of wave spectra from depth 15 m to 7 m at absence and at presence of mud bank has been shown at figure 1. The bimodal structure of spectra with well-expressed peaks at frequencies of 0.06 Hz and 0.09 Hz conserve during the wave propagation in the coastal zone both in case of presence and absence of mud banks. The calculated values of squared bi-coherence functions, shown at figure 2, prove the nonlinear connections of wave harmonics provided by these spectral peaks. Relatively high values of bi-coherence at the frequencies of main spectral peaks demonstrate the existence summary triad wave interactions that transfer energy to summary frequency. High values of bi-coherence at negative frequency range (not shown here due to lack of space) confirm the backward energy transfer the energy from the summary harmonic to the first ones.The no uniform frequency redistribution of backward energy transfer provides the relative grows of energy at lower spectral sideband. The similar nonlinear features of wave spectra transformation and much stronger dissipation of wave energy in cases of presence than at absence of mud banks permit us to separate the influence of nonlinearity and dissipation on wave transformation process over the mud banks. It was revealed that the nonlinearity is responsible for the energy redistribution in the spectrum, whereas the dissipation is responsible on the diminishing of the total wave energy only. The phase shift between the harmonics and it influence on cohesive sediment transport will be discussed during the presentation.
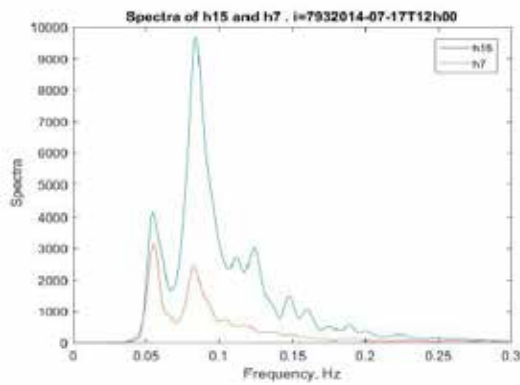
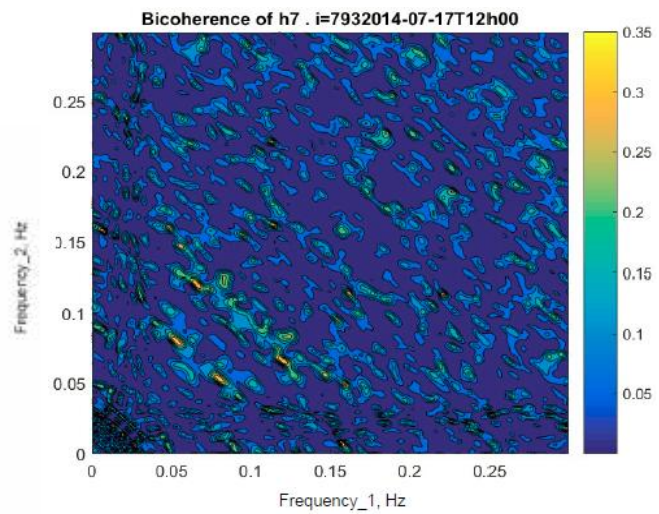**INTERCOH - Intertidal & Subtidal Areas**
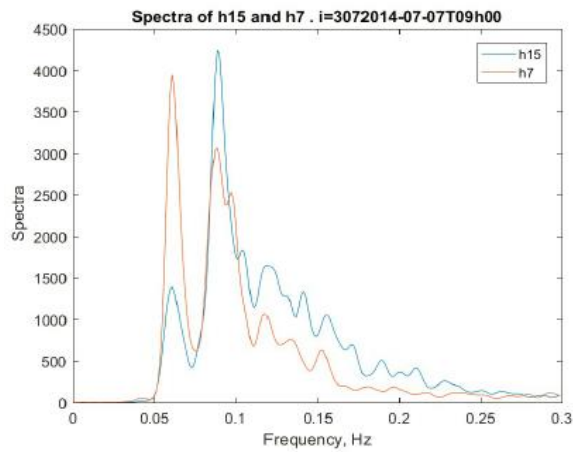
a)
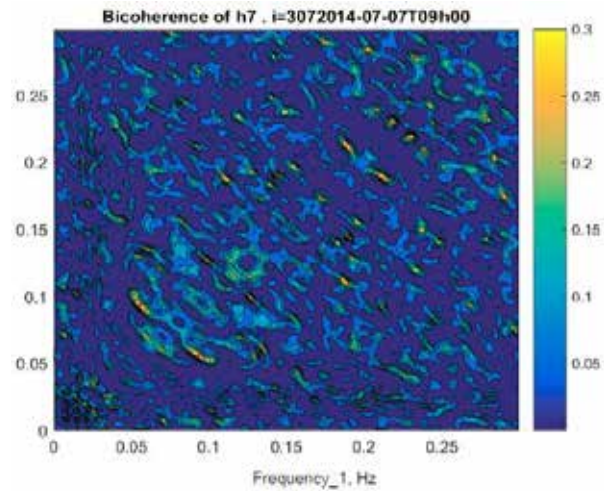
a)

b)

b)

Figure 1. Two peaks (0.06 Hz and 0.09 Hz) wave spectra evolution from depth of 15 m to 7 m. a) at absence of mud bank a) at presence of mud bank

Figure 2. The bi-coherence squared of waves at 7m depth that spectra are shown at Figure1.

INTERCOH - Intertidal & Subtidal Areas

O1016 - WINTER INTERTIDAL SEDIMENT DYNAMICS IN SUBARCTIC ST. LAWRENCE ESTUARY CANADA
Intertidal & Subtidal Areas

Atif Waqas [1], Urs Neumeier [1], André Rochon [1]
Université Du Québec À Rimouski, Institut Des Sciences De La Mer De Rimouski (ismer), Rimouski-Canada [1]

The presence of microalgal biofilm on intertidal sediments has been shown to consolidate the sediment surface and play a vital role for the erosive response to shear stresses generated by waves and currents. The objective of this study is to determine the sediment erodability associated with biofilm on an intertidal area in winter, when it is covered by sea ice during several months. In the St. Lawrence Estuary, the land-fast ice is typically 0.5 m thick. It attenuates strongly waves, modifies the currents, and can transport sediment by ice rafting.

Field sampling was undertaken at Nazareth tidal flat and marsh located west of Rimouski on the southern shore of Lower St. Lawrence Estuary (Canada). This intertidal area is about 1.3 km wide with a spring tidal range of about 4.9 m. A cross-shore transect was established with 8 stations covering low marsh, mudflat and sandflat. Critical erosion threshold was quantified using a Cohesive Strength Meter (CSM Mk IV). Small sediment cores (36 mm φ) were frozen in the field. Concentrations of chlorophyll a and carbohydrate (proxy for Extracellular Polymeric Substances, EPS) were measured in the upper 3 mm. The erosion threshold and the concentration of chlorophyll a and carbohydrates were measured in February 2018 and in March 2019. Samples for grain size and organic content determination were collected in March 2019.

The mean sediment particle size is between 5 and 68 μm, with over 90% of all samples having a mean grain size finer than 26 μm. The poor sorting of sediments directs towards the contribution of sediments transport by ice rafting in addition to the hydrodynamic transport processes in this subarctic intertidal area. Our erosion threshold results show that the sediments are much less stable under land-fast ice than in ice-free periods (in average 0.80 N m-2 vs. 1.10 N m-2). The average chlorophyll a concentrations reduced from 18 μg g-1 in ice-free periods to 14 μg g-1 in winter. However, the EPS concentration substantially increased in winter (in average 600 μg g-1 vs. 250 μg g-1). There is a positive correlation between erosion threshold and organic matter content measured by loss on ignition. However, erosion threshold does not correlate significantly with chlorophyll a or EPS, which are not good indicators for sediment stability in subarctic winter conditions. There is also no significant correlation between mean grain size and critical erosion threshold. This study highlights the implications of intertidal sediment exposure to winter conditions with sea ice cover and consequently lower erosion threshold. The sediments were less stable in winter than in ice-free periods, probably because the algal biomass is reduced due to the low temperature and the partial light blockage by the sea ice cover. This could suggest a higher sediment mobility in winter, but there are no bed shear stress peaks due to high wave events in winter. Further fieldwork will look at the differences in hydrodynamic conditions between winter and summer.

INTERCOH - Intertidal & Subtidal Areas

O1018 - NUMERICAL MODELING OF SEDIMENT BUDGETS IN INTERTIDAL AND SUBTIDAL MUD FLATS OF A MACROTIDAL ESTUARY AND ITS ADJACENT COAST INFLUENCE OF HYDRO METEOROLOGICAL FORCING
Intertidal & Subtidal Areas

Melanie Diaz [1], Florent Grasso [1], Pierre Le Hir [1], Benedicte Thouvenin [1], Matthieu Caillaud [1]
Ifremer, Ode/dyneco/dhysed, Plouzane-France [1]

Introduction
Coastal environments are directly influenced by terrigenous inputs coming from rivers through estuaries. Quantifying the amount of nutrients and contaminants brought by sediments, especially fine particles, from continental areas to the sea is of major interest for marine resource protection. The presence of an Estuarine Turbidity Maximum (ETM) may affect the sediment exchanges at the mouth and intertidal mudflats undergo dynamic mechanisms leading to trapping or resuspension of fine sediment within the estuary (Allen *et al.*, 1980; Grasso *et al.*, 2018). The complexity of the intra-estuarine dynamics, associated with the strong variability of meteorological forcing in the adjacent continental shelf (e.g. wind, waves), makes it difficult to quantify the residence time of particles within the estuary and the accumulation and dispersion areas offshore the mouth. Moreover, the dynamics of fine sediment trapping areas in the adjacent continental shelf (e.g. temporary or permanent storage) remains extremely challenging to address. This study focuses on the macrotidal Gironde Estuary (France) and its adjacent continental shelf in the Bay of Biscay. It is one of the largest estuary of Western Europe and its ETM is one of the most developed in Europe. The surficial sediment map established by Allen and Castaing (1977) and Lesueur *et al*. (1996) exhibited the presence of two subtidal mud fields offshore the mouth, on the continental shelf: the West- and South-Gironde mud patches. Based on a realistic process-based numerical model, the aim of this work is to investigate the dynamics of sediment accumulation and dispersion areas in order to describe the role played by the intertidal mudflats and the subtidal mud patches on sediment trapping and potential further resuspension.

Methods
The hydrodynamic numerical model MARS3D is applied over a large domain including the Gironde Estuary (South-West of France) and the continental shelf seaward (Bay of Biscay). Based on a curvilinear grid, the model is forced by the main tidal components at the sea boundary, wind conditions and meteorological surges provided by a meteorological model and realistic river discharges. Waves are simulated using the WAVE WATCH III® model. The hydrodynamic core is coupled with the multi-layer module MUSTANG (Le Hir *et al*., 2011), accounting for erosion, suspension, deposition and consolidation processes for sand and mud mixtures. Five classes of particles are considered and initially uniformly distributed: one mud (30%), 3 sands with a median diameter d=100, 250 and 400µm (20% of each) and one gravel (d=3mm, 10%). In order to ensure the simulation relevance, numerical model results are obtained after one year spin-up preceding the analysis period. The hydrodynamics and hydrology were validated in terms of water elevation, velocity current and salinity measurements within the estuary. The sediment model was validated with local measurements of Suspended Sediment Concentration (SSC) within the estuary and seaward of the mouth.

INTERCOH - Intertidal & Subtidal Areas

Results and discussion

The simulated sediment distribution is analysed after one year simulation over the realistic year 2015, revealing a simulated mud accumulation area north-west of the estuarine mouth, in agreement with the observed West-Gironde Mud Patch (WGMP) location (figure 1). This area is less energetic than closer to the mouth were the wave-induced bed shear stress is stronger, allowing mud to settle down. Within the estuary, mud is also trapped on intertidal mudflats and in the channel, where the ETM is located (not shown). The accumulated mud mass dynamics in the simulated WGMP (defined by the orange square in figure 1) is evaluated over the year in order to investigate the impact of storms and river discharge on mud trapping. The integrated mud mass was monthly-averaged and the changes from one month to the next one is analysed in figure 2 versus the wave-induced bed shear stress. The monthly-averaged mud mass changes are always positive, revealing that the mud accumulates over the year, without any significant erosion event. Waves significantly influence the trapping efficiency in this area by limiting mud deposition during energetic conditions. However, the impact of storms on mud accumulation is reduced during high river discharge. The mud trapping efficiency is enhanced by comparison with same waves conditions during low river discharge due to largest export of sediment by the turbid plume. In addition, mud dynamics in the intertidal mud flats within the estuary will be discussed. The impact of natural processes on the residence time of particles within the accumulation areas will be investigated by considering diverse hydro-meteorological conditions. In particular, the temporal or permanent trapping patterns, associated with potential sediment resuspension and dispersion, will be analysed.
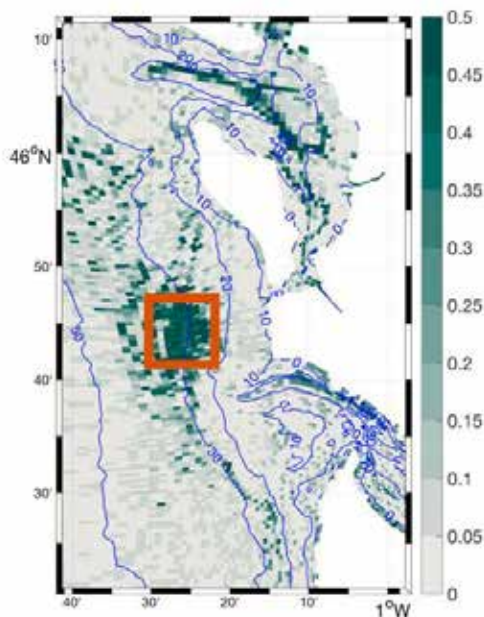

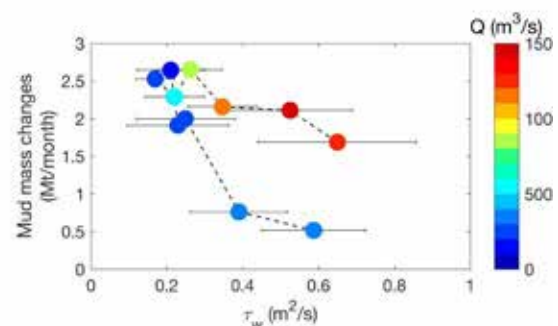Figure 1. Mud fraction in the surficial layers on the continental shelf offshore the Gironde Estuary

Figure 2. Monthly averaged mud mass changes within the simulated mud field on the continental shelf versus the waveinduced bed shear stress, along with the corresponding river discharge.

References

Allen G.P. and Castaing P. (1977). Carte de répartition des sédiments superficiels sur le plateau continental du golfe de Gascogne. Bulletin – Institut de Géologie du bassin d'Aquitaine (Bordeaux), 21: 255-261.

Allen G.P., Salomon J.C., Bassoullet P., Du Penhoat Y. and de Grandpré C. (1980). Effects of tides on mixing and suspended sediment transport in macrotidal estuaries. Sedimentary Geology, 26(1-3): 69-90.

Grasso F., Verney R., Le Hir P., Thouvenin B., Schulz E., Kervella Y., IKhojasteh Pour Fard I., Lemoine J.P., Dumas F. and Garnier V. (2018). Suspended Sediment Dynamics in the Macrotidal Seine Estuary (France): 1. Numerical Modeling of Turbidity Maximum Dynamics. Journal of Geophysical Research: Oceans, 123(1): 558-577.

Le Hir P., Cayocca F., and Waeles B. (2011). Dynamics of sand and mud mixtures: A multiprocess-based modelling strategy. Continental Shelf Research, 31(10): S135-S149.

Lesueur P., Tastet J.P. and Marambat L. (1996). Shelf mud fields formation within historical times: examples from offshore the Gironde estuary, France. Continental Shelf Research, 16(14): 1849- 1870.

INTERCOH - Intertidal & Subtidal Areas

O1020 - FROM MUD TO LAND HOW COHESIVE SEDIMENTS HELP TO KEEP THE NETHERLANDS DRY AND SAFE
Intertidal & Subtidal Areas

Thijs Van Kessel [1]
Deltares, Mcs, Delft-The Netherlands [1]

An important part of the Netherlands lies below mean sea level and to protect the land against the sea and river floods dikes and dunes are used. These require regular maintenance. With raising mean sea level induced by climate change regular strengthening is also required. On top of this, channel deepening and land reclamation within estuaries such as the Scheldt have resulted in substantial raising of high water levels. In the past millennium, flood protection policy was initially quite unreliable, as flood disasters still occurred regularly and caused major damage and claimed many lives. However, this policy grew more and more successful with increasing technical knowledge, economical means and centralized approach and the last flood disaster in the Netherlands is now 65 year ago. The question is to which extent this policy is sustainable into the next centuries. A too extreme difference between sea and land levels imposes many risks and costs. Shouldn't we gradually switch from raising dikes to raising land? To control water and salinity intrusion, shouldn't we allow 'sediment intrusion'?

The Dutch soils consist of sand, clay and peat. Peat is formed in place if conditions are favourable. Sand can only be transported naturally at high current speeds, limiting its natural deposition to a narrow strip along rivers and coasts. Mud can be transported over much longer distances, making is suitable for the creation of gradual water-land transitions. In consolidated form it is quite resistant to erosion and has a low permeability, which is advantageous for the reduction of water and salt seepage.

The question is how much cohesive sediments are available in the Netherlands for this land-building function and how this material can be applied best. To address the second questions, a number of field pilots are presently being carried out. Two major ones are Markerwadden and 'Kleirijperij' (Fig. 1). The first aims at wetland formation using mud from Markermeer. The second aims at converting dredged mud from harbours into clay suitable for dike and foreshore reinforcement.

The presentation will address the questions about availability and application techniques. These include the sensitivity of consolidation and ripening (i.e. densification and soil formation in unsaturated conditions) to cohesive sediment properties, deposition rate and local hydrological and meteorological conditions. Also, uncertainties and open questions with regard to observations and modelling are identified to steer further research.

15th INTERNATIONAL CONFERENCE on
COHESIVE SEDIMENT TRANSPORT PROCESSES
13 - 17 OCTOBER 2019 • ISTANBUL / TURKEY
YILDIZ TECHNICAL UNIVERSITY - YILDIZ CAMPUS

INTERCOH - Intertidal & Subtidal Areas

Fig. 1. Aerial view of Markerwadden (left) and Kleirijperij (right) pilot sites in the Netherlands. The yellow lines represents 1000 m in the left panel and 500 m in the right panel.

INTERCOH - Measurement Techniques

O1053 - COMBINED CURRENT PROFILING AND BIOLOGICAL ECHOSOUNDING RESULTS FROM A SINGLE ADCP
Measurement Techniques

Cristobal Molina [1], Herman Huitema [1], Sven Nylund [2], David Velasco [2]
Nortek, Sales, Rud-Norway [1] Nortek, R&d, Oslo-Norway [2]

Abstract
The present work describes a newly-developed Acoustic Doppler Current Profiler (ADCP) that has a fully integrated single-beam wide-band biological echosounder, thus serving a dual purpose: current measurement and biomass assessment. The system comprises a traditional 4-beam Janus configuration head, which is responsible for profiling the currents, with a vertically oriented center beam for collecting high-resolution acoustic backscatter data for subsequent biomass analysis. The system belongs to the Signature Series family of ADCPs launched in 2013 by Norwegian scientific instrumentation company Nortek. Named Signature100, it is powered by the AD2CP electronics platform, described in United States Patent 7.911.880. The four slanted beams (current profiling beams) operate at a center frequency of 100 kHz and have a range of up to 400 m with 4 m spatial resolution and sampling rate up to 1 Hz. The center vertical beam (echosounding beam) has a wider frequency band of approximately 70-120 kHz with a high dynamic range (~130 dB), and presently operating in up to three discreet pulse characteristics from a single beam set: 1) 70 kHz monochromatic, 2) 120 kHz monochromatic, and 3) 91 kHz chirp with 50 percent bandwidth and pulse compression. Acoustic pulses from the echosounder beam are interweaved with pulses for the current profiling beam for synchronous data collection. In this work we describe the system's configuration, capabilities and results from initial trials.

Keywords
echosounding, ADCP, currents, biomass

I. INTRODUCTION

The continual global increase in human population is prompting governments to assess protein sources with greater detail. Global demand for animal-derived protein is expected to double between now and 2050 [1], driven by increasing urbanization (especially in emerging economies), improved recognition of protein's role in a healthy diet, and increased need for protein in the elderly community. Fish stocks are one source of animal-derived protein which is receiving considerable attention due to their potentially vast contribution to addressing global protein requirements. In fact, global fish production far surpass the production of all other animal protein in the world, and fish also contain many essential micronutrients, minerals and essential amino acids [2].

Fisheries scientists use a variety of tools in understanding the structure, dynamics, function and quantity of fish stocks. Acoustic technology (in the form of biological echosounders) is widely used in quantifying fish stock biomass volumes and their behavior. Acoustic technology (in the form of ADCPs) has also been used to accurately measure currents in all of the world's major water bodies over the last 30 years.

As ADCP and echosounder data complement each other well, they are often used in the same project and deployed together. However, these two technologies have historically been developed by separate companies, with different objectives, leaving the end user to integrate

INTERCOH - Measurement Techniques

the two solutions together. Nortek's approach has been to leverage its expertise in underwater acoustic technology, transducer manufacturing, electronics and firmware architecture design to combine these two tools into a single instrument. This reduces the complexity of the system, increases the ease of use to the operator (data are precisely synchronized) and drives down cost as a single instrument can do the job of two.
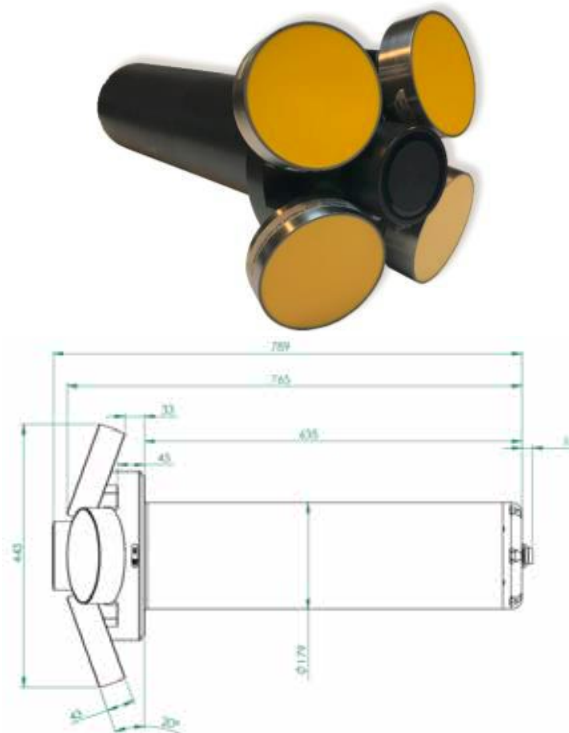

Fig. 1. Nortek's Signature100 ADCP. The four yellow transducers are responsible for measuring the currents. The center black transducer is a biological echosounder. All dimensons in mm.

II. SYSTEM DESCRIPTION

A. Core AD2CP Functions
Powered by the AD2CP platform [3], the Signature100 (Fig. 1) belongs to Nortek's Signature Series family of Doppler profilers, which presently span operating frequencies from 1000 kHz to 55 kHz. Although some application-oriented features are unique to just some of the Signature Series systems, there are several elements common to all of them:

- Current profiling using proper Broadband processing, with frequency coding of the transmit pulse as opposed to phase coding, thus providing improved configuration flexibility.
- Concurrent Mode Technology (described under US Patent 7.911.880), allowing for different types of pings to be collected at the same time (within measurement interval).
- Support for vertical beam operation independent of velocity beams.
- Ethernet communication, allowing for high bandwidth communication and support of standard network protocols (HTTP, FTP, UDP, PTP, and Telnet).

- Automatic recording of raw magnetometer data, enabling post-deployment compass calibration.
- Large memory bank (presently up to 128 GB) for extended deployment time as well as ability to record high volume data such as multiple echograms.
- Significantly reduced power consumption, owing to modern electronics, high efficiency transducers, and intelligent firmware architecture.
- External LED indicator for visual confirmation of instrument's status.
- Support for internal high-accuracy Attitude and Heading Reference Sensor (AHRS) for real-time bin mapping in dynamically moving installations, such as surface buoys.

B. Dual Purpose Applications

The above characteristics come together in the two key functions of the Signature100: current profiling and biological echosounding. The current profiling (traditional ADCP) portion of the Signature100 is comprised of four slanted beams in a Janus configuration, operating at a center frequency of 100 kHz, with 6.1° beam width. These can profile currents over a range of up to 400 m with 4 m spatial resolution and sampling rate up to 1 Hz. The biological echosounder portion of the instrument is comprised of an independent center beam with a wider frequency band (70-120 kHz), a high dynamic range of approximately 130 dB, a beam angle of 15° at 70 kHz and 8.7° at 120 kHz and maximum output power of 120 W. This center beam can ping at the same rate as the velocity beams and also reach the same full range (400 m). When both current profiling and biological echosounding are used together, it is expected that the Signature100 can last one full year with standard battery power options in a typical configuration.

C. Novel Transducer Design

Traditional ADCP transducer stacks are generally comprised of three main parts: a piezoelectric ceramic, a matching layer at the front, and damping material on the back. These are encased in a cup-like housing. This housing acts to support the transducer stack and connect it to the ADCP body, but otherwise plays no active part in the acoustic performance of the entire assembly. The Signature100's slanted (current profiling) transducers are unique in the ADCP industry in that all mechanical parts in the transducer design, including the cup, actively contribute to its acoustic performance and efficiency. This approach allows the entire assembly to have a depth rating of at least 1500 m yet have a total thickness of only 43 mm, never before achieved on an ADCP of this frequency (100 kHz).

In addition to the novel design, the piezoelectric element used in the Signature100 slanted transducers are composite broadband ceramics, rather than solid disks often used on ADCPs. Although not unique to the Signature100 (Nortek's Signature55 also uses composite broadband ceramics), they are made by dicing standard ceramics and filling with a special epoxy resin. This process increases the final transducer's sensitivity while maintaining a wide usable bandwidth, two critical parameters in determining the system's ultimate profiling range, flexibility and power efficiency.

D. Echogram Processing for Wideband Chirp

The main function of the center single-beam transducer in the Signature100 is to record echograms that provide information on the structure and dynamics of marine biota. Echograms can be generated from up to three different pulse types: 1) 70 kHz monochromatic, 2) 120 kHz monochromatic, and 3) wide bandwidth (50%) linear chirp ranging from 68 kHz to 113 kHz centered at 90.9 kHz. The monochromatic pulses are

15th INTERNATIONAL CONFERENCE on COHESIVE SEDIMENT TRANSPORT PROCESSES
13 - 17 OCTOBER 2019 • ISTANBUL / TURKEY
YILDIZ TECHNICAL UNIVERSITY - YILDIZ CAMPUS

INTERCOH - Measurement Techniques

processed internally using standard algorithms, but the chirp can be processed in one of two ways: using pulse compression or using a binned frequency response. The pulse compression technique is widely used in echosounder applications and it allows for increased range resolution as well as improved Signal-to-Noise Ratio (SNR). The resolution after pulse compression is 1.65 cm, and the internal processing can average this into a minimum bin size of 37.5 cm. In the binned frequency response method, the return is processed into five separate echograms each containing approximately one fifth of the total bandwidth.

In this work, the Signature100's echosounder beam was not calibrated for absolute backscatter. However, Nortek is developing a process to allow operators to perform this calibration such that accurate Volume Backscatter Strength (Sv) and Target Strength (TS) can be computed. As such, all backscatter data presented here is relative to the instrument itself and reported as SNR in decibels (dB).

E. Raw Return Signal Storage

In order to expand the system's flexibility, the Signature100 is able to store the complex demodulated return signal. The system allows storage of the in-phase (I) and quadrature-phase (Q) components of the return signal at 45.45 kHz (50% of the center frequency). Additionally, the system can also store the transmit pulse for a complete data set. Despite the system having a large memory bank, recording of raw demodulated signal can surpass the memory's limits, so a configurable recording scheme is implemented. The operator can specify the spacing between the pings or their interval (e.g. store every Nth ping, or all pings for N minutes every hour). The ability to store the raw return signal allows the operator to post-process the data using whatever technique is most suitable for their particular application, as well as perform post-processing calculations for TS and Sv.

III. FIELD VALIDATION

Field trials have been done as part of the Signature100's development, and here we highlight one such deployment carried out in the Mediterranean Sea. The location was just south of Toulon, France, and the deployment lasted from the morning of 10/Nov/2017 until the afternoon of 15/Nov/2017. Water depth at the site was about 470 m and the instrument was mounted up-looking on a subsurface buoy at the top of a short mooring. Raw heading data from the Signature100 (not shown) indicates the buoy observed a strong spin moment on its 7 minute descent, rotating at about 3-4 revolutions per minute, which is not unreasonable during such deployments. For fixed installations (not this case), this spinning can be a source of raw magnetometer data allowing for compass calibration in post-processing. After about 3 hours on the bottom, the buoy stabilized and subsequent data shows the mooring was very stable throughout the rest of the deployment, with only a gentle rotation (less than one revolution every few hours) and a very minor variation in tilt (less than 1°).

A. Current Data

The ADCP portion of the instrument was configured to transmit 60 pings at 0.25 Hz, repeating the sequence every 5 minutes, with single ping data being recorded for quality control purposes. Current profiling was set for 60 depth cells of 10 m each (15 ms pulse) with a blanking distance of 1 m. Variable particle distribution in the water column caused the maximum usable range to oscillate from about 230 m to 420 m (beyond the instrument's specifications), especially during the first half of the deployment, as evidenced by the SNR data of the four slanted beams shown in Fig. 2. As expected, times of reduced SNR coincide

15th INTERNATIONAL CONFERENCE on COHESIVE SEDIMENT TRANSPORT PROCESSES
13 - 17 OCTOBER 2019 • ISTANBUL / TURKEY
YILDIZ TECHNICAL UNIVERSITY - YILDIZ CAMPUS

INTERCOH - Measurement Techniques

with lower along-beam signal correlation values, indicating limit of usable data which is taken at 50% correlation. But despite the variations in particle distribution, over 68% of the data is above this 50% correlation threshold.
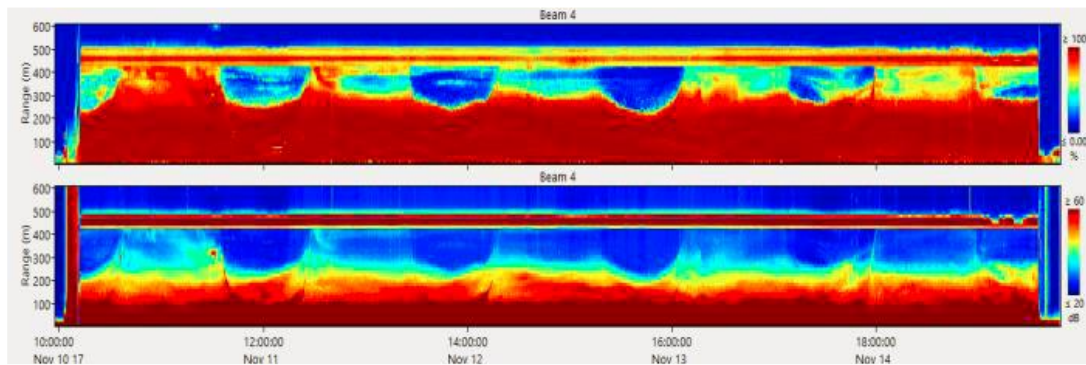

Fig. 2. Signal correlation (top) and SNR (bottom) from the slanted beams for the duration of the deployment.

A mid-depth current maxima is observed early in the deployment, although most of the fastest currents appear to be confined to the top of the water column (Fig. 3). Unfortunately these are not well captured some parts of the deployment due to limited quantity of scattering particles from about 300 m above the instrument, but can be seen during other times when increased particle distribution drives longer profiling ranges.
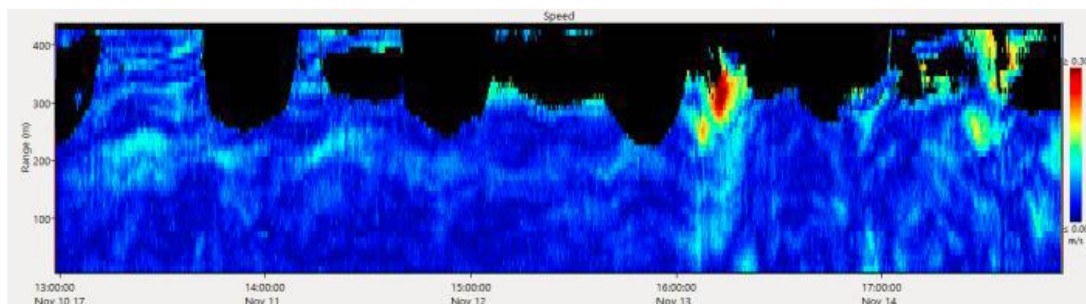

Fig. 3. Current speed for duration of deployment.

B. Echosounder Data
The echosounder portion of the Signature100 was configured to transmit all three pulse types supported, although only the 70 kHz monochromatic is presented here. Each pulse had a 1 ms transmit duration and were transmitted at 1 Hz. The echosounder pulses interweaved with the current profiling pulses at a ratio of 3:1 (i.e. every three echosounder pings to one current profiling ping). The echosounder pulses' return was recorded in 0.75 m depth cells.

From the echosounder data (Fig. 4) it is possible to identify schools of fish, swarms of smaller organisms (krill and/or zooplankton) and even individual fish. Although the present lack of a calibrated return signal prevents calculation of Sv, insights about the distribution, structure and presence/absence of biota over time and depth can be drawn from this deployment. Additionally, echograms coupled with interweaved current profiles into a single system provide valuable information on the behavior marine life.

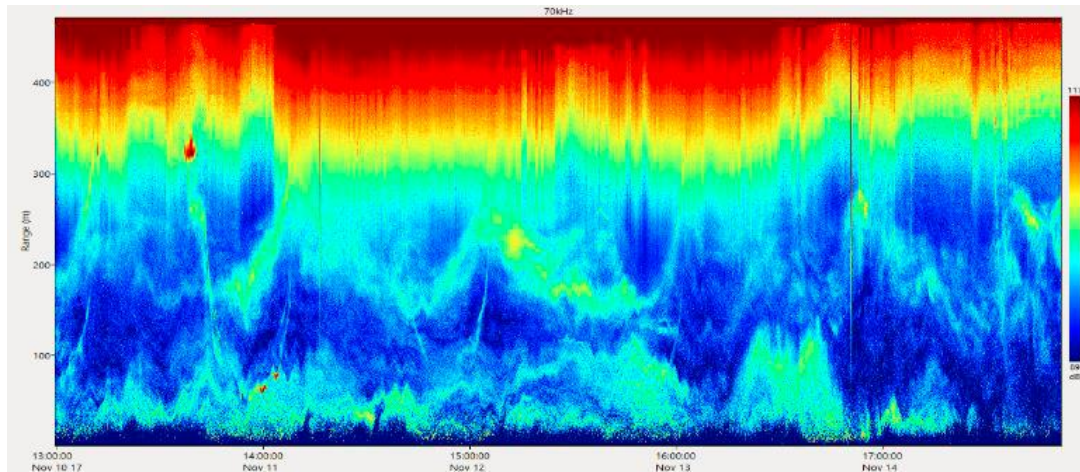**INTERCOH - Measurement Techniques**

Fig. 4. Echogram from 70 kHz monochromatic pulse for duration of deployment. Scale is relative to instrument (not Sv) in dB. Closer details are provided in subsequent figures.

Four different features were selected from the echogram for presentation: plankton/krill diel migration, internal wave structures, passing surface vessels, and migration due to changes in current regime. The first type of feature is shown on Fig. 5. Although no trawling was conducted during the deployment to ground-truth the nature of the scatterers, it is reasonable to assume the features shown represent either plankton or krill (or both) migration, as the same patterns are widely observed in similar data [4]. The diel nature of the movement drives measurable vertical currents of approximately 5 cm/s upward during dusk hours, with the reverse pattern at dawn.
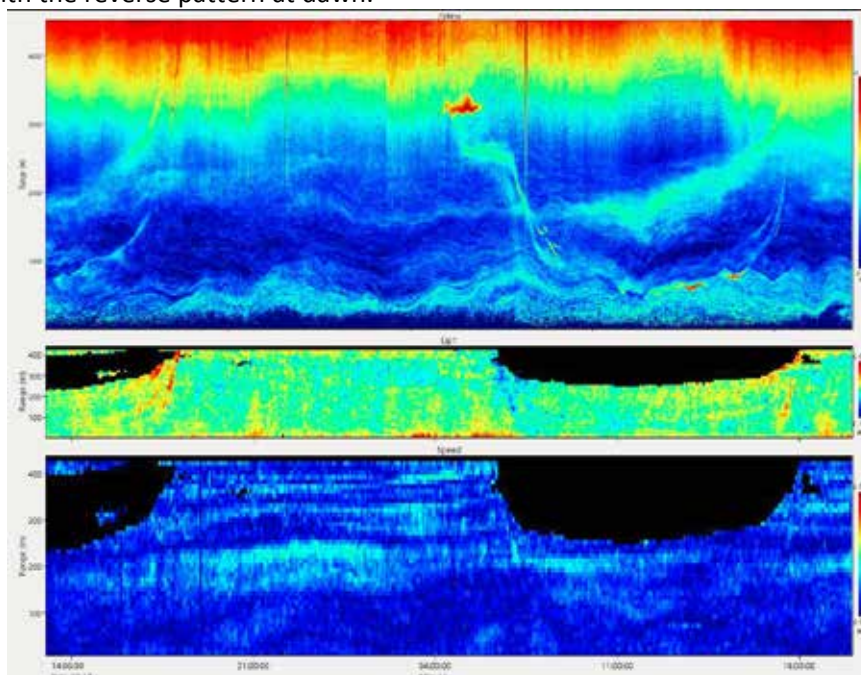

Fig. 5. 70 kHz Echogram (top), vertical velocity (middle), and horizontal current speed (bottom) for the first two days of the deployment.

INTERCOH - Measurement Techniques

Another interesting feature identifiable in the echograms are internal oscillations at varying depths and lasting up to a few hours. The echogram on Fig. 6 clearly shows their presence, distribution and duration. Internal waves are a common feature in the Mediterranean Sea, being described as earlier as the 1960s [5]. They are generated by the interaction of the mostly semidiurnal tidal flow with the variable bottom bathymetry and especially through narrow passages such as the Straits of Gibraltar and others. For the sample shown, it is estimated that some of these reach 10-15 m in height with periods of approximately 90 minutes. Although the spatial resolution of the current data (10 m depth cells) does not allow for as clear identification of these oscillations as the echogram does, nevertheless we can approximate a downward and upward velocity of about 1 cm/s with the passage of this particular event.
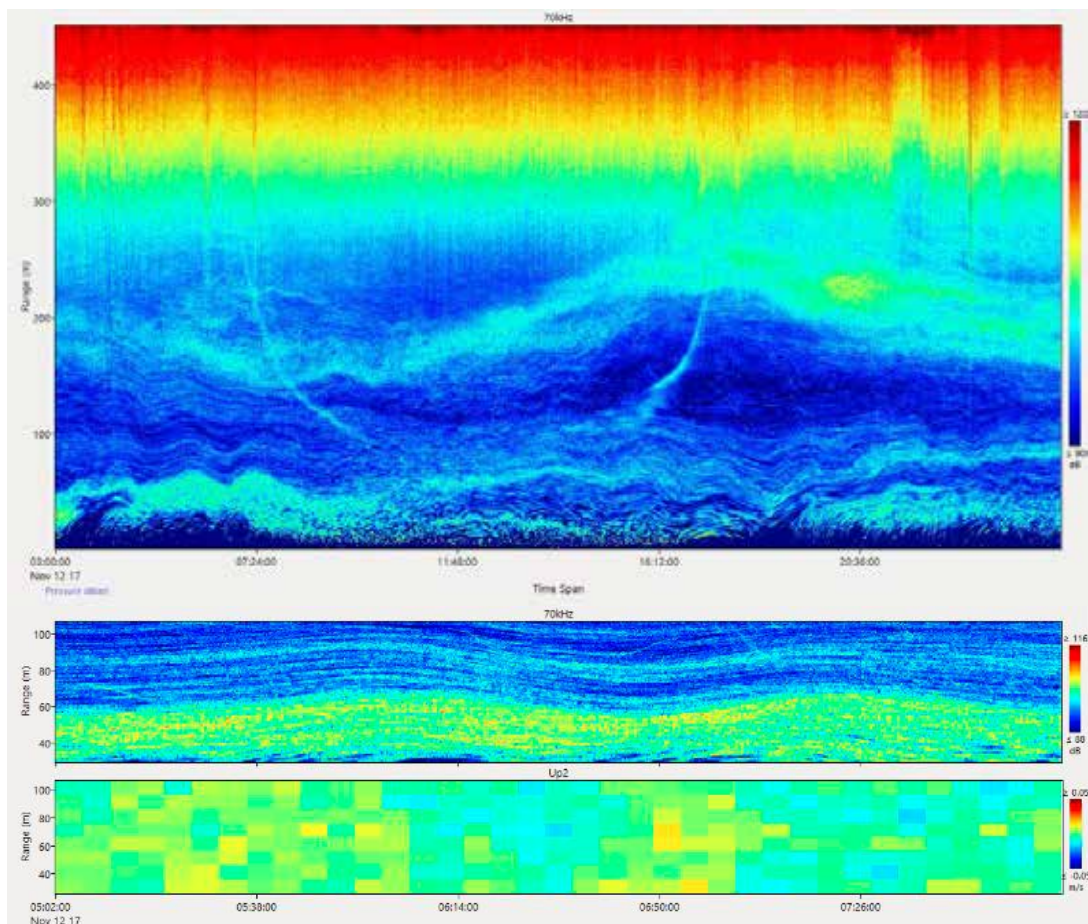

Fig. 6. Internal oscillations observed 70 kHz echogram on 12/NOV/2017 (top). Inset is a particular structure showing the echogram (middle) and the vertical velocity (bottom).

Following the terminology of [5], undesirable echogram features (noise) can be divided into three main categories: Impulsive Noise (IN), Transient Noise (TN), and Background Noise (BN). IN occurs over less than one acoustic ping and can often be traced to interference from a nearby acoustic source of same or similar frequency. TN can last several pings and have variable sources, such as ships passing near the echosounder (for fixed systems) or waves colliding with the vessel's hull (for vessel-mounted systems). BN lasts for hours or longer and may be traced to any continuously generated signal of same or similar frequency, such as an

INTERCOH - Measurement Techniques

underwater turbine. Fig. 7 shows both IN and TN from what we interpret as a passing surface vessel. The TN reaches almost the entire profiling range of the instrument, with increasing attenuation with depth, an inverted arch pattern typical of a single strong reflector, followed by increase near-surface noise in the vessel's wake. The echogram also suggests the vessel had an active acoustic source onboard, as IN features are clearly visible in the leading and trailing edges of the main signal.
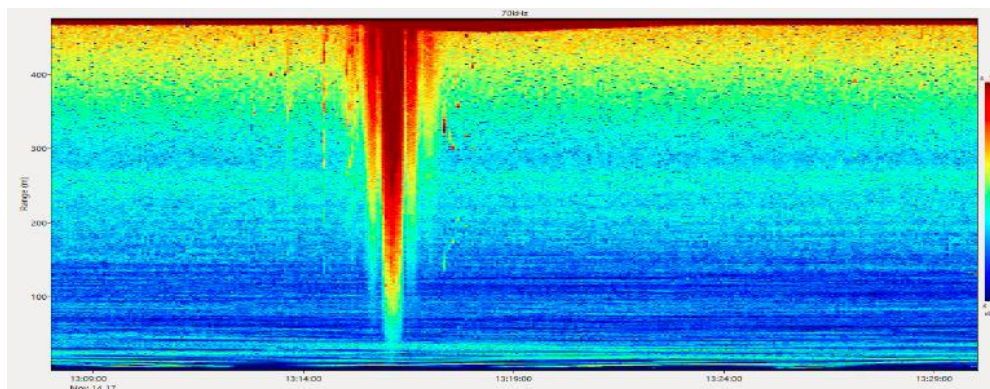

Fig. 7. Echogram showing the passage of a surface ship.

The echogram data also captures a change in the near-bottom activity, which is correlated with a change in current direction near the bottom (Fig. 8). Starting around midday on 14 November, and lasting through the end of the deployment, the echosounder returned signal strength first increased within the bottom 100 m of the water column, and then it diminishes noticeably. Overall currents speeds around this time indicate negligible change (not shown). Although the data is inconclusive as to the reason for this reduction, the correlation with the relatively sudden change in current direction may be a driver. For the 30 hours preceding this change, the mean current direction at 50 m above the instrument was holding relatively steady towards the SSE, but then changed (over the course of less than 3 hours) to flow primarily to the NNW, following some further variations over the subsequent 24 hours. This means that currents that were flowing mainly from the continent switched to flow mainly from the open Mediterranean Sea. It is therefore speculated that this change impacted the local biota, shifting its location towards the continent, away from the instrument.
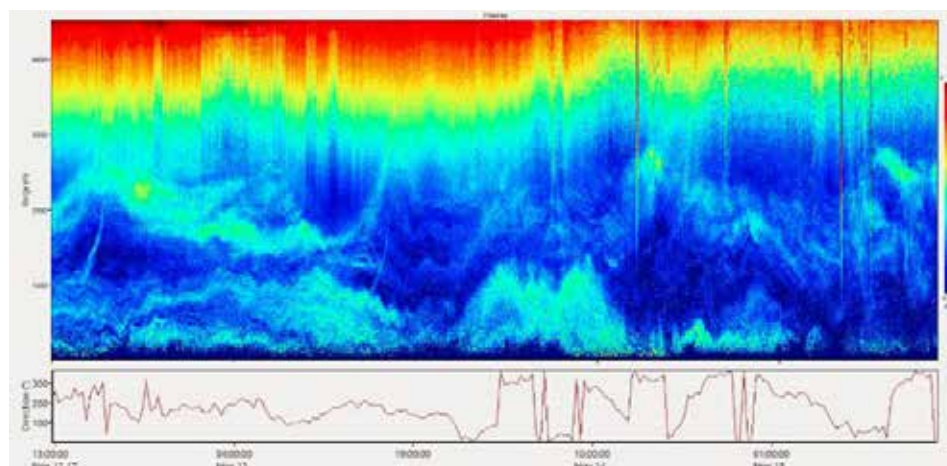

Fig. 8. 70 kHz echogram for second half of deployment (top) and current direction at 100 m above the instrument (bottom).

15th INTERNATIONAL CONFERENCE on COHESIVE SEDIMENT TRANSPORT PROCESSES
13 - 17 OCTOBER 2019 • ISTANBUL / TURKEY
YILDIZ TECHNICAL UNIVERSITY - YILDIZ CAMPUS

INTERCOH - Measurement Techniques

IV. CONCLUSIONS

A newly-developed Acoustic Doppler Current Profiler (ADCP) with a fully integrated single-beam wide-band biological echosounder has been developed and presented. The system belongs to the Signature Series family of ADCPs launched in 2013 by Norwegian scientific instrumentation company Nortek and is powered by the AD2CP electronics platform (US Patent 7.911.880). Named Signature100, it performs two key functions simultaneously over a maximum nominal range of 400 m: current profiling and biological echosounding. Some of its key features include a novel transducer design, three distinct echosounder pulse types, data processing with pulse compression, and the capability of recording the complex demodulated return signal. Details from a field validation deployment in the Mediterranean Sea were presented, with a focus on the 70 kHz echogram created by the instrument. Four main features of the echograms were discussed: plankton/krill diel migration, internal wave structures, passing surface vessels, and migration due to changes in current regime. The current profiling data complemented the echosounder data, providing greater insights into the distribution, structure and behavior of the marine life at the test site during the deployment.

REFERENCES

[1] World Bank. Fish to 2030 Prospects for Fisheries and Aquaculture. World Bank Report No. 83177-GLB. Washington, DC, 2014.

[2] C. Béné, M. Barange, R. Subasinghe, et al., "Feeding 9 billion by 2050 – putting fish back on the menu," Food Security, vol. 7, issue 2, pp. 261-274, April 2015.

[3] A. Lohrmann, S. Nylund, "A New Long Range Current Profiler, Development of the Signature75," MTS Oceans Conference 2013, San Diego, CA.

[4] C. Winant, T. Mettlach, S. Larson, "Comparison of buoy-mounted 75-kHz acoustic Doppler current profilers with vector-measuring current meters," J. Atmos. Oceanic Tech., vol. 11, pp. 1317-1333, 1994.

[5] J. Ziegenbein, "Short internal waves in the Strait of Gibraltar," Deep Sea Research and Oceanographic Abstracts, vol. 16, issue 5, pp. 479-482, November 1969.

[6] T. E. Ryan, R. A. Downie, R. J. Kloser, G. Keith, "Reducing bias due to noise and attenuation in open-ocean echo integration data," ICES Journal of Marine Science, vol. 72, issue 8, pp. 2482–2493, October 2015.

INTERCOH - Morphodynamics

O1022 - INCORPORATING WEIGHTING FACTOR OF FIELD OBSERVED MORPHOLOGICAL CHANGES TO SIMULATE SEVERE SEDIMENTATION UNDER FLOOD DOMINANT ENVIRONMENT Morphodynamics

Seung-won Suh [1], Hyeon-jeong Kim [1], Sang-cheol Yoo [2], Ike-jang Ann [3], Ki-jae Lee [3], Won kyung Park [4]
Kunsan National University, Ocean Science And Engineering, Kunsan-Korea, South [1] The Sea-born Experts, , Kunsan-Korea, South [2] Hyein Engineering And Construction, , Seoul Korea, South [3] Dae Young Engineering Corporation, , Seoul-Korea, South [4]

In the west coast of Korea (WCK), macro-tidal areas with a mean spring tidal range of 8 m and a mean depth of 10 m dominate the tidal hydrodynamics and affect coastal sedimentation. In addition, diverse anthropogenic activities during the last four decades (Suh et al., 2014) have caused the tidal change, crossing the tipping point from an ebb- to a flood-dominant environment in the mid-WCK. This is where the study area including the small-sized Eoyoojeong harbor (EH) used by fishing boats is located. EH encountered severe sedimentation, 0.7 to 2.6 m/yr, with cohesive sediments being the predominant ones. Coastal anthropogenic development also yielded up to 2.0 m/yr of sedimentation along an estuarine harbor (Kunjang harbor, KH) after the closure of a dam in the Geum river estuary (Kim and Suh, 2017) in the mid-low region of the WCK. Both sites exhibit similar tidal asymmetry of flood-dominant environments and thus have encountered continuous sedimentation.

To investigate and predict sedimentation, both field observations and numerical simulations have been applied using the sedimentation model, EFDC. However, any numerical models have not been able to satisfactorily generate such large amounts of annual sedimentation because of limited model capabilities or inaccurate input parameters. Essentially, measured depth data, which involve diverse variations in the external force that are not fully incorporated in any sedimentation model, sometimes showed severe sedimentation of 3 m/yr. In a previous study on the KH (Kim et al., 2017), the shrunken bed shear force induced a reduced tidal prism owing to the construction of the estuarine dam construction. The study used extensive archives of depth measurements to assess the variations in the bottom shear stress. As a result, a correlation between annual sedimentation and the bottom shear stress was established and applied to a numerical model as an empirical factor to compensate for the inaccuracy in the simulation itself. This approach was applied in the KH with a weighting factor of 0.5 (0.15) for the empirical sedimentation rate and a numerical model factor of 0.5 (0.85), regarding bottom shear stress values greater than 0.8 (or below 0.2) (Kim et al., 2017). Thus, to account for site-specific conditions and to overcome the limitations of the morphological model, we needed to correct the optimized weighting factor to 0.5. However, the ratio of empirical to numerical simulation should be accounted for in accordance to local geological coastal hydrodynamic environments. Nevertheless, the combination of empirical weighting factors can be regarded as a reasonable attempt because even sedimentation models cannot completely account for real natural variation in hydrodynamic and sedimentation.

For the simulation of the EH, the domain is small compared to that used of the KH; thus, relatively small time steps should be applied in accordance with a very fine grid. The overall computational burden exponentially increases up to 48 h for a month-long simulation. Thus, it

INTERCOH - Morphodynamics

is highly recommended that an empirical formula of sedimentation rate be incorporated with regard to the bottom shear stress; this can be easily computed from any circulation model regardless of the grid resolution and time limitation. In this study, we built two grids: one for the large domain encompassing the Gyeonggi-bay and another nested finer grid considering the study area, EH, as shown in Fig. 1 (a). As nonlinear shallow tides are a major factor in tidal hydrodynamics in the mid-WCK (Suh et al., 2014), a total 10 tidal constituents (M_2, S_2, K_1, O_1, N_2, K_2, P_1, Q_1, M_4, and MS_4) were applied along the open boundary in EFDC simulations. Then, the simulated results were implemented as the input of the finer nested grid system.

Simulated results were obtained based on the empirical formula (Sedimentation rate= $1.72\ln(\tau) - 0.42$) correlating bottom shear stress (N/m^2) and sedimentation rate (m/yr), which were observed between 2015 to 2018 through EH field measurements, extracted by EFDC computations using a grid considering a wide region. The results indicated a correlation coefficient of 0.84 and τ_c of 0.79 (as shown in Fig. 1(b)) for the critical bottom shear stress for the study area. In order to account for this empirical formula, the study domain was divided into sub-sections, as shown in Fig. 2, where the bottom shear stresses for the computational grids were normalized to each section to obtain representative sedimentation rates for those sub-sections.

The computed results based on this approach showed up to 3 m/yr of sedimentation, particularly in front of the EH dock area. This trend is almost consistent with the sedimentation observed around the study area. Thus, the proposed scheme can be satisfactorily applied to other areas regardless of the model grid resolution or uncertainty in input parameters. However, determination of the site-dependent optimized weighting factor should be further investigated to derive overall formulas.
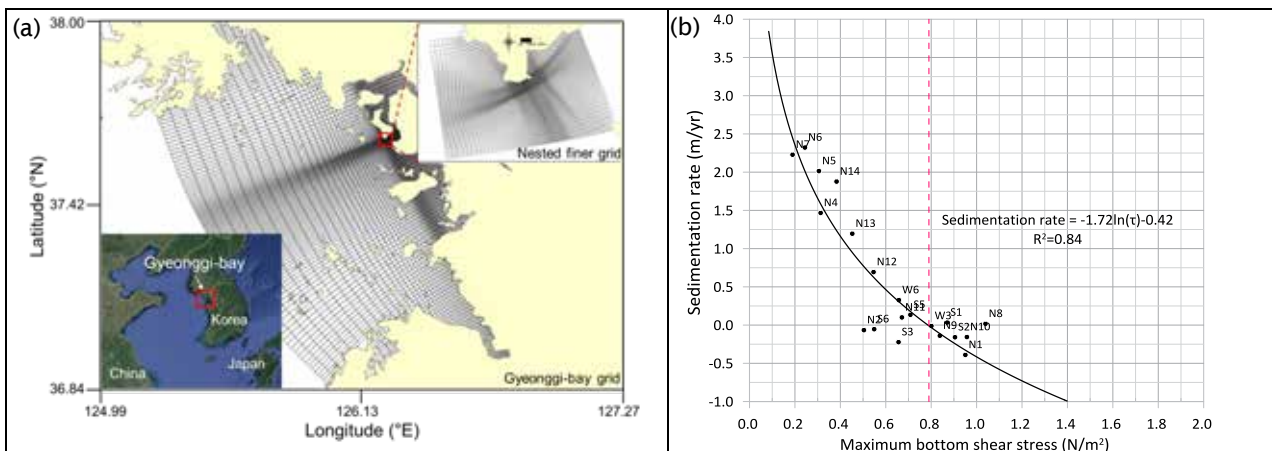

Fig. 1. (a) Study area with curvilinear grids and nested domain with finer grids, and (b) sedimentation rate vs shear stress.

INTERCOH - Morphodynamics

O1035 - SMALL SCALE BEDFORM PATTERNS UNDER COMBINED FLOW IN THE GEDIZ RIVER MOUTH TURKEY
Morphodynamics

Sinem Oguz Kaboglu [1], Gokhan Kaboglu [1], Dogan Kisacik [1]
Dokuz Eylul University, Institute Of Marine Sciences And Technology, Izmir-Turkey [1]

Improving knowledge on bedforms in combined flow areas is important for a more realistic determination of sediment transport. This knowledge will also contribute to define river-sea interactions and depositional sedimentary environments. Although there are many studies about bedforms, the findings (e.g. prediction formulae, phase diagrams) are still in conflict with each other and more research is needed. On the other hand, the combined flow condition is the least studied subject when compared to other flow conditions (oscillatory and unidirectional).

We analyzed the bedforms and related hydrodynamic conditions in the Gediz River mouth, in the Izmir Bay (middle of the Turkish Aegean coast). Field measurements were carried out in two periods (July and October 2017) in order to present rainy and dry season conditions. Bedform observations were conducted by diving and sample photographs were taken at each station. Sediment samples were collected by grab and then analyzed in order to obtain seabed surface sediment compositions. The current measurements were made at three stations during each field study. Furthermore, long-term wind measurement was made to determine the wave parameters of the study area. Additionally, stationary CTD (Conductivity, Temperature, Depth) measurements were performed to define the physical parameters of seawater. After obtaining the necessary parameters, several prediction formulae (e.g. Khelifa and Ouellet, (2000); Soulsby, Whitehouse, and Marten, (2012)) and phase diagrams (e.g. Kleinhans, (2005); Perillo, Best, and Garcia, (2014)) were tested by using these parameters. In this study, we present only the results of the combined flow phase diagram of Kleinhans (2005), which was produced by a large dataset.

The Gediz River mouth has a shallow and wide pro-delta area (0.5-12.5 m). Study area shows a cohesive characteristic with an average of 29.5% clay proportion. Low unidirectional flow velocities (0.03-0.07 m/s) were measured and about 1 m wave heights were obtained from the SWAN model by using measured wind data. Calculated oscillatory flow velocities were 15 times higher than the measured unidirectional flow velocities in the area. The angles between river flow direction and the significant wave direction in rainy and dry seasons were 220° and 255°, respectively.

Both ripples and plane beds were observed in the study area. The ripples were small and located where the sand proportion was above 70%. These ripples had both 2D and 3D planform geometries (Fig.1 a & b) and were categorized as wave ripples. Based on the measured parameters, wave and current Shields values (Θw and Θc) in Kleinhans, 2005 (formula (13)) were plotted on the combined flow phase diagram, which was presented as Figure 7 in the same reference work. As shown in the Fig. 1 c, except for only one record, ripples at Gediz River

mouth are located in 'wave only' hydrodynamic region. This is mainly due to the low flow regime of the Gediz River during study periods. Although this result was as expected, the majority of the plotted data stands out of the border of the Upper Stage Plane Bed (USPB). The referred phase diagram was created according to the criteria for sediment grain size D=0.21 mm. However, the seabed sediments of the study area had an average of D=0.007 mm, with a max value of D=0.03 mm. Despite other possible effects, the reason for this situation is concluded to arise from this variation in the sediment grain size D. Thus, our further research will focus on testing parameters affecting ripple generation and their representation in existing phase diagrams, with enlarged in-situ datasets (e.g. Büyük Menderes River mouth). We will additionally integrate our results of in-situ bedform measurements, such as ripple dimensions and calculated ripple indexes, in order to classify the bedforms and enhance our assessments.

INTERCOH - Morphodynamics

O1041 - EVALUATING THE EFFECTIVENESS OF SEDIMENT RECYCLING WITHIN THE STOUR ORWELL ESTUARY SYSTEM
Morphodynamics

Tom Benson [1], Jeremy Spearman [1]
Hr Wallingford, Coasts & Oceans, Wallingford-United Kingdom [1]
Email: t.benson@hrwallingford.com

Management of port development is increasingly challenging because of the competitive requirement for deeper channels and because of the need to preserve important coastal wetlands which function as both habitat and flood defence. These twin pressures are encouraging coastal developers to consider so –called "building with nature" development solutions which achieve the desired development whilst enhancing the
natural environment.

The present paper investigates the efficacy of a sediment recycling approach to offsetting the predicted effects of channel deepening in the Stour/Orwell Estuary system, a system which has experienced considerable historic development and morphological change. The estuary system is internationally important for its wetland bird populations and the intertidal areas of the estuary system are protected under European legislation. It is also the location of the Port of Felixstowe which is the biggest container terminal in the UK. In 1998/2000 the approach channel to the Port of Felixstowe was deepened from -12.5 m to -14.5 m below Chart Datum (CD). To offset the anticipated effects of the deepening on estuary habitat, mitigation was implemented in the form of sediment recycling (Figure 1).
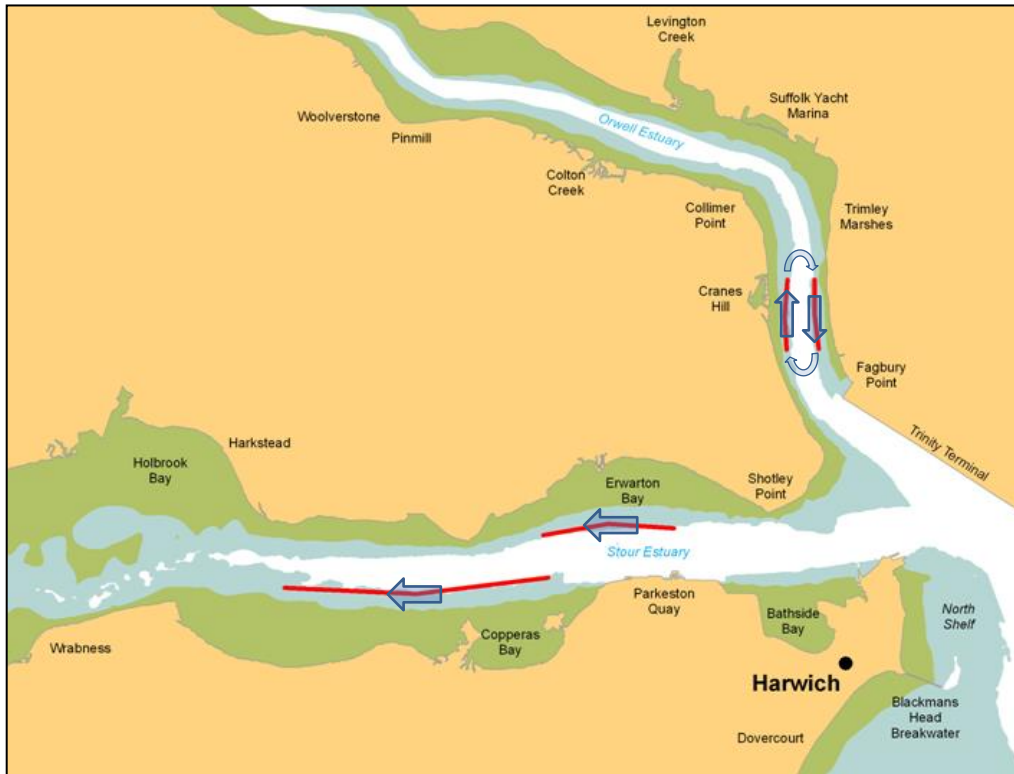
Figure 1 Sediment recycling locations and movement of dredging during placement
Sediment recycling has been undertaken by the developer, Harwich Haven Authority (HHA), over the 20 years since the deepening. Detailed monitoring has allowed HHA to evaluate the evolution of the estuary system over this period – which has shown a significant change in the evolution of intertidal areas, from that of erosion to accretion.

A 3D morphological model of the Stour/Orwell system was developed and calibrated based on ADCP transects of flow and sediment, 5 yearly bathymetric/LiDAR surveys and detailed dredging records. This calibrated model was used to evaluate the effectiveness of the sediment recycling strategy.

The modelling confirmed that the sediment recycling strategy has not only offset the adverse impact of the capital dredge on intertidal area but has caused a significant further increase in intertidal area, indicating that both development and nature enhancement had been achieved.

INTERCOH - Morphodynamics

O1063 - LONG TERM EVALUATION OF SEDIMENT DYNAMICS IN THE SAKARYA RIVER DELTA COAST
Morphodynamics

Cihan Sahin [1], Mehmet Ozturk [1], H. Anil Ari Guner [1], Yalcin Yuksel [1], Ahmet Altunsu [1], Ilgar Safak [2]

Yildiz Technical University, Department of Civil Engineering, Istanbul-Turkey [1] University of Florida, Department of Civil And Coastal Engineering, Gainesville-United States [2]

Karasu Beach is located in the southwestern Black Sea (100 km east of Istanbul) and impacted by the Sakarya River plume. The shoreline has a WNW–ESE general orientation and stretches approximately 30 km to the west side and 50 km to the east side of the Sakarya River mouth. River discharge and energetic wind and wave climate are among the major physical processes that control the sediment transport pattern along the shoreline and cause formation of natural beach areas with dunes behind. Sands of the inner shelf display a seaward-fining texture and show a cohesive behavior in deep areas. The series of large volume reservoirs along the Sakarya River stream, related to hydroelectric power stations, reduces the sediment runoff and the input of sediment into the Sakarya River mouth. Due to the decrease of the sediment runoff to the coast, and also a construction of a harbor at the west side of the river mouth, significant erosion occurred at the east side of the river, with the 7.5 m/yr year retreat of coastal line. The erosion problem threatens the coastal area and also the Acarlar Floodplain Forest at the west side of the river behind the dunes on the coast which support a very rich ecosystem.

In this study, wave, current, and sediment dynamics along the Karasu coastline are investigated using field observations and numerical model results. The field campaigns were conducted in the vicinity of the Sakarya River region of influence, covering different meteorological and hydrological conditions, and therefore allow for observations under different forcing conditions. Two shipboard surveys were conducted in February and July 2019 and consisted of three transects (one cross-shore and two longshore transects) around the Sakarya River mouth. Measurements of waves, vertical structures of currents, turbidity, temperature, and salinity were collected. The CTD and turbidity probes were lowered at 0.2–0.4 m/s, covering the entire water column. The CTD and turbidity downcast data were averaged in 0.5 m bins. An upward-looking ADCP at 20 m measured waves and the profiles of current and backscatter continuously at 2 Hz for one week in each campaign.

Waves, hydrodynamics, and sediment processes were modeled using the MIKE modeling suite. The model domain is the Black Sea closed basin between 27.62°-41.78°E and 40.97°-46.68°N. The numerical wave model used in this study is the MIKE 21 Spectral Wave (SW) model, a new generation spectral wind-wave model based on unstructured meshes. Waves between 1978 and 2019 were modeled within a coarse-resolution grid that covers the closed Black Sea basin, by using the wind fields obtained from the ECMWF (European Center for Medium-Range Weather Forecasts) and calibrating with the measured wave conditions. The evolution of the wave climate in the last 41 years was evaluated. Mike 3 Flow Model FM and Mike 21 ST coupled model were used for modeling the hydrodynamics and sediment processes along the Karasu coastline. A higher-resolution grid that covers the Karasu nearshore region was nested in this Black Sea grid and forced with waves at its boundaries. After calibrating this grid also using the

in-situ measurements of waves, hydrodynamics and sediment processes, the model setup is being run over decadal scales for evaluating the long-term sediment transport patterns of the region. The results will be used to investigate to respective impacts of climate-change associated and the anthropogenic influences.

INTERCOH - Mud Rheology and Fluid Mud

O1067 - ASSESSMENT OF MORPHOLOGICAL CHANGES BY TSUNAMI ATTACK; A CASE STUDY FOR IZMIR BAY

Gozde Guney Dogan [1], Isikhan Guler [1], Ahmet Cevdet Yalciner [1]

METU Civil Engineering Ankara-Turkey [1]

Recent tsunami events (September 2018 Sulawesi and December 2018 Sunda Strait Tsunamis) reminded the coastal communities of the extent of destruction on coastal facilities as well as morphological changes by tsunami waves. Water motion related to long waves (tidal wave, storm waves and tsunami) in shallow water zone, especially inside the ports and basins, cause sediment movement. Tsunamis can carry considerable amount of sand and erosion and/or deposition on harbors which reduce the port functions and also influences the safety of maritime traffic. In the case of tidal wave, the morphological changes take long time whereas the change occur in a short time during the tsunami action.

In this study, the sediment transport and morphological changes due to long wave action in Izmir Bay are investigated and discussed. Izmir bay, which is located in Aegean coast of Turkey, is particularly selected due to several reasons. The region is prone to earthquakes and tsunamis because of the nearby active fault zones and their recent activities. There is an active shoaling process in the basin due to the alluvial material transported by Gediz River. The decrease in the circulation within the bay is also another reason for becoming shallower of the basin. The Izmir Harbor and its location in the inner basin make the area vulnerable against marine related phenomena for maintenance of proper and successful operations. Furthermore, there is a planned project of two channels planned to be dredged in order to facilitate the navigation and circulation in the bay (Figure 1). The navigation channel will be 12km long, 250m wide and 14m deep. The circulation channel is 13km long, 250m wide and 6m deep. All these sediment transport related issues necessitate a complete assessment of morphological changes in the region.

The study is performed by numerical modeling which is commonly used as an important tool to estimate the response and behavior of water motions. The possible effects of tsunamis and or long waves in terms of tsunami induced sedimentation and amplification effects in Izmir Bay are assessed by following the methods given in Pamuk (2014) and Kian (2015). First, the numerical model NAMI DANCE is utilized to determine the hydrodynamic parameters in Izmir Bay under long wave conditions as well as selecting the spatial and temporal changes of main tsunami parameters for Izmir region from Dogan et al. (2018). Then, the water level and current amplifications as well as current pattern variations are computed. After evaluation of the grain size distribution of sediment in the selected region to employ the settling velocity and hence Rouse number, the consequent morphological changes are determined in terms of instantaneous Rouse numbers during the simulations. Finally, the Rouse numbers computed are used to assess the morphological changes due to tsunami attack by identifying the transport modes of sediments. Thus, the critical locations for the sediment movement inside Izmir bay are determined. The possible morphological changes and their effects on the navigation in Izmir bay are also discussed.

Keywords: tsunami, long wave, sediment transport, rouse number, harbor, bay

References
Dogan G. G., Yalciner A.C., Kilic N., Yucemen S. (2018), "Tsunami Hazard Assessment for Izmir Bay, Turkey", 16th European Conference on Earthquake Engineering, Thessaloniki, Greece, June 2018.
Kian, R. O. Z. I. T. A. (2015). Tsunami Induced Wave and Current Amplification and Sedimentation in Closed Basins (Doctoral dissertation, Ph. D. Dissertation, Middle East Technical University, Ankara, Turkey).
Kian, R., Velioglu, D., Yalciner, A. C., & Zaytsev, A. (2016). Effects of Harbor Shape on the Induced Sedimentation; L-Type Basin. Journal of Marine Science and Engineering, 4(3), 55.
Pamuk, A. Y. K. U. T. (2014). Assessment of Inland tsunami parameters and their effects on morphology (Doctoral dissertation, MS Thesis, Middle East Technical University).

15th INTERNATIONAL CONFERENCE on COHESIVE SEDIMENT TRANSPORT PROCESSES
13 - 17 OCTOBER 2019 • ISTANBUL / TURKEY
YILDIZ TECHNICAL UNIVERSITY - YILDIZ CAMPUS

INTERCOH - Mud Rheology and Fluid Mud

O1005 - USING THE K OMEGA MODEL IN A HOLISTIC MODEL APPROACH

Mud Rheology and Fluid Mud

Andreas Malcherek [1], Oliver Chmiel [1], *Johanna Schmidt* [1]

University of The German Armed Forces Munich, Institute of Hydromechanics and Hydraulic Engineering, Neubiberg-Germany [1]

Abstract

In numerical models, it is difficult to precisely define the boundaries between fluid mud and a suspension on the one hand and fluid mud and consolidating mud on the other hand. It therefore seems favourable to employ a holistic simulation approach in which fresh water, suspensions, fluid and consolidated mud are simulated using one set of equations only.

One major challenge in this approach is the formulation of a turbulence model. While turbulence is apparent in a pure water flow, it is damped in stratified suspensions and non-existent in fluid and consolidated mud. In a holistic simulation model, the turbulence model should therefore be able to simulate free turbulence, turbulence damping, laminar rheological flow, as well as the absence of turbulence in consolidated mud.

This paper demonstrates that the kω-model can cope with such a demanding task. The lower boundary is chosen to be located in the consolidated bed, where no movement and therefore no turbulence is expected. At this boundary, the turbulent kinetic energy (TKE) is set to zero while ω is set to a constant large value. The turbulent kinetic energy thus remains zero and ω remains constant in the consolidated bed. This approach reveals that ω must be interpreted as a potential to dissipate TKE instead of an actual dissipation rate, as there is no TKE within the consolidated bed.

When a fluid mud layer is superimposed on the consolidated bed, the TKE there is also zero due to laminar rheological flow. In this case the simulation model calculates the effective viscosity of the mud according to its rheological properties. Finally, in the superimposed suspension, the turbulent viscosity is calculated by the turbulence model. Furthermore, a function is introduced, describing the transition from settling velocity to consolidation velocity.

In order to test this model approach, it is implemented in a 1DV-model. The vertical discretisation is realized by a non-equidistant formulation, which allows the water depth to vary over time. This procedure enables the implementation of frequencies, phases and amplitudes of tidal constitutes.

The simulation results show the ability of the kω-model to be used in a holistic model approach where pure water, suspensions, fluid mud as well as a consolidated bottom are simulated by one set of equations.
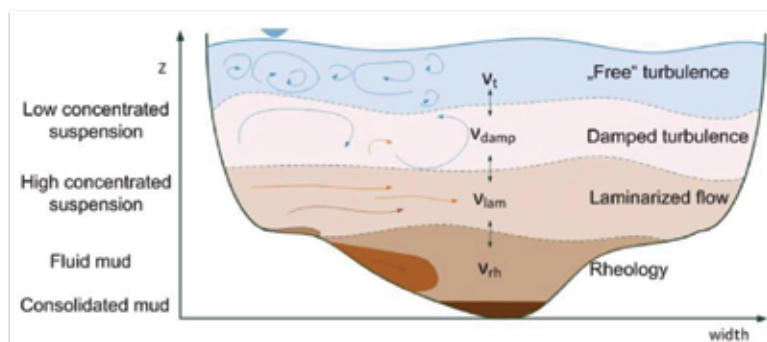
Figure 1: Scheme of the holistic model approach.

INTERCOH - Mud Rheology and Fluid Mud

O1008 - SEASONAL VARIATION OF FLUID MUD THICKNESS AROUND RIVER MOUTH IN NORTH WESTERN JAVA ISLAND INDONESIA
Mud Rheology and Fluid Mud

Yasuyuki Nakagawa [1], Bagyo Widagdo [2], Masayuki Banno [3], Gugum Gumbira [2], Taichi Kosako [3], Hitoshi Tamura [4], Dinar Istiyanto [2]
Kyushu University, Faculty of Engineering, Fukuoka-Japan [1] Bppt, Center of Technology for Maritime Industrial Engineering, Jakarta-Indonesia [2] Port and Airport Research Inst, Coastal and Estuarine Sediment Dynamics Group, Yogyakarata-Japan [3] Port and Airport Research Inst, Marine Information Group, Yokosuka-Japan [4]

Introduction
For the prediction of coastal bathymetry evolution around the river mouth delta, it is crucial to understand sedimentary process considering discharged sediment through the river. In case that fine sediment is dominant, the transport process becomes complicate with the formation of fluid mud, which may be an important role on the transport and distribution of muddy sediment. The present study focused on the seasonal variation of sediment discharge which may be a key factor for the deformation of the bathymetry around river mouth.

Field Measurement
The target site of the study is around the mouth of the Cipunagara river near the Patimban coast at the north west of Java island in Indonesia (Fig.1). At the monitoring points we located around the river mouth, we deployed several measurements for the vertical profiles of salinity and turbidity with a CTD censors, AAQ1183 (products of JFE-Advantech Co.), and an in-situ densimeter of XL-4, the product of Hydramotion Ltd., for the bulk density measurement through the water column including near bed fluid mud layer. Bottom sediment and suspended sediment sampling were also carried out and the current velocity measurement with the ADCP was also deployed at each monitoring points. The field works were carried out in February and August, 2017, as wet and dry season survey, respectively.

Measurement Results
By the bulk density measurements, it reads around 1,000 kg/m3 for fresh water layer and 1,020 kg/m3 for the sea water layer. For the near bed layer, the density increased up to 1,300 kg/m3 through 1,400 kg/m3 in the consolidated mud bed. Transient layer with the bulk density of 1,100 – 1,200 kg/m3 are apparently observed between the sea water and the consolidate mud layer and it is defined as so called fluid mud layer (e.g. Whitehouse et al. 2000). The measured profiles at the monitoring station at Stn B1, which is the nearest to the mouth of the branch of the Cipunagara Riv., are shown in Fig 2. It is noteworthy that three layers structure above the consolidated mud bed appears in the vertical profile of the bulk density in the wet or higher river discharged season, as indicated in Fig 2(a). The fresh water layer, however, does not appear in the dry season as in Fig 2(b) and fluid mud layer is thinner than that of measured in the wet season. Field surveys were carried out with monitoring of spatial distribution of suspended sediment and fluid mud in the estuarine system under a tropical climate environment with a wet and dry season.

INTERCOH - Mud Rheology and Fluid Mud

Summary

We successfully captured the difference between the wet and dry season in vertical structure of bulk density through the water column from the sea surface through consolidated mud bed. Observed data including the seasonal variation of fluid mud thickness can be applied for the modelling works of the fine sediment transport process in the target site, which is our future work.

References

Whitehouse, R., R. Soulsby, W. Roberts and H. Mitchener (2000): Dynamics of estuarine mud, Telford Publishing, 210p.

INTERCOH - Mud Rheology and Fluid Mud

O1013 - MEASURING MUD MONITORING NAUTICAL DEPTH AND FLUID MUD CONSOLIDATION IN THE PORT OF ROTTERDAM WITH SUB BOTTOM AND IN SITU RHEOLOGY PROFILING TECHNIQUES

Bart Ursem [1]
Stema Survey Services B.V. Poppenbouwing 52, 4191NZ Geldermalsen - The Netherlands[1]
E-mail: bart.ursem@stema-systems.nl

Keywords

Fluid mud; nautical depth; sub-bottom profiling; rheology; density; yield stress; Port of Rotterdam

Abstract

A long-term monitoring campaign in the Port of Rotterdam, the Netherlands, is used as a case study to emphasise combining sub-bottom and in situ rheology profiling techniques to solve fluid mud issues. This monitoring is performed by using a combination of the Stema EBP system and RheoTune and accompanying software suites. This study shows significant consolidation of fluid mud in both seismic and rheological data over the first three weeks after preliminary dredging. From four until ten weeks after dredging, almost no more subsidence of the top of the fluid mud layer and shallowing of the nautical depth occurred. Continuous imaging of the nautical depth in this fluid mud layer ensures safe passage of vessels and could lead to a considerable reduction of dredging volumes and costs.

Introduction

Safe vessel passage in harbours and their access channels is of vital importance for port authorities since it ensures secure navigation and manoeuvrability and therefore a stronger competitive position of harbours. Generally, harbours are areas where the nautical depth is affected by siltation. A further increase in harbour traffic and increase vessel draught over the last decade make accurate information on the nautical depth very imperative.

Traditionally, a combination of a singlebeam echosounder with a high frequency (~200kHz) and low frequency acoustic signal (15–38kHz) and multibeam echosounder (200–400kHz) is used to map the water–fluid mud interface and fluid mud–(pre-)consolidated mud interface. High frequencies are supposed to line up with multibeam data and the top of a fluid mud layer, whereas low frequencies should line up with the bottom of this layer. In practice it turns out that the acoustic signal of the multibeam and high frequency signal of the singlebeam gives unreliable, spiky data of which depth values might vary on a short timescale (de Boer & Werner, 2016). Moreover, these techniques do not provide any information on the nautical depth. This depth is generally bound to a certain density value, although yield stress is a more direct parameter for nautical depth than density (Fontein & van der Wal, 2006). A big score could be done in determining the nautical depth by using a combination of full-wave sub-bottom and in situ rheology profiling techniques.

INTERCOH - Mud Rheology and Fluid Mud

This study is focused on a compartment of (650x120m) in the Calandkanaal (Rotterdam, the Netherlands) is deepened by performing water injection dredging (WID). Dredging of this compartment was followed by a four-month monitoring campaign without any dredging activities in the compartment itself. In the past, the WID method has been applied successfully in other parts of the port of Rotterdam (Kirichek et al., 2018).The port's nautical depth is determined at a density level of 1200 g/L.

Equipment and approach

The monitoring setup existed of a Stema EBP system, a 38kHz sub-bottom profiler, and Stema's in situ density and yield stress profiler: the RheoTune. The EBP system ensures ultra-high resolution sub-bottom profiling of the full seismic signal. The RheoTune—which measurements are based on a tuning fork principle—provides the end user with in situ density and yield stress depth profiles.

Every survey day comprised thirteen seismic lines, ranging from 600–1,600m long with a spacing of 50m. Three of those lines intersected the WID compartment. Thirty RheoTune measurements were taken in the compartment, equally distributed over the those three lines. The spacing between two RheoTune measurements on the same seismic line is 60m.

The seismic and rheological data are matched in interpretation software Silas Processing, resulting in the correlation of seismic reflections to rheological point data on this line. Ultimately, this enables the end user to indicate yield stress and density levels—such as the nautical depth—along an entire seismic line.

Field experiment and results

The monitoring campaign resulted in a comprehensive overview of consolidation of fluid mud and development of the nautical depth over a period of ten weeks. One week after water injection, the compartment was filled with a homogeneous fluid mud layer of 1.46m thick (figure 1a). The nautical depth corresponded with the bottom of the WID compartment, located at 25.09m below CD. According to both the seismic images and homogeneous RheoTune profiles, a negligible amount of consolidation occurred in this first week.

Three weeks after water injection, the thickness of the fluid mud layer decreased to 1.13m due to consolidation. The nautical depth was determined at 24.32m below CD, resulting in a navigable fluid mud layer of 0.36m. Density and yield stress significantly rose in all examined RheoTune profiles. Seismic sections through the WID compartment show sharper reflections, presupposing an increase in sound velocity and density in the fluid mud layer (figure 1b).

INTERCOH - Mud Rheology and Fluid Mud

From four until ten weeks after injection, the top of the fluid mud layer remained more or less at the same depth below CD. Ten weeks after injection, the thickness of navigable fluid mud decreased to 0.22m implying a nautical depth of 24.12m below CD. This decrease did not
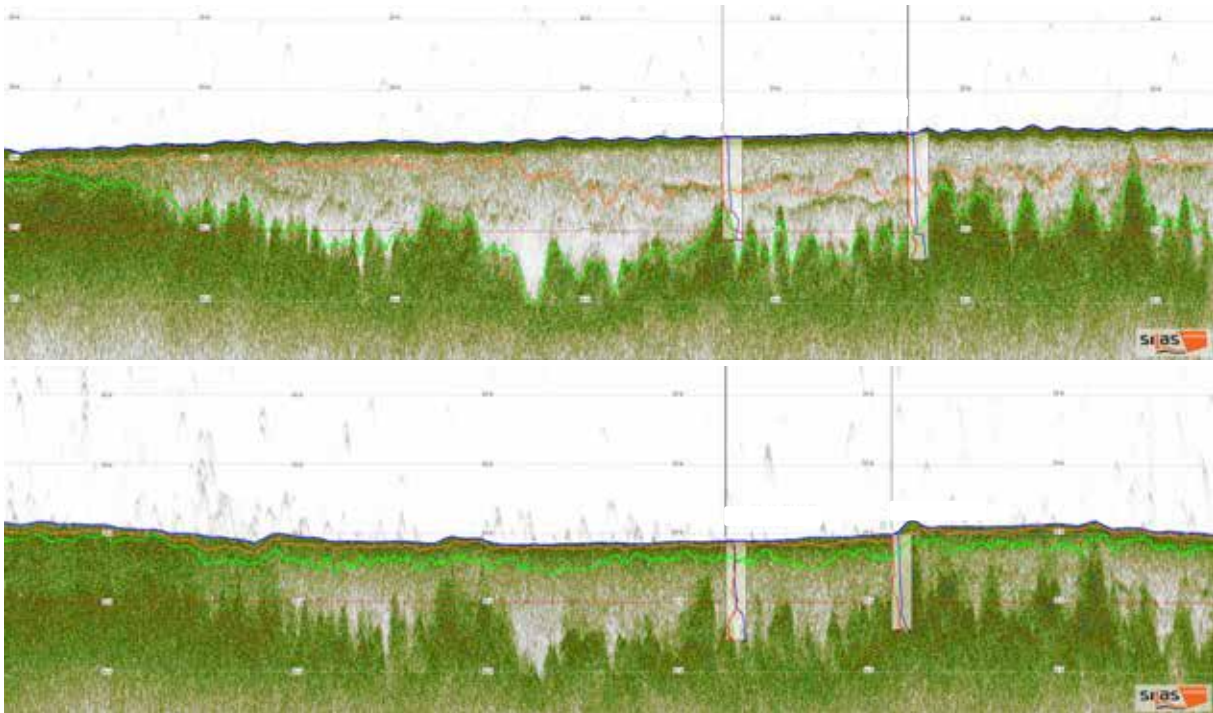

Figure 1a (above):   *Seismic line no. 3 through the WID compartment showing a fluid mud layer of 1.46m with a homogeneous density and yield stress distribution.*

Figure 1b (below):   *Seismic line no. 3 through the WID compartment showing shrinking of the fluid mud layer to 1.13m with higher densities and yield stresses and sharper seismic reflections, resulting in a navigable fluid mud portion of 0.4m.*

The 1030 g/L (blue), 1130 g/L (orange), and 1200 g/L levels (green) are indicated in both figures.

occurred entirely gradual, since ongoing sediment supply in the waterway resulted in the continuing siltation.

Conclusion

This study case at the Calandkanaal shows that monitoring fluid mud areas with a combination of the Stema EBP system and RheoTune gives an comprehensive overview of the actual nautical depth and its development over long periods. Mostly all consolidation of the fluid mud and shallowing of the nautical depth occurred in the first three weeks after injection.

Ongoing consolidation and therefore shallowing of the nautical depth over time have enormous implications for the timing of dredging and sediment volumes that need to be dredged. Constant monitoring of the nautical depth ensures safe vessel passage and enables increased loading of container vessels, minimized environmental impact, reduced dredging volumes and costs, and less hindrance from dredging vessels.

References

de Boer, P. J., & Werner, C. J. (2016). Provide end users with the most accurate nautical depth

INTERCOH - Mud Rheology and Fluid Mud

measurement by using the combination of echo sounders and density measurement equipment. In *Hydro International* (p. 13). Rostock-Warnemünde, Germany.

Fontein, W. F., & van der Wal, J. (2006). Assessing Nautical Depth Efficiently In Terms Of Rheological Characteristics. In *International Hydrographic Conference*. Antwerp, Belgium.

Kirichek, A., Rutgers, R., Wensween, M., & van Hassent, A. (2018). *Sediment management in the Port of Rotterdam*. Rotterdam, The Netherlands.

Background author

INTERCOH - Mud Rheology and Fluid Mud

O1014 - OBSERVATIONS OF LAYERED TRANSPORT IN A HYPERTURBID TIDAL CHANNEL A CLOSER LOOK AT THE EFFECT OF STRATIFICATION
Mud Rheology and Fluid Mud

Marius Becker[1], Christian Maushake[2] and Christian Winter[1]

[1] Institute of Geosciences, Kiel University, Germany Otto-Hahn-Platz 1, 24118 Kiel, Germany
E-mail: marius.becker@ifg.uni-kiel.de

[2] Federal Waterways Engineering and Research Institute (BAW), Hamburg, Germany

Introduction

Due to the interaction between stratification and vertical mixing, mud transport in hyperturbid tidal channels is susceptible to variations in hydrodynamic conditions. Transport characteristics may change on different time scales, i.e. in response to variations in discharge, during the neap-spring cycle and potentially also due to the diurnal inequality. At this stage, understanding of mud transport is still limited due to the lack of high resolution field data, which reflects these different time scales. Data used in this study show the intratidal variability of transport in different hydrody-namic conditions. These data are analysed regarding the influence of stratification on transport.

Study area and observations

Mud induced periodic stratification was measured in the tidal channel part of the Ems estuary, lo-cated at the border between The Netherlands and Germany (Winterwerp et al., 2017; Becker et al, 2018). The study is based on four 13h data sets, representing different hydrodynamic conditions, all collected at on location (Jemgum) in the fluid mud reach (Talke et al., 2009). Two consecutive surveys conducted in 2015 show conditions in between neap and spring tide. Two tidal-cycles measured in 2017 depict neap and spring tide conditions, respectively. Data was acquired and pro-cessed as described in Becker et al. (2018).
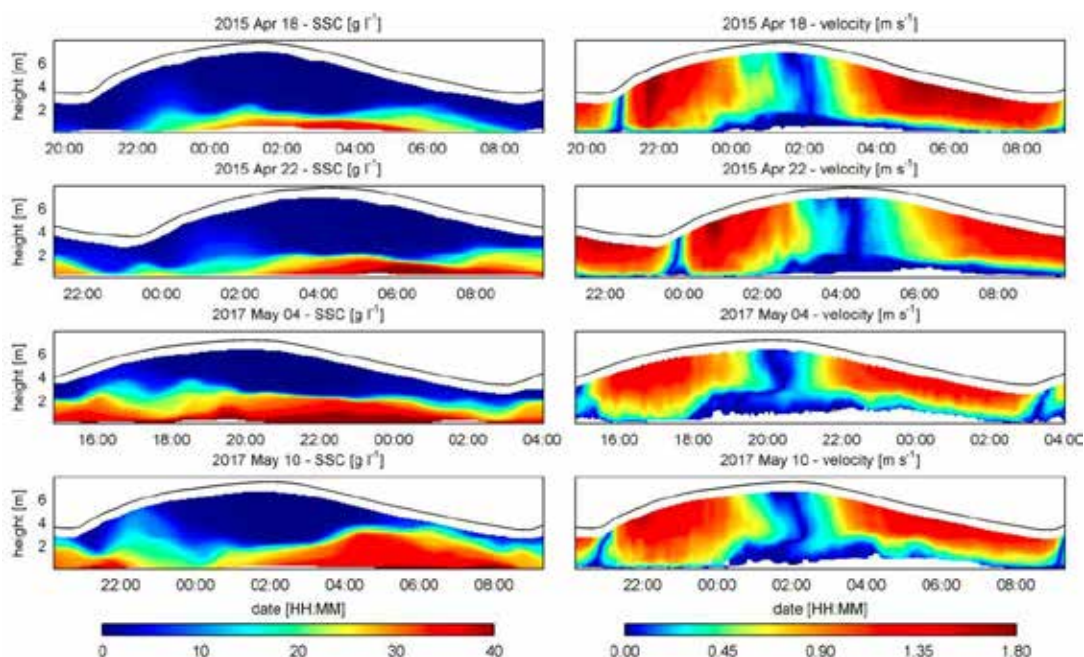

Fig. 1. SSC (left) and current velocity (right) at Jemgum in the Ems river. Results are shown for dif-ferent conditions, i.e. between spring and neap tide as measured in 2015 (row 1 and 2), and for neap (row 3) and spring (row 4) conditions as measured in 2017.

INTERCOH - Mud Rheology and Fluid Mud

In addition to differences in current velocity and current shear, these data also show differences in the characteristics of stratification (Fig. 1). In 2017, highest fluid mud layer thickness and the high-est vertical density gradients were observed during neap tide conditions, while layer thickness and density gradients were slightly reduced during the following spring tide. In 2015, layer thickness was average lower, compared to 2017. Despite this range in conditions, entrainment was substan-tially asymmetric. Quasi-instantaneous entrainment and rapid vertical mixing occur at the beginning of the flood tide. During the ebb, entrainment is limited to the fluid mud layer surface, leading to a gradual reduction in layer thickness throughout the ebb. The observations confirm previous con-cepts on intratidal stratification (Winterwerp 2001), and the recent analysis by Becker et al. (2018).

Differences in sediment transport are observed for different conditions. During the transitional situation between neap and spring in 2015, integrated transport during the ebb exceeds transport during flood, with minor differences between the two tidal-cycles.

A similar situation is found during spring tide, despite higher velocities. During neap tide con-ditions however, flood transport exceeds ebb transport. In both 2015 and 2017, flood transport is almost the same in two consecutive measurements, and the significant difference in net-transport is controlled by variations of transport during the ebb phase.

A similar situation is found during spring tide, despite higher velocities. During neap tide con-ditions however, flood transport exceeds ebb transport. In both 2015 and 2017, flood transport is almost the same in two consecutive measurements, and the significant difference in net-transport is controlled by variations of transport during the ebb phase.

In situations with significant ebb-entrainment, i.e. 2015 and during spring tide conditions in 2017, local gradient Richardson numbers indicate reduced vertical mixing in the upper part of the water column. Reduced mixing is

Fig. 2. Transport integrated vertically and in time, ebb and flood separately.

spatially related to increased stratification by suspended sediments. Persisting throughout the ebb phase, this stratification delineates the upper boundary of a turbulent mixing layer, which is characterized by fluid mud entrainment. Regarding the vertical distribution of high transport rates, ebb transport is restricted to a narrow band. Observations indicate that this band of transport covers the upper part of the mixing layer, and the lower part of the region of reduced mixing.

Transport patters
To elucidate this spatial relation, the vertical distribution of the gradient Richardson number is used to relate the occurrence of high transport rates to regions characterized by increased or reduced mixing. To simplify, high transport rates, co-located with increased and decreased mixing, are de-scribed as *turbulent* and *laminar transport*, respectively. Results (not shown)
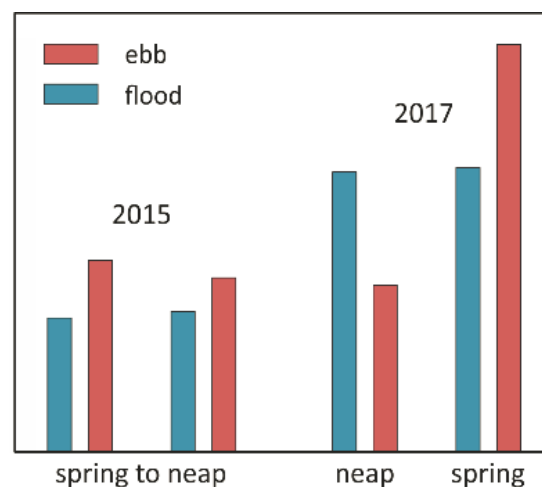
indicate that transport exhibits a layered structure during the entire period of ebb entrainment. A layer of negligible transport above the bed is located below a layer of turbulent transport, which is followed by a lami-nar transport layer. Very low transport occurs in the upper water column. Turbulent transport oc-curs at the surface of the fluid mud layer, where entrainment leads to vertical mixing. Laminar transport occurs in the region of significantly higher velocities but increased stratification, and re-duced mixing. In the uppermost part of the water column, sediment concentrations are compara-tively low, such as the transport rate, as a result of reduced mixing.

Summary and outlook

Despite the different hydrodynamic conditions, transport always showed the described characteris-tics during ebb, with a clear separation between laminar and turbulent transport layers. Previous analysis of mud transport in turbid estuaries discussed the tidal pumping of sediments and implicit-ly stressed the importance of strong flood currents. By contrast, this study indicates that net transport depends significantly on the ebb phase, which is controlled by the feedback of stratifica-tion on mixing. These results will be further analyzed regarding the influence of fluid mud layer thickness and the effects of ebb transport on the spatial structure of the fluid mud layer.

References

Becker, M., C. Maushake and C. Winter (2018). Observations of Mud-Induced Periodic Stratification in a Hyperturbid Estuary. GRL.

Talke, S. A., de Swart, H. E., & Schuttelaars, H. M. (2009). Feedback between residual circulations and sediment distribution in highly turbid estuaries: An analytical model. CSR.

Winterwerp, J. C. (2001). Stratification effects by cohesive and non-cohesive sediment. JGR.

INTERCOH - Mud Rheology and Fluid Mud

O1015 - ESTIMATION OF FLUID MUD THICKNESS ON SEAFLOOR BASED ON SURFACE WAVE OBSERVATIONS
Mud Rheology and Fluid Mud

Ilgar Safak [1], Ashish Mehta [1], Cihan Sahin [2], James Kaihatu [3], Alex Sheremet [1]
University of Florida, Civil and Coastal Engineering, Gainesville-United States [1] Yildiz Technical University, Civil Engineering, Istanbul-Turkey [2] Texas A&m University, Civil Engineering, College Station-United States [3]

Surface wave dissipation over muddy seafloors is dramatically greater than over sandy seafloors (e.g., Jiang and Mehta, 1996; Sheremet and Stone, 2003). The dissipation rate depends on wave parameters, which are relatively easy to measure, and on mud properties which not only are site-specific and highly variable throughout a storm but also require labor-intensive field experiments for high-resolution observations using advanced instrumentation. These complexities have forced wave-mud interaction studies to use wave models in an inverse manner (Sheremet et al., 2011; Safak et al., 2013, 2017). In order to run these models in the forward manner and thereby improve their prediction capability, the relation between fluid mud thickness, an essential mud parameter that controls wave dissipation, and surface wave conditions has been investigated.

A comprehensive data set of field observations of wind, waves, currents, sediment and near-bed conditions was collected in Winter 2008 at five locations, three of which being along a cross-shore transect between 8 m and 4 m depths on the muddy Atchafalaya Shelf of the Gulf of Mexico (Figure 1). Near-bed wave orbital velocity, which is a function of surface wave height, period and water depth, is taken as a proxy for wave energy reaching the seafloor and estimated from the surface wave observations at all five locations. The thickness of the fluid mud layer formed at all locations throughout the experiment is estimated from the near-bed sediment volume fraction and profiles of acoustic backscatter.
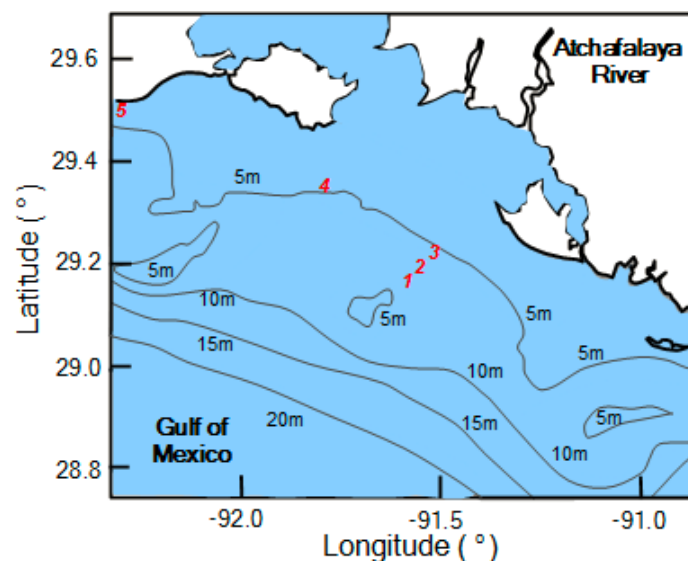

Figure 1 – Field experiment locations (numbers labeled in red) in the Gulf of Mexico.

INTERCOH - Mud Rheology and Fluid Mud

Preliminary analysis of the wind and near-bed conditions at one of the sites during part of the experiment suggests a correlation between fluid mud thickness and storms (Figure 2). In this example, the three most energetic storms (with wind speeds reaching 15 m/s) caused evident changes in the near-bed conditions and fluid mud thickness. Although this behavior is unsurprising, its quantification for field conditions is necessary (and is therefore the goal of this study) for wave modeling. A physics-based relation between surface waves and fluid mud thickness will be evaluated with respect to wave frequency and the phase of the storm. The results will be compared and discussed relative to the findings of a related study based on laboratory experiments (Vinzon and Mehta, 1997).
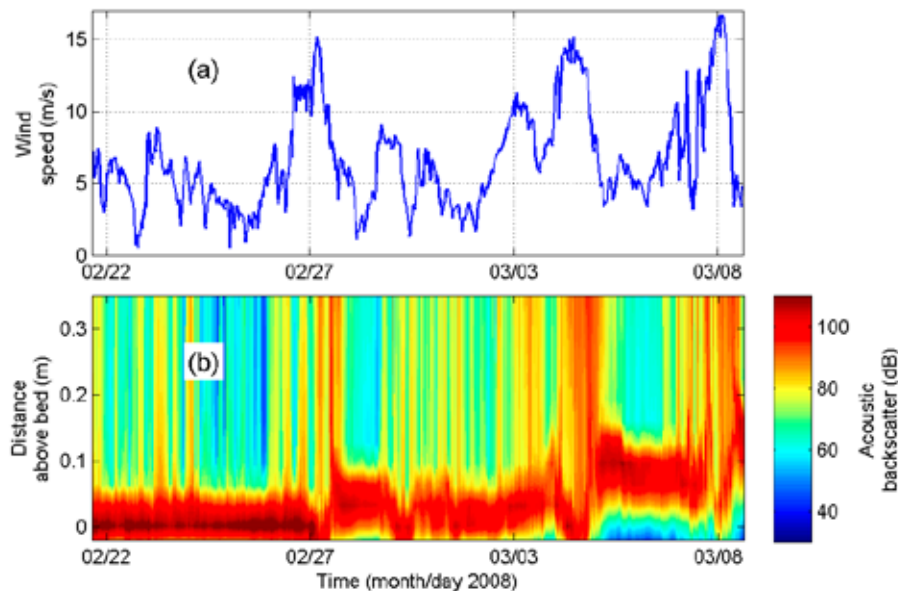

Figure 2– Observations of (a) wind speed, and (b) vertical structure of near-bed acoustic backscatter (dB) at one of the experiment sites (4 m deep) at the Gulf of Mexico.

References:

Jiang, F., Mehta, A.J., 1996. Mudbanks of the southwest coast of India V: Wave attenuation, Journal of Coastal Research 12, 890-897, CERF.

Safak, I., Sahin, C., Kaihatu, J.M., Sheremet, A., 2013. Modeling wave-mud interaction on the central chenier-plain coast, western Louisiana Shelf, USA, Ocean Modelling 70, 75-84.

Safak, I., Sheremet, A., Davis, J., Kaihatu, J.M., 2017. Nonlinear wave dynamics in the presence of mud-induced dissipation on Atchafalaya Shelf, Louisiana, USA, Coastal Engineering 130, 52-64.

Sheremet, A., Stone. G.W., 2003. Observations of nearshore wave dissipation over muddy sea beds, Journal of Geophysical Research 108, C11, American Geophysical Union.

Sheremet, A., Jaramillo, S., Su, S.-F., Allison, M.A., Holland, K.T., 2011. Wave-mud interactions over the muddy Atchafalaya subaqueous clinoform, Louisiana, USA: wave processes. Journal of Geophysical Research 116, C06005, American Geophysical Union.

Vinzon, S., Mehta, A.J., 1997. Mechanism for formation of lutoclines by waves, Journal of Waterway, Port, Coastal and Ocean Engineering 124, ASCE.

INTERCOH - Mud Rheology and Fluid Mud

O1025 - MANAGEMENT OF THE FLUID MUD IN XIAMEN WATERWAY CHINA
Mud Rheology and Fluid Mud

Qixiu Pang [1]
Tianjin Research Institute of Water Transport Engineering, Research Central of Coastal and Esturine Engineering, Tianjin-China [1]

Introduction

The Xiamen waterway is excavated on muddy estuarine bay, where fluid mud often arises in the segments near the estuary after the typhoon and river flood. The typhoon-induced river flood water brings a high concentration of suspended sediment layer near the bed, which deposits or pours directly into the deep-dredged waterway to form fluid mud. The typical bulk densities of fluid mud are between 1030 and 1250 kg/m3 with sediment concentration approximately 50 to 400 kg/m3, resulting that the efficiency of dredging away the fluid mud is very low. An alternative to the dredging is urgently needed to deal with the fluid mud.

Many muddy harbours have employed successfully a part of fluid mud with lower density, namely nautical depth, as water depth for navigation to reduce the frequency and the amount of dredging (Pang et al., 2010; Kirby 2013; Metha 2014; McAnally et al., 2016).

Key parameters for application of nautical depth

1 Critical nautical density

The sediment deposited in the waterway was fine cohesive sediment. The median particle size of the sediment was 0.0073 mm, and it contained 46.9 wt.% of clay. The critical limit of nautical bottom is usually represented by the density of mud. The critical nautical density is generally less than 1250 kg/m3, for example, Lianyungang Harbour, Guangzhou Harbour and Shenzhen Harbour (Pang et al., 2010). We determined the critical nautical densities of the nautical bottom to be 1235 kg/m3 based on rheological tests and vessel model tests on the sediment sampled from Xiamen waterway.

2 Survey of nautical depth

In Xiamen waterway, the instruments of nautical depth survey are the Silas survey system which is combination of a dual-frequency sounder and a Rheotune density meter. The low frequency is about 24 kHz. And then, with the field data, a map of nautical depth is drawn and published, where nautical thicknesses are given in parentheses.

Application of nautical depth

The waterway had not been dredged for several months, after Typhoon Meranti in September 2016. During this period, the nautical depth was employed for navigating and berthing. In most cases, the nautical thickness was used as under-keel clearance, which is less than 10% of the vessel's draught. It did not show any effect on the safety when the vessels were navigating or berthing with nautical depth. But it is suggested that the vessel's high intake should be used to take circulating water, and the lower intake is closed to avoid blockage. By the application of nautical depth, the dredging interval is prolonged, and the dredging efficiency is improved, thereby a large amount of maintenance dredging cost is saved.

INTERCOH - Mud Rheology and Fluid Mud

However, fluid mud consolidates gradually as a result of self-weight. After the fluid mud consolidation, the dredging is still need to keep the required water depth. Further, new techniques extending the usage time of nautical depths has been studied. Microbial extracellular polymer substance has been reported to play an important role in delaying settling over periods of up to several months (Kirby, 2013; Pang et al., 2018 ; Pang et al., 2018), and it might be helpful to promote the application of nautical depths in harbors.

Conclusions

Nautical depth has successfully employed to reduce dredging frequency and volumes, which offers significant economic and environmental benefits. The techniques are mainly applied in muddy harbours with fine cohesive sediment, which median particle size of sediment is smaller than 0.03 mm, and content of clay is larger than 30 wt.%.

References

Kirby R. (2013). Managing industrialised coastal fine sediment systems. Ocean and Coastal Management, 79: 2-9.

McAnally W.H., Kirby R., Hodge S.H., Welp T.L., Greiser N., Shrestha P., McGowan D., Turnipseed P. (2016). Nautical Depth for U.S. Navigable Waterways: A Review. Journal of Waterway, Port, Coastal and Ocean Engineering. 142(2): 04015014.1-04015014.13.

Mehta A.J., Samsami F., Khare Y.P., Sahin C. (2014). Fluid mud properties in nautical depth estimation. Journal of Waterway, Port, Coastal and Ocean Engineering, 140(2): 210-222.

Pang Q.X., Han P.P., Zhang R.B., Wen C.P. (2018). Delaying effect of extracellular polymer substances on fluid mud consolidation and application for nautical depth. Journal of Waterway Port Coastal & Ocean Engineering. 144 (3) DOI: 10.1061/(ASCE)WW.1943-5460.0000441

Pang Q.X., Yang S.S., Yang H., Han X.J. (2010). Research and application of the technique of nautical depth in muddy Harbours. Hydro-Science and Engineering. 3: 33–39. (in Chinese)

Pang Q.X., Zhang R.B., Wen C.P., Han P.P. (2018). Fluid mud Consolidation Delayed by Extracellular Polymer Substances (EPS). Environmental Technology. 39(19) :2534-2541.

INTERCOH - Mud Rheology and Fluid Mud

O1043 - A MODIFIED K ε TURBULENCE MODEL FOR COHESIVE SEDIMENT TRANSPORT WITH A FLUID MUD LAYER
Mud Rheology and Fluid Mud

Erik Toorman [1], Samor Wongsoredjo [1], Mohamed Ouda [1]
Ku Leuven, Hydraulics Division, Dept. of Civil Engineering, Leuven-Belgium [1]

Abstract

When a hyperconcentrated fluid mud layer (defined as having a bulk density above the gelling point) is present on the seabed or the bottom of a channel, the generation of turbulence by shear flow cannot properly be modelled with a standard turbulence model (like *k-epsilon*) because the growth of turbulent eddies in inhibited by the multitude of sediments in hyperconcentrated conditions just above the bed and the large amount of energy required to transport the particles is no longer available to turbulence production. This mechanism of turbulence damping is most clearly observed in the data from the flume experiments with sand by Cellino (1998).

In the present study the k-epsilon turbulence model is chosen, being the most commonly used turbulence model for vertical mixing in coastal engineering. The proposed method is designed for sediment transport models based on mixture theory. Two major modifications are needed:
1) the fluid viscosity should be replaced by the effective viscosity of the mud suspension or fluid mud, and
2) low-Reynolds damping functions to generate proper values of turbulent kinetic energy (TKE = k) and turbulent dissipation rate (TDR = ε) in the inner boundary layer, where the standard model fails since turbulence is no-longer fully developed here.

The analysis of data from new dedicated experiments in a rotational rheometer with vane spindle strongly supports the hypothesis that the equilibrium flow curve for fluid mud is well described by a perfect Bingham model in the laminar flow regime. The parameters of the rheological model are empirically related to the sediment concentration. The experimental data from Celino (1998) for sand give further insight how a non-Newtonian suspension generates additional granular stresses in the transient regime. These concepts are combined to develop a closure for the effective viscosity of the sediment-water mixture, additionally making use of the insights from a newly developed hybrid mixture/two-phase flow model in OpenFOAM, which is used as a numerical laboratory (Ouda & Toorman, 2019).

Low-Reynolds damping functions have been derived from DNS data for smooth-wall turbulence as a function of non-dimensional wall-distance. By rescaling the non-dimensional wall coordinate ($z_+ = zu_*/v$) and the model constants with the effective (non-Newtonian) mixture viscosity, similar damping functions can be used for fluid mud as for clear water. Based on these modifications, the law of the wall is also corrected to define proper near-bottom boundary conditions in the case of coarse vertical meshes.

Both types of closures are implemented in a 1DV model for steady uniform open-channel flow, where the turbulence model is implemented in a similar way as in the well-known GOTM model (Umlauf et al., 2007). Equilibrium concentration profiles are computed for various steady shear velocities. By lack of data for experiments with cohesive sediments, the methodology is validated with Cellino's (1998) flume data for high-concentrated sand transport.

In addition, attention has been payed to improving the accuracy of the numerical implementation of the turbulence equations. The high non-linearity of the two turbulence variables, approximated (most commonly) by linear interpolation functions between neighbouring grid points, can induce large deviations and errors, in particular in the last grid cell near the bottom. This has large consequences regarding the accuracy of both hydrodynamics and sediment transport. Moreover, this problem has been found to be mesh dependent. Therefore, the near-wall boundary conditions are redefined to minimize the errors. The alternative conditions are based on three criteria: conservation of flux and correct values of wall shear stress and near-wall TKE (i.e. correct force and energy balance). Moreover, the TKE production term is also discretized in an alternative, more accurate way.

The method is tested on different vertical mesh resolutions: a high-resolution mesh to resolve not only the fully-developed outer layer, but also the inner layer all the way down to the immobile bed, and coarse resolution meshes to define minimal requirements for large-scale 3D simulations which are expensive because of their large horizontal domain scale.

The modified numerical formulation has been tested in the 1DV model, before being implemented and tested into the TELEMAC3D code.

The methodology is then further extended for the case where the fluid mud layer thickness is smaller than the vertical mesh size. In this case the fluid mud flow is a subgrid scale phenomenon. A method is being designed to describe fluid mud flow as a bed load transport formula, which provides also the near-bed reference concentration for the resolved suspension flow in the outer layer.

References
Cellino, M. (1998). Experimental study of suspension flow in open channels. PhD thesis No.1824, Ecole Polytechnique Fédérale de Lausanne, Switzerland.
Ouda M., Toorman E.A. (2019). Development of a new multiphase sediment transport Model for free surface flows. *International Journal of Multiphase Flow*, 117(8): 81-102.
Umlauf, L., Burchard, H., Bolding, K. (2007). GOTM. Source code and test case documentation
Version 4.0. http://gotm.net

INTERCOH - Mud Rheology and Fluid Mud

O1048 - NUMERICAL MODELLING OF WAVE INDUCED MUD TRANSPORT USING INCOMPRESSIBLE SMOOTHED PARTICLE HYDRODYNAMICS (ISPH) BASED ON AN IMPROVED INTER PARTICLE AVERAGE METHOD
Mud Rheology and Fluid Mud

Abolfazl Aslani [1], Kourosh Hejazi [2], *Mohsen Soltanpour [1]*
K. N. Toosi University of Technology, Civil Engineering, Tehran-Iran [1] K. N. Toosi University of Technologyk. N. Toosi University of Technology, Civil Engineering, Tehran-Iran [2]

Abstract
Waves-induced siltation and contaminant transport have a great significance to the civil and environmental engineers. Waves-induced mud transport has been investigated theoretically and experimentally in several studies, but very few numerical model developments has been reported in the literature. In this paper, improved incompressible smoothed particle hydrodynamics (ISPH) method based on the improved inter-particle average method has been deployed in order to handle the discontinuity across the interface in simulating wave-mud interaction. The improvements are made in the free surface and interface treatment and viscous term. Mud layer is considered as a Non- Newtonian fluid in this study. For validating the model, the simulation results have been compared with the experimental results which showed good agreements.

Keywords: mass transport velocities; inter-particle average method; wave-mud interaction; ISPH.

Governing equations and the ISPH formulation
The two-dimensional governing equations of mass and momentum conservation were used in Lagrangian form. The ISPH method based on the inter-particle average method originally presented by Hu and Adams (2007). Despite having a robust technique in handling the discontinuity between the two media, due to some shortcomings of this method found in simulating of free surface and simplification of interface treatment, it requires some improvements and modification in governing equations. A way out for the aforementioned problems in the free surface is use of imaginary mirror particles outside the free surface leading the below pressure gradient for the free surface particles:

$$(1+k)\sigma_i \sum_j \frac{A_{ij}}{r_{ij}} \frac{P_{ij}}{k\rho_i + \rho_j} = \frac{1}{\Delta t} \sum_j A_{ij} \left(\frac{k\mu_i v^*_i + \mu_j v^*_j}{k\mu_i + \mu_j} \right) . e_{ij}$$

(2)

Bingham-Papanastasiou model was used for the rheology of mud layer. Noting that the neighbouring particles are involved in determining the shear stress of reference particle, the effect of all neighbouring particles on determining the magnitude of shear rate is involved in this study. The present method uses prediction–correction fractional steps with the temporal velocity field integrated forward in time without enforcing incompressibility in the prediction step. Hu and Adams (2007) assumed that the interface was exactly between the two particles of two different fluids. This assumption disregards the real particle distance from the interface. Therefore, an improved Poisson equation for pressure considering the real distant of interface from particles to find the exact particles pressure is rewritten as:

INTERCOH - Mud Rheology and Fluid Mud

Where $A_{ij} = \left(1/\sigma_i^2 + 1/\sigma_j^2 \right) \partial W_{ij}/\partial r_{ij}$, σ_i is the particle number density, W is the interpolation kernel function, $\vec{r}_{ij} = \vec{r}_i - \vec{r}_j = r_{ij}\boldsymbol{e}_{ij}$, $\boldsymbol{e}_{ij}$ is the unit vector from particle i to particle j which is the neighboring particle, ρ represents the density, the superscript (*) refers to prediction step, $\boldsymbol{v}$ is the velocity, Δt is time step and k is the correction factor in order to improve the formulation. After finding the pressure the corrective particles velocity and position are obtained. Since the SPH is a Lagrangian method, it can be easy to trace the position of each particle at every time. The displacement of each particle in the mud layer divided by the specified time period Δt gives the mud mass transport velocity. Due to periodic characteristic of overlaying wave, the Δt should be a multiple of wave period to satisfy a thorough orbital motion of each particle under wave enforcement.

Model application

Fig. 1 shows the schematic of the simulation set-up of wave-mud interaction. A piston wave maker was used to generate a sinusoidal wave at the entrance of a channel with the length of 10 m. The number of particles employed in the computation was about 40000, and the initial particles spacing and the time step were set equal to 0.01 m and 0.001 s respectively.
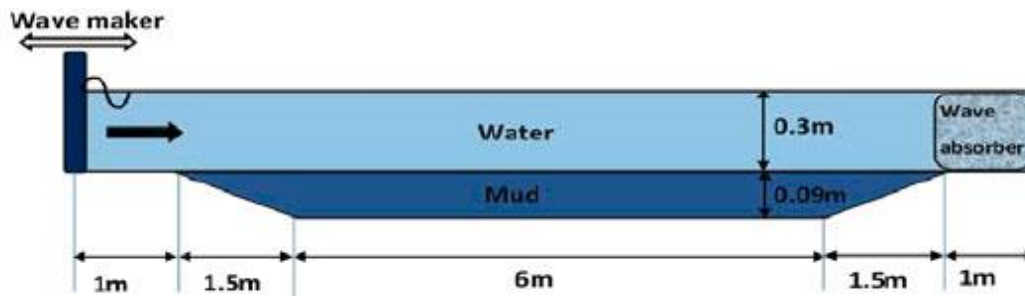

Fig. 1. Schematic of the simulation set-up

Results and Discussion

A comparison between the simulated and measured mud mass transport velocity distributions has been presented over the mud layer depth in Fig.2. The figure indicates that reasonable agreement exists between the present simulated results and measured ones given by Soltanpour et al. (2016). The effect of wave height on the mass transport velocity is significant so that an increase of wave height from 5 to 7 cm results in a twofold increase in the mass transport velocity due to relatively greater driving force to move mud as reported by Sakakiyama and Bijker (1989) that the mud mass transport is proportional to a higher power than the square of the surface wave height.
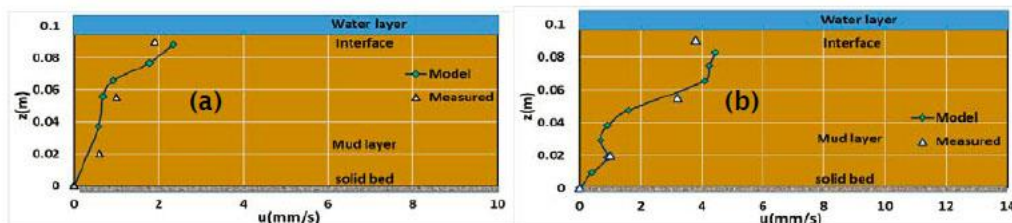

Fig. 2. Comparisons between the experimental (Soltanpour et al., 2016) and simulated results of mud mass transport velocity; a) T=1.1 s, H=5.0 cm; b) T=1.1 s, H=7.0 cm.

INTERCOH - Mud Rheology and Fluid Mud

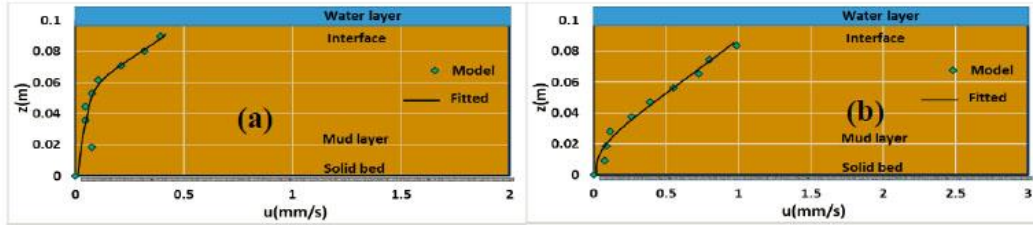Fig. 3. Mass transport velocity; H0≈4.0 cm, mud density=1370 3kgm , Wave Period ≈0.9s; (a) without interface spacing treatment (b) with interface spacing treatment

References

Hu X.Y., Adams N.A. (2007). An incompressible multi-phase SPH method. Journal of Computational Physics, 227: 264–278.

Sakakiyama T., Bijker E.W. (1989). Mass transport velocity in mud layer due to progressive waves. J Waterw Port Coast Ocean Eng, ASCE 115(5):614–633.

Soltanpour M., Shamsnia H., Shibayamab T., Nakamurac R., Tatekoji A. (2016). A study on wave-induced particle velocities in fluid mud layer.Coastal Engineering Proceedings 35.

INTERCOH - Mud Rheology and Fluid Mud

O1055 - SPECTRAL WAVE GENERATION MODELING IN AN OPEN SEA SHALLOW MUDDY ENVIRONMENT
Mud Rheology and Fluid Mud

Fatemeh Ameri [1], Sarmad Ghader [1], S. Abbas Haghshenas [1], Daniel Yazgi [2], Azadeh Razavi Arab [3], Edris Delkhosh [1]
Institute of Geophysics - University of Tehran, Oceanography, Tehran-Iran [1] Institute of Geophysics - University of Tehran, Space Physics, Tehran-Iran [2] Louisiana State University, Oceanography, Baton Rouge-United States [3]

Introduction
The interactive effects of mud-induced wave dissipation in shallow water and wind-induced wave generation are still poorly understood and needs more attention to be paid in details. Considerable decay of wave energy along the wave trajectory over muddy beds makes a different wave generation/transformation in comparison with sandy/rocky environments. The role of soft mud to dissipative waves has been implemented to SWAN wave model by Kranenburg et al. (2011). They implemented a new dispersion relation obtained from a viscous two-layer model in the wave-forecasting model, SWAN-mud, to consider wave decay in coastal areas due to the presence of fluid mud deposits. The dispersion relation was derived for a viscous layer overlying by an inviscid upper layer. Assessing the two-dimensional, wave fields in shallow waters, they showed a satisfactory performance for their model in real muddy environments. Significant wave heights over gentle muddy slopes are usually overestimated using default SWAN model setup. It is while it is expected that using SWAN-mud setup improves the correlation between model simulations and real field measurements. However, considering the viscous assumption of mud behavior in developing new dispersion relation the model results are highly dependent on the assumed mud rheology and mud behavior in reality. This research aims to adopt various facilities implemented in SWAN wave model to regenerate a set of two station wave measurements over the muddy bed of Northern Persian Gulf with acceptable accuracy. A number of about 30 model configurations are considered for wave generation over the mud coast of Deylam Bay and favorable results are obtained at the end. The focus of this study is to develop a proper hindcast/forecast system for predicting wave characteristics in the North-Western Persian Gulf including the mud induced wave dissipation in the areas covered with soft muddy deposits.

Study Area and Field Program
The North-Western part of the Persian Gulf is covered with mud deposits originated mainly from the Arvand River catchment area. Mud deposits up to 20 meters thickness is observed at the very shallow coast of Deylam Bay, which implies high rates of wave dissipation in the area; something which should be taken in to consideration for wave climate estimations. A set of 37-day field measurements was available, conducted at the field site, from the 20th of February to the 28th of March, 2007 (Haghshenas and Soltapour, 2009). Directional wave spectra and vertical current velocity profiles were simultaneously recorded at one deep and one shallow water stations. Mud samples from the top 1-meter layer were also collected to define mud characterics. At the same period of time, there are data available in the middle part of the Persian Gulf at Naiband Bay wave buoy. The latter set of data will be used for validation of model performance in an area with no mud-induced wave dissipation.

INTERCOH - Mud Rheology and Fluid Mud

Numerical Model

The 3rd Generation SWAN model version 41.20 is employed to simulate spectral wave generation and propagation over the entire Persian Gulf simulation domain. Adopting structured and un-structured simulation grid, different wave generation configurations and including/excluding mud-induced wave dissipation, a number of more than 30 model configurations are considered for wave generation over the entire Persian Gulf. At the muddy coast of Deylam Bay, mud induced dissipation effects are considered using the software option in some certain run cases. For input wind data, the WRF (Weather Research and Forecasting) model as a mesoscale meteorological numerical model is used which can provide accurate and high-resolution simulation of surface fields (such as wind). WRF is a fully parallel three dimensional atmospheric simulation system that numerically solves the fully compressible and non-hydrostatic equations governing the atmosphere. Wind simulations over the Persian Gulf and the Oman Sea are performed for the period of data availability and the system performance was verified. The simulated wind field is applied to simulate wave generation over the entire model domain by using SWAN model. Observational directional wave data are used to verify the model predictions at the three mentioned stations. The results of different model runs are investigated in Deylam Bay adopting wave dissipations and against field data over the muddy beds. Figure 1 shows one of the selected simulation grids for instance, as well as measurement station locations. Comparisons between the measured and simulated wave heights for one of the modified model runs are presented in Figure 2, which show fair agreement with the observations.
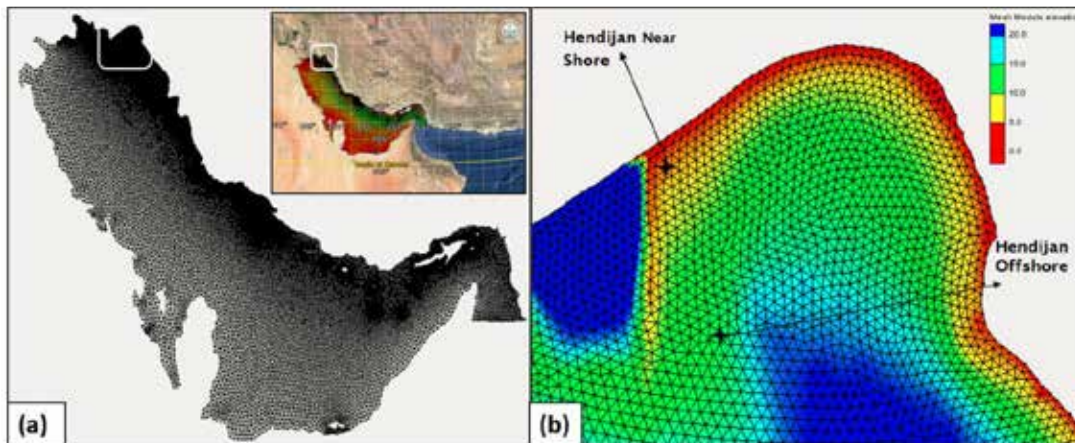

Figure 1. (a) Unstructured simulation grid for the Persian Gulf wave model domain, (b) the study area - location of wave measuring stations are shown with black astricks.
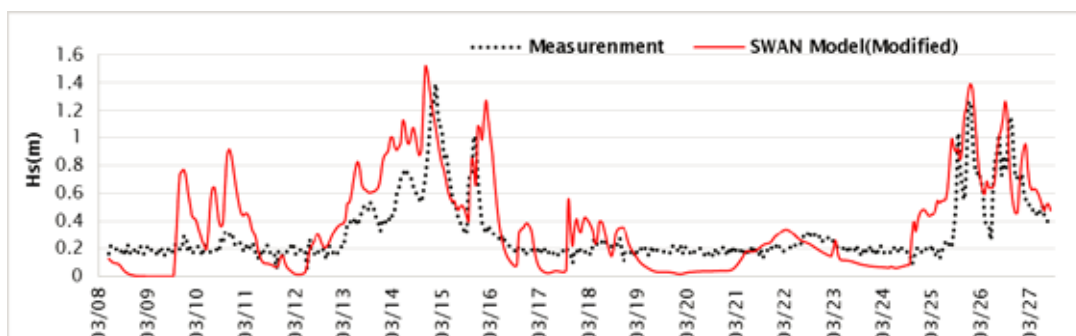

Figure 2. Simulated significant wave height at Deylam Bay offshore station, the North-Western Persian Gulf, in comparison with field measurements – February and March 2007.

INTERCOH – Mud Rheology and Fluid Mud

A two-layer analytical wave-current-mud interaction model

Kamrooz Mahshid[1], Hadi Shamsnia[2], S. Abbas Haghshenas[1], Sarmad Ghader[1]

[1] Institute of Geophysics, University of Tehran
North Kargar Ave., Tehran, PC 1439951113, Iran
E-mail: sahaghshenas@ut.ac.ir

[2] K. N. Toosi University of Technology
Tehran, PO Box 1346, Iran

Introduction

There are several coastal areas covered by soft mud normally adjacent to big rivers where the bottom layer has been covered with soft mud. In these environments, the discharges of the big adjacent rivers usually play a significant role on the behaviour of mud under wave action. Since Gade (1958), the interaction of waves and muddy beds has been studied in several ways. Wave attenuation and mud mass transport are two major phenomena that have received the most attentions (e.g., Dalrymple and Liu, 1978; Sakakiyama and Bijker, 1989; Ng, 2000). There have also been some efforts to formulate the combined effects of waves-currents-mud interaction system. An and Shibayama (1994) conducted some laboratory wave flume experiments to observe wave-mud interaction with current presence. Both wave height attenuation and mass transport were measured. Nakano (1994) performed laboratory experiments to measure wave height attenuation on a horizontal muddy bed introducing a following current. The effect of current on wave-mud interaction has also been included in a few recent studies (Zhao et al., 2006, Soltanpour et al., 2018).

The present study offers an analytical wave-mud-current interaction model to simulate wave transformation as well as velocities in water and mud layers. Performance of the newly established model is examined by using different available laboratory experiments.

Governing Equations

The fluid system is divided into two layers. A fully viscous layer is considered for the water layer with three different current velocity profiles: 1) uniform current, 2) lineal current profile, and 3) second order varying current profile. The governing equations of the wave field for the wave-current-mud interaction are written as follows (Zhao et al., 2006)

$$\frac{\partial \tilde{u}_w}{\partial t} + U\frac{\partial \tilde{u}_w}{\partial x} + \tilde{v}_w\frac{\partial U}{\partial z} = -\frac{1}{\rho_w}\frac{\partial \tilde{p}_w}{\partial x} + \nu_w\left(\frac{\partial^2 \tilde{u}_w}{\partial x^2} + \frac{\partial^2 \tilde{u}_w}{\partial z^2}\right) \tag{1}$$

$$\frac{\partial \tilde{v}_w}{\partial t} + U\frac{\partial \tilde{v}_w}{\partial x} = -\frac{1}{\rho_w}\frac{\partial \tilde{p}_w}{\partial z} + \nu_w\left(\frac{\partial^2 \tilde{v}_w}{\partial x^2} + \frac{\partial^2 \tilde{v}_w}{\partial z^2}\right) \tag{2}$$

$$\frac{\partial \tilde{u}_m}{\partial t} = -\frac{1}{\rho_m}\frac{\partial \tilde{p}_m}{\partial x} + \nu_m\left(\frac{\partial^2 \tilde{u}_m}{\partial x^2} + \frac{\partial^2 \tilde{u}_m}{\partial z^2}\right) \tag{3}$$

$$\frac{\partial \tilde{v}_m}{\partial t} = -\frac{1}{\rho_f}\frac{\partial \tilde{p}_m}{\partial z} + \nu_m\left(\frac{\partial^2 \tilde{v}_m}{\partial x^2} + \frac{\partial^2 \tilde{v}_m}{\partial z^2}\right) \tag{4}$$

$$\frac{\partial \tilde{u}_f}{\partial x} + \frac{\partial \tilde{v}_f}{\partial z} = 0 \tag{5}$$

where $\tilde{u}$, $\tilde{v}$ are the horizontal and vertical velocities corresponding to the x and z directions respectively, $\tilde{p}$ is the dynamic pressure, t represents the time, ν is the kinematic viscosity, $f=w$, m denote the water and mud respectively, and U is the current velocity.

By considering the wave field variables to be periodic in x and t we will have

$$\tilde{u}_f = u_f e^{i(kx-\sigma t)} \tag{6}$$

INTERCOH – Mud Rheology and Fluid Mud

$$\tilde{v}_f = v_f e^{i(kx-\sigma t)} \tag{7}$$

$$\tilde{p}_f = p_f e^{i(kx-\sigma t)} \tag{8}$$

where k is the wave number, and σ is the wave frequency.

By substitution of Eqs. (6)-(8) into Eqs. (1)-(5), the following ordinary differential equations are obtained in water and mud layers

$$v_w'''' - (k^2 + \lambda_w^2 + ikU/v_w)v_w'' + \left(\frac{ik}{v_w}\frac{dU}{dz}\right)v_w' + \left(-k^2\lambda_w^2 - \frac{1}{v_w}\frac{dU}{dz} - \frac{ik}{v_w}U\right)v_w = 0 \tag{9}$$

$$v_m'''' - (k^2 + \lambda_m^2)v_m'' + k^2\lambda_m^2 v_m = 0 \tag{10}$$

where, $\lambda_{m,w}^2 = k^2 - i\sigma/v_{m,w}$

The current field equations are written as

$$\rho_w v_w \frac{\partial^2 U}{\partial z^2} = -\frac{\partial P_w}{\partial x} \tag{11}$$

where P is the averaged steady pressure.

Solution

The general solution of Eqs. (9), (10) reads as

$$v_w = \sum_{n=1}^{\infty} A_{w,n} z^n \tag{12}$$

$$v_m = A_m \sinh k(h+z) + B_m \cosh k(h+z) + C_m \sinh \lambda_m(h+y) + D_m \cosh \lambda_m(h+y) \tag{13}$$

The solution of current equation, Eq. 11 is given as

$$U = Az^2 + Bz + C \tag{14}$$

Appropriate boundary conditions are applied to obtain the constants of wave and current solutions.

Results

Figure 1 presents a sample of mud particle velocity versus the current values. As observed in the figure, by an increase in the reference value of the current velocity, the mud particle velocities are decreased.
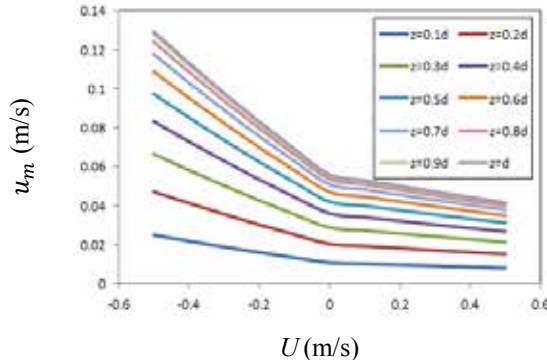

Fig. 1 Particle velocity amplitudes versus a reference current velocity at different depth in the mud

References

An, N. N., Shibayama, T. (1994). Wave-current interaction with mud bed, Proceedings of 24th Coastal Engineering Conference, ASCE: 2913–2927.

Dalrymple, R.A., Liu, P.L.-F. (1978). Waves over soft mud: a two-layer fluid model, J. Phys. Oceanogr. 8: 1121–1131.

Gade, H. G. (1957). Effects of a non-rigid, impermeable bottom on plane surface waves in shallow water, PhD Thesis, Texas A&M University, USA.

Nakano, S. (1994). Wave damping and mud transport. PhD Thesis, Kyoto University, Japan, 212 pp, (In Japanese).

Ng, C. O. (2000) Water waves over a muddy bed: a two-layer Stokes' boundary layer model, J. Coast. Eng. 40: 221-242.

Sakakiyama, T., Bijker, E.W. (1989). Mass transport velocity in mud layer due to progressive waves, J. Waterw. Port. C-ASCE, 115: 614–633.

Soltanpour, M., Shamsnia, S. H., Shibayama, T., & Nakamura, R. (2018). A study on mud particle velocities and mass transport in wave-current-mud interaction, J. Appl Ocean Res. 78: 267-280.

Zhao, Z. D. , Lian, J. J., Shi, J. Z. (2006). Interactions among waves, current, and mud: numerical and laboratory studies, Adv. Water Res. 29: 1731-1744.

INTERCOH - Sediment Characterization and Mixtures

O1029 - SEDIMENT MOBILISATION EXCITED BY EARTHQUAKES IN THE SEA OF MARMARA
Sediment Characterization and Mixtures

Christos Papoutsellis [1], Pierre Henry [1], Cristele Chevalier [2], Nurettin Yakupoğlu [3], Sinan Özeren [4], Nazmi Postacioğlu [5]
Aix Marseille Univ, Cnrs, Ird, Inra, Coll France, Cerege, Cerege, Marseille-France [1] Aix Marseille Univ, Universite De Toulon, Cnrs, Ird, Mio, Mio, Marseille-France [2] Istanbul Technical University, Maslak, Geological Engineering, Istanbul-Turkey [3] Istanbul Technical University, Maslak, Eurasia Institute of Earth Sciences, Istanbul-Turkey [4] Istanbul Technical University, Maslak, Physics, Istanbul-Turkey [5]

Observations of sediment cores from the seabed of the sea of Marmara show cyclic occurrence of turbidites-homogenites that present a basal layer with an alternation of coarse (sand/silt) and finer (clay silt) laminae ("turbidite") followed by a layer of apparently homogenous mud ("homogenite") and are generally interpreted as earthquake deposits. Previous studies hypothesized that oscillatory currents ("seiches") resulting from earthquakes and tsunamis play a major role in shaping these deposits. The understanding of processes of turbidite-homogenite deposition and their relationships with the hydrodynamic characteristics of the sea of Marmara is the subject of the present study. From a hydrodynamical point of view, the sea of Marmara is characterised by a water column stratification due to the density difference between the dense Aegean waters and brackish Black sea waters, passing through the Dardanelles and Bosporus respectively. Moreover, the Sea of Marmara is also affected by water column oscillations (seiches) or internal waves that are excited by meteorological perturbations, e.g. strong atmospheric pressure gradients, or earthquakes originating from the North Anatolian Fault. Such a complex configuration requires performing numerical modelling of hydrodynamical processes as a first step before considering coupling with sediment transport. Our analysis is based on existing data of bottom pressure, temperature and current in conjunction with a two-layer 3D numerical model implemented by using the code CROCO.

INTERCOH - Sediment Characterization and Mixtures

O1057 - CONSISTENCY AND RHEOLOGY OF MIXED SEDIMENTS AND EFFECTS OF EXTRACELLULAR POLYMERIC SUBSTANCES ON ITS BEHAVIOR
Sediment Characterization and Mixtures

Farzin Samsami [1], Mansour Yadegari [2], Ashish J Mehta [3]
Iau West Tehran Branch, Civil Engineering, Tehran-Iran [1] Iau Sciences and Research Branch, Civil Engineering, Tehran-Iran [2] University of Florida and Nutech Consultants, Civil & Coastal Engineering, Gainesville-United States [3]

Introduction

Mixed mineral sediments are common in estuarine environments. Biologically cohesive, or adhesive, extracellular polymeric substances (EPS), or exopolymers, generated by microorganisms can significantly influence these sediments. Thus far, many studies have been carried out on mixtures of cohesive (clayey) and cohesionless (silt and sand) sediments and their behavior under waves and currents. The consistency (characterizing the soil) and rheological properties of such sediments are essential to understand the interaction of waves and currents with the sedimentary bed, and modeling sediment transport. In this study, consistency and rheological properties of selected mixed sediments were investigated through a series of Atterberg Limits and rheometric tests, respectively. The effect of adding EPS to the mixture was additionally examined. Kaolinite was used as the cohesive fraction, very fine sand/silt as the non-cohesive fraction, and xanthan gum as a proxy for EPS. The mixtures were prepared with different fractions (by weight) of kaolinite, silt and xanthan gum at different water contents.

Experimental Methods

The samples were prepared by thoroughly mixing kaolinite, silt and xanthan gum. The weight fractions of the materials were varied in range of 100%-70% for kaolinite, 0%-30% for silt, 0%, 0.01%, and 0.05% for xanthan gum. In order to obtain the consistency of each sample, Atterberg Limits tests were performed through the standard procedure (i.e. ASTM D4318: Standard Test Methods for Liquid Limit, Plastic Limit, and Plasticity Index of Soils). The measurements included Plastic Limit (PL) and Liquid Limit (LL). These data were used to characterize the type of soil according to Casagrande (1948). Rheology tests were performed in rotary and oscillatory modes. An Anton Paar Physica MCR302 rheometer equipped with a parallel-plate geometry was used to obtain the viscoplastic and viscoelastic parameters (Mehta et al. 2014).

Analysis and Discussion

The soil was classified by plotting the Plasticity Index PI versus the LL based on the Casagrande Plasticity Chart (Fig. 1). Figure 2 shows the results for PI and Fig. 3 classifies the soils. In the latter it is observed that the samples can be categorized as ML (i.e. clayey fine sands, or clayey silts with slight plasticity), CL (i.e. silty clays with low plasticity), and OL (i.e. organic silty clays of low plasticity). Their significance is discussed in the full paper.

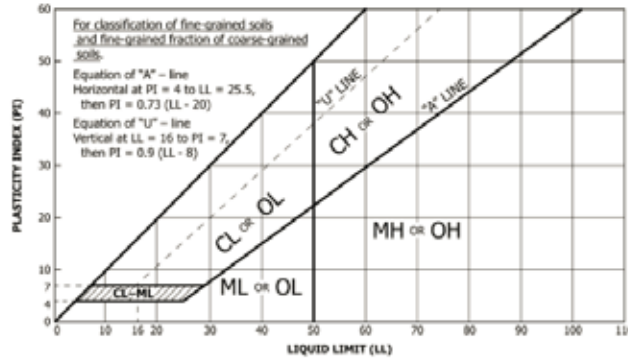## INTERCOH - Sediment Characterization and Mixtures
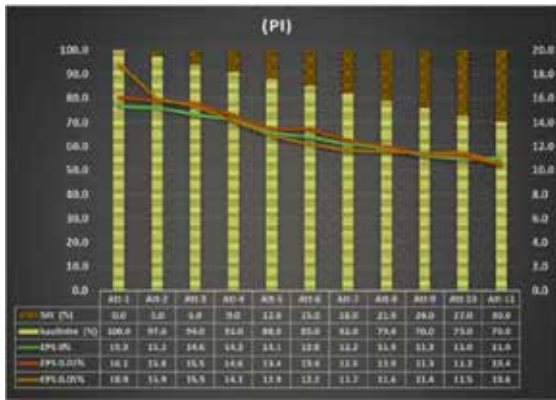

Fig. 1. Casagrande (1948) Plasticity Chart.

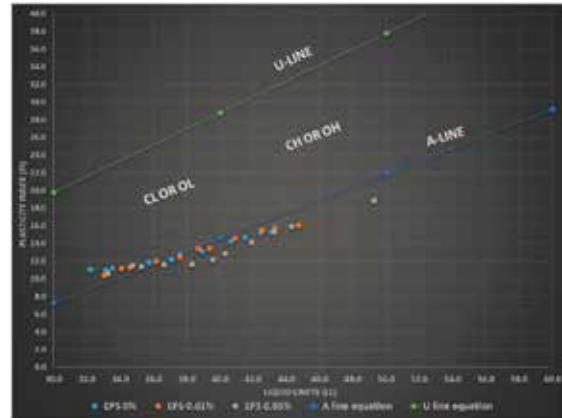Fig. 2. Plasticity index (PI) from Atterberg Limits tests.

Fig. 3. Soil classification.

Based on the Bingham viscoplastic model, the yield stress and viscosity of each sample were deduced from the rotary rheocurve, and the storage and loss muduli from the oscillatory data. Figure 4 illustrates oscillatory output results for a sample. The oscillatory yield stress and flow point stress τf (discussed in the paper) were obtained from such tests (Table 1).

TEST No.	clay %	silt %	EPS %	W (%)	Rotary η_B (pa.s)	Rotary τ_B (pa)	Oscillatory τ_f (pa)
Rh80-1-I	100	0	0	80	2.057	103.32	45.3
Rh80-1-II	90	10	0	80	1.668	76.04	33.4
Rh80-1-III	80	20	0	80	1.243	48.11	23.2
Rh80-1-IV	70	30	0	80	0.774	26.02	14.0
Rh80-2-I	100	0	0.01	80	2.874	149.15	59.8
Rh80-2-II	90	10	0.01	80	2.238	89.76	40.8
Rh80-2-III	80	20	0.01	80	1.493	45.24	21.6
Rh80-2-IV	70	30	0.01	80	3.922	153.19	15.0
Rh80-3-I	100	0	0.05	80	2.686	97.92	69.8
Rh80-3-II	90	10	0.05	80	2.955	100.01	39.5
Rh80-3-III	80	20	0.05	80	2.242	56.53	38.6
Rh80-3-IV	70	30	0.05	80	0.936	23.57	13.6
Rh70-4-I	80	20	0.05	70	2.496	86.94	35.3
Rh90-4-II	80	20	0.05	90	1.074	27.14	15.7
Rh100-4-III	80	20	0.05	100	0.529	13.97	7.5

Table 1. Yields stress, viscosity and flow point stress.
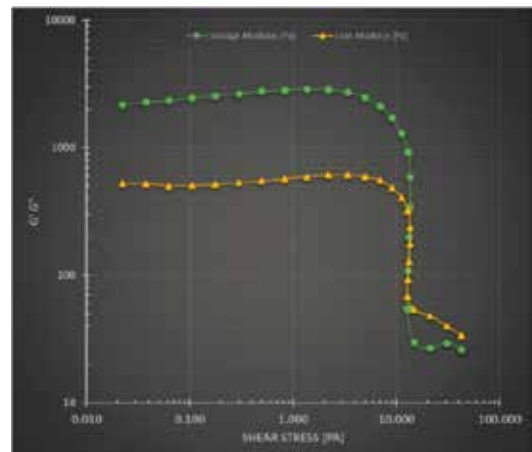
Fig. 4. Sample result of an oscillatory test.

The rheometric tests showed that with increasing water content (W), the characteristically viscoplastic yield stress and viscosity decreased, and the viscoelastic storage and loss moduli were also reduced.

Moreover, by increasing the fractions of cohesive sediment and EPS, i.e. reducing the non-cohesive sediment fraction, the yield stress and viscosity as well as the storage and loss moduli increased. The overall significance of all the tests, role of xanthan gum and use of the results are described in the full paper.

References

Casagrande, A. (1948). Classification and identification of soils. Trans. Amer. Soc. Civ. Engrg., 113, 901-930.

Mehta A., Samsami F., Khare Y., Sahin C. (2014). Fluid mud properties in nautical depth estimation. J. Waterway, Port, Coastal, Ocean Eng., 140(2): 210–222.

INTERCOH - Sediment Characterization and Mixtures

O1019 - SEDIMENTARY DYNAMICS ON A THE TOLIARA HIGH TURBID LAGOON (MADAGASCAR) EFFECT OF TIDE AND REEF BREAKING WAVE ON THESE DYNAMICS
Siltation Dredging and Plumes

Moustapha Sow [1], Bamol Ali Sow [2], Cristele Chevalier [3], Jean Luc Devenon [3]
Laboratoire D'océanographie, Des Sciences De L'environnement et Du Climat (losec), Physics, Marseille-France [1] Laboratoire D'océanographie, Des Sciences De L'environnement et Du Climat (losec), Physcis, Ziguinchor-Senegal [2] Institut Méditerranéen D'océanographie (mio), Physics, Marseille-France [3]

This paper investigates the relative influence of the river sediment discharge, the wind-induced current, the tidal current and the incident ocean swell on the sediment (sand and mud) mobility of a micro-tidal of the environment the Toliara reef lagoon (South-West of Madagascar). Fine sands are mainly transported in suspension. The methodological approach combines and compares field measurements with numerical modeling and satellite imagery. The model is based on the 3D hydrodynamic model CROCO, which takes into consideration a set of non-cohesive sediment transport equations, a bottom boundary layer wave-current interaction model and different parametrization of bottom characteristics as geometry and friction coefficient. In this study, we will test different parametrization of settle velocity, deposition rate and erosion to reproduce the high level of turbidity inside the lagoon. Then, we will analyze the respective effects of tidal currents, stormy waves superimposed on tidal currents and wind on lagoon sedimentary process in order to estimate how the lagoon functioning may evolve in the global changing context.

INTERCOH - Siltation Dredging and Plumes

O1036 - ASSESMENT AND FEASIBILITY STUDY FOR IMPLEMENTATION OF NAUTICAL DEPTH APPROACH IN BUSHEHR PORT AND ACCESS CHANNEL
Siltation Dredging and Plumes

Farzin Samsami [1], S. Abbas Haghshenas [2], Mohsen Soltanpour [3], Robert Kirby [4], Mohammad Hossein Nemati [5]
Iau West Tehran Branch, Civil Engineering, Tehran-Iran [1] University of Tehran, Institute of Geophysics, Tehran-Iran [2] K. N. Toosi University of Technology, Civil Engineering, Tehran Iran [3] Semaso Uk, -, Taunton-United Kingdom [4] Ports And Maritime Organization, Coastal Engineering Office, Tehran-Iran [5]

Introduction
Siltation and sedimentation in ports and their navigation and access channels are major problem and navigational control and vessel manoeuvrability will be difficult due to the reduction of the distance between the ship and the bed. The consequent dredging in the basin and access channel is also increased the costs of maintaining and operation in ports. These issues intensify in those areas where the origin of bed material is fine-grained sediment due to the complexity of muddy and also mixed bed behaviour. Ports of Bushehr and Imam Khomeini in the Persian Gulf and port of Anzali in the Caspian Sea are confronted with these issues. In the Bushehr port access channel, due to presence of fine-grained and muddy deposits in the inner and outer channel, special arrangements need to be considered to ensure that the port is accessible and safe for navigation. The upper layer of the bed is usually formed from a fluid mud and dredging of this layer can be very expensive. Increasing the draught of ships causes the ships under keel touch this fluid layer and the ships manoeuvrability is significantly affected. To reduce the amount of dredging and its costs and utilize the scientific and practical methods, some approaches are applied such as active and passive nautical depth. Nautical depth as "the level at which physical characteristics of the bottom reach a critical limit beyond which contact with a ship's keel causes either damage or unacceptable effects on controllability and manoeuvrability" is defined by PIANC (1997). The main goal of this study is to investigate about the possibility of implementing the nautical depth approach in the Bushehr port and access channel.

Sediment Sampling and Laboratory Tests
Eight grab samples were collected from inner and outer channels during a field trip in October 2016 by Darya Negar Pars field survey Team (Darya Negar Pars Consulting Engineers, 2018). The sediment samples were collected using a Van Veen grab sampler and all of them are of the disturbed type. A handy Garmin GPS and also a portable handy depth sounder were used to specify the sediment samples location and depth, respectively. In order to investigate the sediment characteristics in the channel following laboratory tests were designated to be performed: particle size distribution; organic and carbonate contents; rheometry; density, concentration and water content parameters Tests. Particle size distribution was performed in the laboratory of Institute of Materials and Energy using Laser Particle Sizer "analysette22". This Particle Size Analyser is a high-performance particle size analysis system incorporating modes for measuring both dry and liquid samples in the range from 0.16μm to 1160μm. Organic matter influences many properties of sediments as sediment structure, compressibility and shear strength. In addition, it also affects the water holding capacity, biological activity, and water and air infiltration rates. In order to obtain the organic content, we performed test instruction based on ASTM D2974 "Standard Test Methods for Moisture, Ash, and Organic Matter of Peat and Organic Soils". X-ray Fluorescence Spectroscopy (XRF) is

INTERCOH - Sediment Characterization and Mixtures

used to detect sediment elements such as carbonate content. The rheology tests were performed in the Laboratory of Institute of Materials and Energy using "Anton Paar Physica-MCR301" to investigate the changes of the shape (deformations) and quasi-fluid flow of the mud samples. The rheological tests were conducted both in rotary (static) and oscillatory (dynamic) modes using vane and cylinder geometry and be repeated 3 times, (I) after stirring of the sample, (II) after 2 days resting, and (III) after 2 weeks resting.

In-Situ Sediment Characteristics

In order to estimate the fluid mud thickness in each part of inner and outer channel, hydrographic surveys were performed using dual frequency echosounder- DESO30. Multifrequency fathometers operating at 200 kHz and 30 kHz are used to identify the thickness of fluid mud layer (Mehta et al., 2014). Two samples of recorded echograms were shown in Figure 1.

Analysis and Discussion

Figure 2 shows the changes in amounts of sand, silt and clay in the taken samples along the channel. Clay values in surface samples are between 20 and 30%. Physical properties and characteristics of all sediment samples are tabulated in Table 1. The amount of organic matter in the samples is between 0.24 and 0.31 percent, and the amount of carbonate content is somehow same in all samples exclusive of one sample with high sand portion. Figure 3 show sample of rheological properties of sediments i.e. the yield stresses obtained from the oscillatory tests versus the concentration. The amount of clay portion in sediment samples indicate that the sediment behavior is cohesive, and the values of yield stresses obtained from rheological tests are less than 80pa in most samples. The relatively high yield stresses were probably due to the use of the Van Veen sampler, which led to sampling at a lower depth than the fluid mud layer. Based on dual frequency echosounding surveys in the access channel a fluid mud layer (up to 4 meters) were observed. The next phases of the project are to develop 3D hydrodynamic and sediment transport model, perform in-situ density measurments, arrange appropriate dredger for conditioning, conduct pilot project and finally plan implementation strategy.

Sample No.	W (%)	Carbonate (%)	Organic (%)	D_{50} (μm)	Clay (%)	Silt (%)	Sand (%)
1	67	52.92	0.25	4.66	25	72	1
2	60.23	57.23	0.24	8.51	18	77	5
3	80.90	56.3%	0.25	5.22	23	77	-
4	59.85	54.79	0.29	3.39	31	69	-
5	99.35	53.06	0.27	3.22	31	69	-
6	37.45	70.62	0.31	63.76	-	48	52
7	60.25	54.57	0.28	3.62	29	71	-
8	75.08	56.09	0.28	6.77	30	67	3

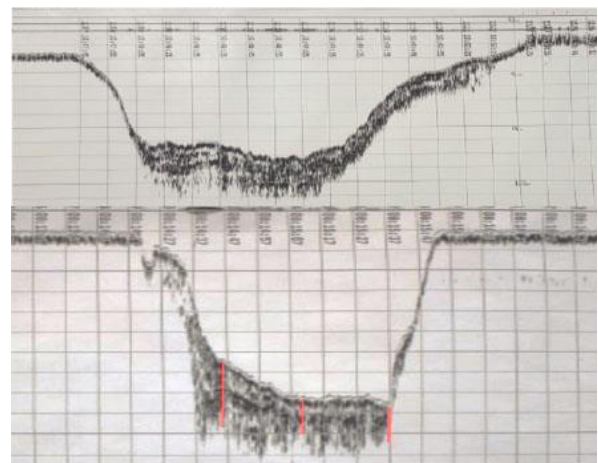Table 1. Physical characteristics of sediment samples

Figure 1. Sample echograms in channel

INTERCOH - Sediment Characterization and Mixtures

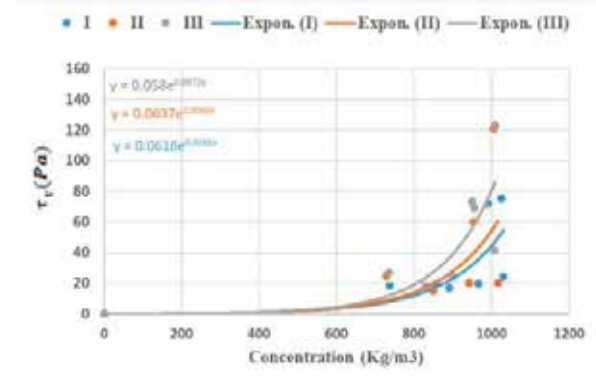Figure 2. Particle sizes along the channel

Figure 3. Yield stresses versus concentration

References

Darya Negar Pars Consulting Engineers, Sediment Sampling and Analysis Report. Prepared for PMO, 2018.

Mehta A., Samsami F., Khare Y., and Sahin C. (2014). Fluid Mud Properties in Nautical Depth Estimation. J. Waterway, Port, Coastal, Ocean Eng., 140(2): 210–222.

PIANC (World Association for Waterborne Transport Infrastructure), "Approach channels, a guide for design", Supplement to Bulletin No. 95, Brussels, Belgium, 1997.

INTERCOH - Sediment Characterization and Mixtures

O1045 - COHESIVE SEDIMENT TRANSPORT THROUGH BOTTOM GRAVITY CURRENTS
Siltation Dredging and Plumes

Firat Testik [1]
University of Texas at San Antonio, Civil and Environmental Engineering, San Antonio
United States [1]

Sediment-driven bottom gravity currents frequently occur in the coastal and oceanic environment. Examples of such gravity currents are sediment underflows formed during coastal dredge disposal operations and turbidity currents formed by dislocations of large volumes of sediment due to geological disturbances. These currents are an important mechanism for sediment transport and are of interest to various engineering and science applications. Depending on the sediment source, both cohesive and non-cohesive sediment gravity currents may occur in the environment. The propagation, deposition, and concentration characteristics of cohesive and non-cohesive currents are vastly different. This study is mainly a laboratory study, and investigates sediment gravity currents of both cohesive and non-cohesive currents in lock-exchange type of tanks. The lock-exchange type tanks consist of two sections: the reservoir section that is initially filled with the current fluid (i.e. sediment-water mixture) and the experimental section that is initially filled with tap water. These two sections are separated by a lock gate, and once the gate is removed, the sediment-water mixture flows into the experimental section as a bottom gravity current. The propagation characteristics of the experimental currents were monitored using video cameras and the concentration structures of these currents were monitored by collecting current fluid at different vertical distances from the tank bottom and at different distances along the tank. Laboratory observations were supplemented with mathematical models and physical interpretations to elucidate the sediment-driven gravity current characteristics. Our efforts revealed that cohesive fluid mud gravity currents exhibited propagation behaviors that are similar to compositional gravity currents with non-Newtonian rheological properties, which differed significantly from their non-cohesive counterparts. The concentration structures and deposition behaviors of cohesive currents and their differences from their non-cohesive counterparts were identified. In this talk, our findings on propagation, deposition, and concentration characteristics of cohesive gravity currents will be discussed, and comparisons with those of non-cohesive gravity currents will be provided. These findings are important in facilitating the development and validation of predictive computational and mathematical models for sediment transport applications, especially for those related to sediment-driven gravity currents.

INTERCOH - Suspended Matter and Flocculation

O1001 - EXPERIMENTAL STUDY ON THE EFFECTS OF ORGANIC MATTERS ON SUSPENDED SEDIMENTS AN INVESTIGATION OF THEIR INTERACTION FORCES AND SETTLING VELOCITIES
Suspended Matter and Flocculation

Jinfeng Zhang [1], Qinghe Zhang [1], Jerome P.-y. Maa [2], Xiaoteng Shen [3], Run Liu [1]
Tianjin University, State Key Laboratory of Hydraulic Engineering Simulation and Safety, Tianjin-China [1] College Of William and Mary, Department of Physical Sciences, Gloucester Point-United States [2] Ku Leuven, Hydraulics Laboratory, Department of Civil Engineering, Ku Leuven-Belgium [3]

Large amounts of organic matters are present in aquatic environments in estuarine and coastal waters (Riley, 1963). Meanwhile, the physical and chemical characteristics of cohesive sediments are largely modified due to the coverage of organic matters (such as humic acid substances and biofilms) on their surface (Maggi, 2009; Fang et al., 2015), which make the effects of organic matters critical on the flocculation process, and thus, the transport of cohesive sediments. To better clarify the biological flocculation processes, two laboratory experiments were conducted in this study: one focused on the impacts of organic matters on the flocculation and settling velocities of cohesive sediments and the other highlighted the interaction forces between the organism-coated suspended particles.
(1) Settling experiments with kaolinite under the various salinity and organic matter conditions in quiescent waters were set up in a settling column. Results show that the settling velocity decreases with an increase of organic matter content in freshwater or in saline water with relatively high salinities (i.e., > 5ppt). In low salinity (i.e., < 1ppt) saline waters, the settling velocity increases first and then decreases, and reaches a peak value when the organic matter concentration is 30mg/L. Based on the above observations, a new empirical formula of settling velocity considering organic matter and salinity is proposed by fitting the experimental results.
(2) The floc morphology against different organic matter contents was also investigated in our experiments. With an increase of organic matter content in the water, the floc size at first increases and then decreases. The interaction forces between latex particles and organism-covered particles were measured by an atomic force microscopy (AFM). Compared with the eXtended DLVO (XDLVO) theory, the repulsive force between particles with biological effects is larger than the extended DLVO force. With the increase of the organic matter content, the Van der waals attraction force between the latex particle and organism-covered particle gradually decreased and the repulsive force increased.
(3) According to the experimental results of the interaction forces between particles under salinities of 200 and 300 mol/L, a new formula of the inter-particle forces between particles with organic matter attaching is proposed, based on the XDLVO theory and regression analysis.

References

Fang, H.W., Zhao, H.M., Chen, Z.H., Chen, M.H., Zhang, Y.F. (2015) 3D shape and morphology characterization of sediment particles. Granular Matter, 17(1): 135-143.
Maggi, F. (2009) Biological flocculation of suspended particles in nutrient-rich aqueous ecosystems. Journal of Hydrology, 376(1–2): 116-125.
Riley,G.A. (1963) Organic aggregates in sea water and the dynamics of their formation

INTERCOH - Suspended Matter and Flocculation

O1004 - THE COMPOSITION OF SUSPENDED PARTICULATE MATTER IN MARINE COASTAL AREAS
Suspended Matter and Flocculation

Fettweis Michael [1], Riethmüller Rolf [2], Verney Romaric [3], Schartau Markus [4], Lee Byung Joon [5]
Royal Belgian Institute of Natural Sciences, Od Nature, Brussels-Belgium [1] Helmholtz Centre, Institute for Coastal Research, Geesthaacht-Germany [2] Ifremer, Laboratoire Dhysed, Plouzané-France [3] Helmhotz Centre, Geomar, Kiel-Germany [4] Kyungpook National University, Department of Construction and Environmental Engineering, Sangju Korea, South [5]

The seasonal dynamics of Suspended Particulate Matter (SPM) along the cross-shore gradient, from the coastal zone to the offshore has attracted considerable attention in recent years (e.g. Maerz _et al._, 2016; Li _et al._, 2017; Fettweis & Lee, 2017; Shen _et al._, 2018). SPM incorporates inorganic minerals of physico-chemical and of biogenic origin and it embeds living and non-living organic matter (OM). The increase of the OM content of the SPM with decreasing SPMC (see Figure 1) and to a first order with distance from the coast is a known general feature (Schartau et al., 2019). Based on water sample Loss-on-Ignition (LoI) and SPMC data from the German Bight, Schartau et al. (2019) have devised an analytical model for estimating fractions of inorganic and two types of OM as a function of SPMC. Applied to satellite SPMC, the model provided insights into temporal and spatial variations in SPM and OM features across the German Bight. However, the model does not resolve how the OM is composed of preserved or refractory and labile portions. Their ratios vary due to the seasonal formation and decay of fresh organic matter by algae bloom and bacterial activity (Ittekkot, 1988; Keil _et al._, 1994). The labile fraction is one control of the SPM transport features as it is linked with the occurrence of transparent exopolymeric particles (TEP) (e.g. Alldredge _et al._, 1993). TEPs may act as biological glue increasing particle stickiness during aggregation, thereby enhancing the formation of larger flocs with larger settling velocities (e.g. Fettweis _et al._, 2014, Lee _et al._, 2019). As an example, nearshore data from the Belgium coast show that Chl-a is high between March and September with the prominent algae bloom in spring and with a secondary peak in summer and low during winter (Figure 2a). The particulate organic carbon (POC) content in the SPM shows little variation over the whole year, except during the spring bloom when the POC content also increases. The POC here includes some persistent fraction of OM. This fraction remains unvalued by Chl-a data that may act only as a proxy for the labile fraction of the OM. The labile fraction is subject to seasonal build-up and decay of fresh OM, e.g. during algal growth or during degradation by bacteria. The "freshness" of the OM, as indicated by the Phaeophytine /Chl-a ratio, is lower in winter compared to the rest of the year, Phaeophytine being associated with decaying Chl-a (Figure 2b).

The aim of the present study is twofold. Firstly, we want to validate the Schartau _et al_. (2019) model with LoI and POC data from other areas. Secondly, we want to investigate how the labile fraction of the OM, as calculated by the model, is correlated with CHL-a and the concentrations of Phaeophytine and TEP to allow model refinements and to generate improved data sets, resolving spatio-temporal characteristics of those OM components that are relevant for the near-shore SPM dynamics and element cycling.

INTERCOH - Suspended Matter and Flocculation

References

Alldredge A.L., Passow U., Logan B.E., Howarth M. (1993). The abundance and significance of a class of large, transparent organic particles in the ocean. Deep Sea Res. I 40, 1131–1140.

Fettweis M., Baeye M., Van der Zande D., Van den Eynde D., Lee B.J. (2014). Seasonality of floc strength in the southern North Sea. J. Geophys. Res. Oceans 119, 1911–1926.

Fettweis M., Lee B.J. (2017). Spatial and seasonal variation of biomineral suspended particulate matter properties in high-turbid nearshore and low-turbid offshore zones. Water 9, 694.

Ittekkot V. (1988). Global trends in the nature of organic matter in river suspensions. Nature 332, 436–438.

Keil R.G., Montluçon D.B., Prahl F.G., Hedges J.I. (1994). Sorptive preservation of labile organic matter in marine sediments. Nature 370, 549–552.

Lee B.J., Kim J., Hur J., Choi I.H., Toorman E., Fettweis M., Choi, J.W. (2019). Seasonal dynamics of organic matter composition and its effects on suspended sediment flocculation in river water. Water Resources Research (accepted).

Li D., Li Y., Xu Y. (2017). Observations of distribution and flocculation of suspended particulate matter in the Minjiang River Estuary, China. Mar. Geol. 387, 31–44. - 2 –

Maerz J., Hofmeister R., van der Lee E.M., Gräwe U., Riethmüller R., Wirtz K.W. (2016). Maximum sinking velocities of suspended particulate matter in a coastal transition zone. Biogeosci. 13, 4863–4876.

Schartau M., Riethmüller R., Flöser G., van Beusekom J.E.E., Krasemann H., Hofmeister R., Wirtz, K. (2019). On the separation between inorganic and organic fractions of suspended matter in a marine coastal environment. Prog. Oceanogr. (in press).

Shen X, Toorman EA, Lee BJ, Fettweis M. (2018). Biophysical flocculation of suspended particulate matters in Belgian coastal zones. J. Hydrol. 567, 238-252.
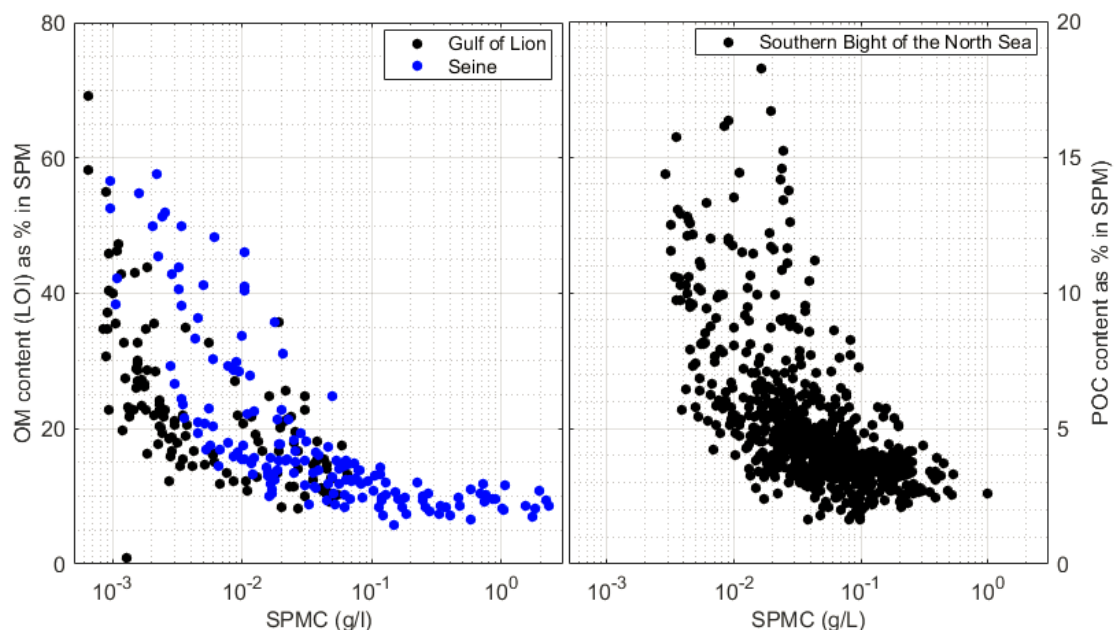
Fig. 1. Organic matter content in the SPM from determined through LoI (left) and element analysis (right). Both data set show that largest variation in organic matter content occurs at low SPMC.

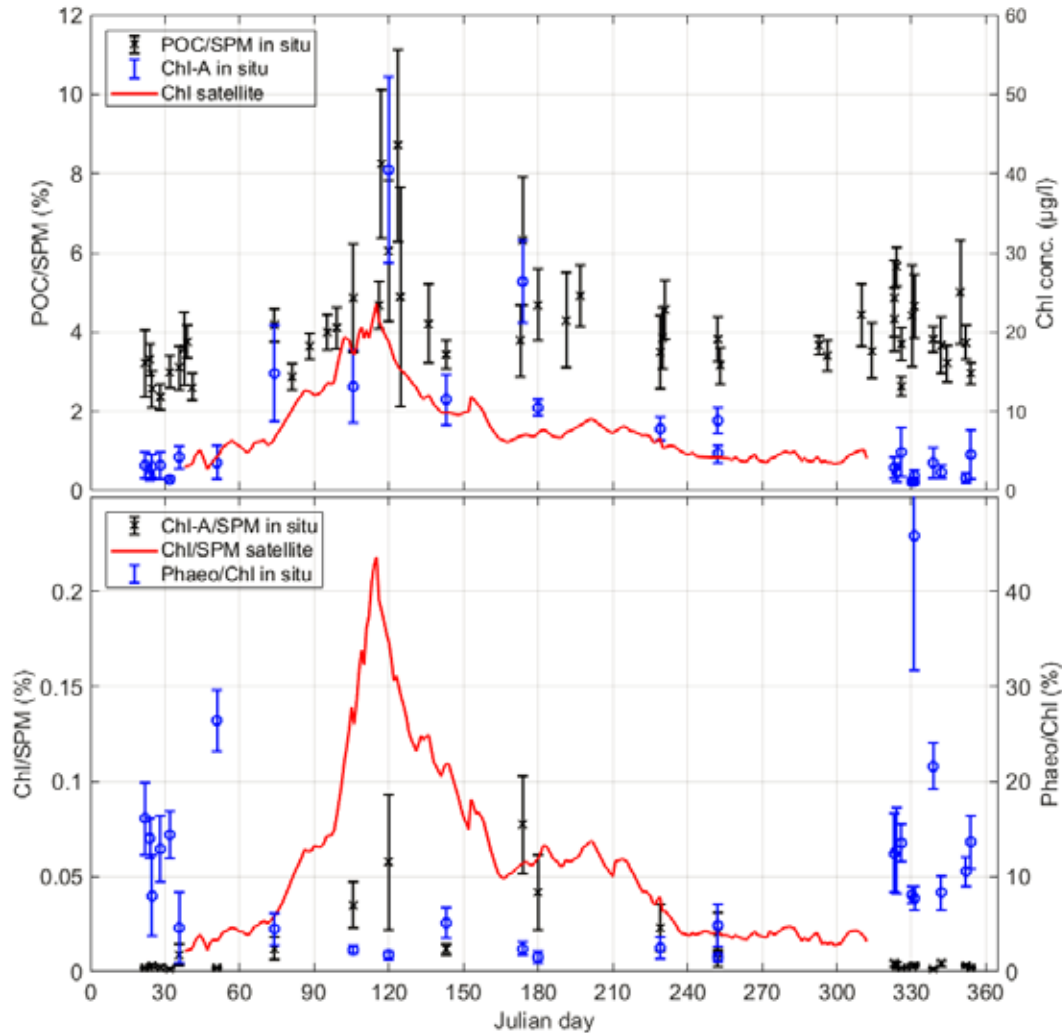## INTERCOH - Suspended Matter and Flocculation

Fig. 2. Seasonal variation of the OM (above) and the Chl and Phaeophytine content of the SPM (below) derived from water samples taken in the Belgian nearshore in 2000-2018. Each dot and errorbar represents the mean and standard deviation of 13 samples taken during a tidal cycle. The solid line is the surface Chl concentration derived from MERIS satellite over the period 2002-2012.

15th INTERNATIONAL CONFERENCE on
COHESIVE SEDIMENT TRANSPORT PROCESSES
13 - 17 OCTOBER 2019 • ISTANBUL / TURKEY
YILDIZ TECHNICAL UNIVERSITY - YILDIZ CAMPUS

YILDIZ TEKNİK ÜNİVERSİTESİ 1911

INTERCOH - Suspended Matter and Flocculation

O1017 - MULTI CLASS FLOC SIZE DISTRIBUTIONS OF COHESIVE SEDIMENTS AT STATION XULIUJING OF THE CHANGJIANG RIVER ESTUARY
Suspended Matter and Flocculation

Xiaoteng Shen [1], Erik Toorman [2], Yuyang Shao [3], Michael Fettweis [4]
Hohai University, Key Laboratory of Coastal Disaster and Defense of Ministry of Education, Nanjing-China [1] Ku Leuven, Department of Civil Engineering - Hydraulics, Leuven-Belgium [2] Hohai University, College Of Harbour, Coastal and Offshore Engineering, Nanjing-China [3] Royal Belgian Institute of Natural Sciences, Operational Directorate Natural Environment, Brussels-Belgium [4]

Introduction

To manage coastal and estuarine waters, it is critical to accurately predict the movements of cohesive and non-cohesive sediments. There are well-established methods to estimate the behavior of non-cohesive sediments; however, without extensive knowledge on flocculation processes it remains difficult to predict the behavior of cohesive sediments. Flocculation is one of the main processes (e.g., erosion, deposition, settling, consolidation and flocculation) in cohesive sediment dynamics. The study of flocculation is an interdisciplinary work since it relates to various physical (e.g., transport, settling and deposition), chemical (e.g., contaminant uptake and transformation) and biological (e.g., community structure activities and metabolism) activities. Nevertheless, a widely-accepted flocculation model that can quantitative simulating the Floc Size Distributions (FSDs) for a relatively large study domain has not yet been fully developed. Recently, Lee et al. (2012) have pointed out that an observed FSD by LISST (Laser In Situ Scattering and Transmissometry) instrument can be decomposed into subordinate lognormal distributions for microflocs, macroflocs and megaflocs. With this three-class FSD decomposition, the accuracies of predicted settling velocities are largely enhanced compared with single-class approach. This method has been used in the well-mixed Belgian coast (Shen et al., 2018). Nevertheless, it is not clear if the FSDs in other regions can be analyzed and simulated in the same way for a broader application. Therefore, this study aims to implement an improved quadrature-based Population Balance Equation (PBE), based on that given by Shen and Maa (2015), on a 1-D vertical hydrodynamic model (Shao et al., 2017), to simulate the floc sub-populations in the Changjiang River Estuary. The long term target is to better investigate the FSDs and the particle dynamics in 3-D estuarine models.

Field measurements

Field work was carried out at station Xuliujing of the Changjiang River Estuary, in the wet season of the year 2016. In this study, navigation data of two typical tidal cycles that represents spring and neap tidal conditions respectively are highlighted to investigate the water levels, flow velocities, turbulences, salinities, suspended sediment concentrations (SSCs) and FSDs. Velocity profiles were collected by a shipboard downward-looking ADCP (Acoustic Doppler Current Profiler), the in-situ flocculated FSDs were measured with the LISST-100 (type C), and samples from different water levels were analyzed to determine the salinities, SSCs and primary particle size distributions. Notably, the measured FSDs were automatically decomposed into microflocs, macroflocs and megaflocs using the software DistFit (Lee et al., 2012).

INTERCOH - Suspended Matter and Flocculation

Flocculation Model

The general transport equation (i.e., the PBE) that includes the kinetics of aggregation and breakage of flocs with size L can be expressed by:

$$\frac{\partial n(L,z,t)}{\partial t} + (w-w_s)\frac{\partial n(L,z,t)}{\partial z} - \frac{\partial}{\partial z}\left(\frac{v_t}{\sigma_t}\frac{\partial n(L,z,t)}{\partial z}\right)$$

$$= \frac{L^2}{2}\int_0^L\left[\frac{\beta\left((L^3-\lambda^3)^{1/3},\lambda\right)\cdot\alpha}{\left(L^3-\lambda^3\right)^{2/3}}\cdot n\left((L^3-\lambda^3)^{1/3},z,t\right)\cdot n(\lambda,z,t)\right]d\lambda$$

$$- n(L,z,t)\int_0^\infty \beta(L,\lambda)\alpha(L,\lambda)n(\lambda,z,t)d\lambda$$

$$+ \int_L^\infty a(\lambda)\cdot b(L\,|\,\lambda)\cdot n(\lambda,z,t)d\lambda - a(L)\cdot n(L,z,t) \qquad (1)$$

where $n(L, z, t)$ is the number density function defined on the basis of floc size L at any location z at time t with

$$n(z,L,t) = \sum_{i=1}^{3} w_i(z,t)\cdot\delta(L-L_i(z,t)) \qquad (2)$$

in which L_i and w_j (i = 1, 2, 3) are the representative sizes and weights of microflocs, macroflocs and macroflocs. Additionally, w is the vertical velocity along, w_s is the settling velocity, v_t is the eddy viscosity, σ_t is the turbulent Prandtl-Schmidt number, β is the collision frequency function, α is collision efficiency function, a is breakup frequency function and b is fragmentation distribution function. The right hand side of Eq. 1 include: (i) the birth of flocs with size L due to aggregation of smaller particles, (ii) the death of flocs with size L due to aggregation with other particles, (iii) the birth of flocs with size L due to fragmentation of bigger particles and (iv) the death of flocs with size L due to breakup into smaller particles. The left hand side terms include, from left-to-right, an unsteady term, an advection & settling term and a diffusion term, respectively.

Results

The results at a well-mixed estuary show that the 1-D vertical model in this study can reasonably reproduce the velocity profiles (Fig. 1). The model predicted sizes $L1$, $L2$ and $L3_3$ also match the sizes of microflocs, macroflocs and megaflocs of the observed FSD. Additional validations of subpopulations of FSDs in Changjiang River Estuary will be represented.

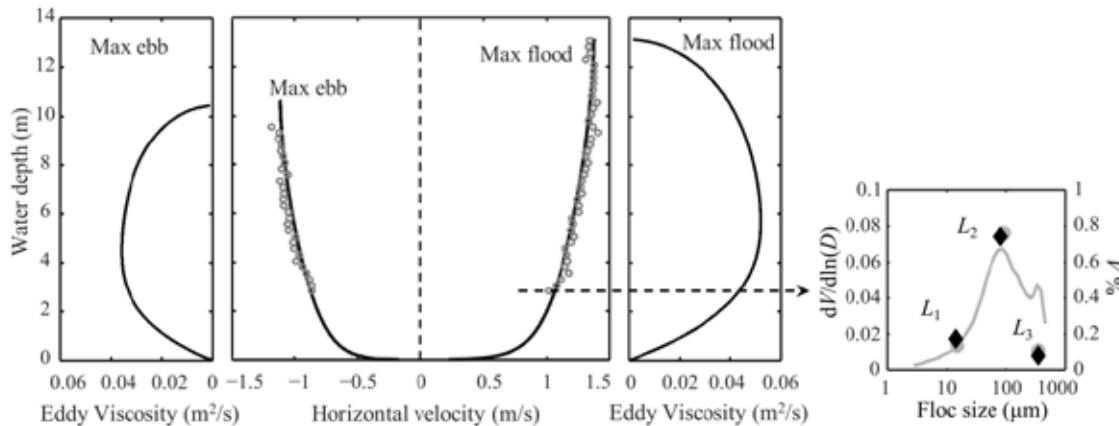**INTERCOH - Suspended Matter and Flocculation**

Fig. 1 An example of predicted velocity and eddy viscosity profiles at the maximum flood and the maximum ebb at a well-mixed estuary (modified from Shen et al., 2018). The FSD at a selected location is presented by subpopulations of microflocs ($L1$), macroflocs ($L2$) and megaflocs ($L3$). Symbols and lines in grey color are measurements and that in dark color are model predictions.

Conclusions

In summary, a framework is proposed based on implementing a quadrature-based PBE in a hydrodynamic model to mimic the representative sizes and their volume fractions of microflocs, macroflocs and megaflocs at station Xuliujing of the Changjiang River Estuary. This study, an integrated flow-turbulence-sediment model, although only validated in a 1-D vertical application at current stage, is a preliminary work to contribute to large scale simulations with comprehensive wave, suspended particles and water quality modules in the future.

Acknowledgements

References

Lee, B.J., Fettweis, M., Toorman, E., Molz, F.J. (2012). Multimodality of a particle size distribution of cohesive suspended particulate matters in a coastal zone. *Journal of Geophysical Research: Oceans*, 117: C03014.

Shao, Y., Shen, X., Maa, J.P.Y., Shen, J. (2017). Simulating high ebb currents in the North Passage of the Yangtze estuary using a vertical 1-D model. *Estuarine Coastal and Shelf Science*, 196: 399-410.
Shen, X., Maa, J.P.Y. (2015). Modeling floc size distribution of suspended cohesive sediments using quadrature method of moments. *Marine Geology*, 359: 106-119.
Shen, X., Lee, B.J., Fettweis, M, Toorman, E.A. (2018). A tri-modal flocculation model coupled with TELEMAC for estuarine muds both in the laboratory and in the field. *Water Research*, 145: 473-486.

module in Telemac to model suspended sediment transport. The mud model is calibrated against the mass balance for the estuary, tidal ensembles of measured suspended sediment concentration (SSC) and estimates of siltation on intertidal flats in the Upper Sea Scheldt. It is important to note that the model does not include morphological feedback, or the effect of SSC on water density.

The effect of different human interventions needs to be quantified with the estuary in an estimated future state (2050). In order to deal with the uncertainty in autonomous development, runs are performed with an ensemble of boundary conditions that reflect different scenarios of climate change and evolution of tidal amplitude in the Scheldt estuary. Planned interventions (eg measures for safety against flooding) are included in the model.

Results

The model shows that the mud dynamics in the Upper Sea Scheldt are dominated by downstream advective transport. This corresponds with a recent sediment balance (mud and sand) for the upper and lower Sea Scheldt (Vandenbruwaene et al., 2017). This result is also checked against eight different measures of (eularian) tidal asymmetry.

When quantifying tidal asymmetry from a model run with limited temporal resolution in its output (1h intervals), the skewness of the distribution of the time derivative of water level is shown to be a good approximation of the ratio of duration of rising to falling tide, which loses a lot of its predictive power when the interval of model output becomes larger than 1h.

Total sediment transport [kg/s] is decomposed in sediment transport related to advection and tidal pumping by decomposition of the cross section, the cross-sectionally averaged velocity and cross-sectionally averaged sediment concentration into their tidal averages and its deviation. Model results are explained in terms of this decomposed sediment transport.

Deepening the Durme tributary (a human intervention, part of implementing a "sustainable bathymetry") is expected to increase bottom shear stress (and thus resuspension capacity) downstream of the tributary and reduce it upstream. The implementation of a sluice at the upstream edge of the estuary, increases reflection of the tidal wave, and increases tidal amplitude.

Expected climate change is parametrised both at the downstream and upstream boundary of the model. Two scenarios for sea level rise are considered (+15cm and +40cm in 2050). The upstream boundaries of fresh water discharge (Q in Figure 1) is a synthetic timeseries that is perturbed due to climate change. The sediment concentrations at the model boundaries are assumed to stay the same. The perturbed fresh water discharge [m³/s] is higher in the 2050 simulations then in the simulations of the current situation, which means higher downstream sediment transport and higher SSC in the Upper Sea Scheldt. The combination of the change in bathymetry and the change in boundary conditions together provide an estimate of the autonomous development in the zone of interest.

The human interventions that have been investigated in the project so far all include a deepening of a canalised river section at the upstream end of the estuary. This deepened section acts as a sediment trap, which dominates the initial response of the model. More sediment is retained upstream, lowering the expected SSC in the Upper Sea Scheldt.

References

Smolders, S.; Bi, Q.; Vanlede, J.; De Maerschalck, B.; Plancke, Y.; Schramkowski, G.; Mostaert, F. (2018). Integraal plan Boven-Zeeschelde: Sub report 6 – Scaldis Mud: a Mud Transport model for the Scheldt Estuary. Version 4.0. FHR Reports, 13_131_6. Flanders Hydraulics Research: Antwerp.

Vandenbruwaene, W.; Levy, Y.; Plancke, Y.; Vanlede, J.; Verwaest, T.; Mostaert, F. (2017). Integraal plan Boven-Zeeschelde: Deelrapport 8 – Sedimentbalans Zeeschelde, Rupel en Durme. Versie 4.0. WL Rapporten, 13_131_8. Waterbouwkundig Laboratorium: Antwerpen.

Vanlede, J., Smolders, S., Maximova, T., & Teles, M. J. (2015). The 3D Unstructured SCALDIS Model. A new high resolution model for hydrodynamics and sediment transport in the tidal Scheldt. The Hague: IAHR.

INTERCOH - Suspended Matter and Flocculation

O1039 - USING SATELLITE IMAGERY FOR STUDYING THE DYNAMICS OF THE RIO DE LA PLATA TURBIDITY FRONT.
Suspended Matter and Flocculation

Francisco Pedocchi [1], Fernanda Maciel [1], Pablo Santoro [1]
Universidad De La Republica, Uruguay, Instituo De Mecanica De Los Fluidos E Ingenieria Ambiental, Montevideo-Uruguay [1]

Both remote sensing and numerical modeling studies heavily rely on field data for calibration and validation, but they are seldom used to validate each other. In this work we used the turbidity front detected from satellite imagery to evaluate the performance of a numerical hydro-sedimentological model of the Rio de la Plata.

The Rio de la Plata is a micro-tidal estuary located between Argentina and Uruguay in South America. It is approximately 280 km long and its width increases from 20 km at the inner part to 220 km at its mouth. Due to its large extension, satellite images are one of the few tools able to provide a synoptic view of the estuary. The estuary receives an annual mean flow of 22.000 m3/s from the Parana and Uruguay rivers, and 160x106 tons/yr of sediment, which are mostly cohesive sediments coming from the upper Parana River basin.

The following data was available for studying the response of the system to the main forcings: daily discharges of the main tributaries from 2001 to 2017 (the mean discharge for the 2014-2017 period was 24250 m3/s); wind data every six hours from the European Centre for Medium-Range Weather Forecasts (ECMWF); CTD salinity measurements at two sites along the northern coast of the Rio de la Plata (just in front of Montevideo and approximately 40 km to the W).

We used images from the MODIS-Aqua satellite mission from 2014 to 2017. The images have a spatial resolution of approximately 1 km and a daily time step, and we used the red channel reflectance (wavelength of 645 nm) to detect the turbidity front location. The turbid river water in the inner and intermediate regions of the estuary has high reflectance, while the clear seawater in the outer zone and continental shelf has negligible reflectance. This allowed us to implement an image-based, autonomous algorithm, defining the turbidity front as a reflectance level that 'best' separates the two reflectance regions.

We analyzed the distribution of the front location over the 2014-2017 period, and found that the front location along the Uruguayan coast is more often located to the E of Montevideo, approximately 60% of the time, being the maximum eastward distance 143 km. On the other hand, we observed that the front could recede up to 70 km to the W of Montevideo. The turbidity front location along the Uruguayan coast presented statistically significant linear correlation with the Parana and Uruguay river discharges, with larger discharges being associated with positions further to the E. Regarding the wind, we observed as a general trend that positions to the W are associated with relatively weaker winds from all directions, while positions to the E show a larger scatter and are more frequently associated with stronger winds. We also observed a general trend in the data indicating that the front location along the north coast was particularly affected by winds coming from the SW and ENE directions.

INTERCOH - Suspended Matter and Flocculation

However, it should be highlighted that strong winds are also more prone to generate waves and induce sediment resuspension, which results on the turbidity front location effectively moving to the E.

The turbidity front location was also obtained from a numerical 3D hydro-sedimentological model for the Rio de la Plata. The model was implemented in TELEMAC MASCARET, with wave generation and propagation simulated with the TOMAWAC module, and hydrodynamics, sediment transport and bottom evolution solved using TELEMAC 3D.

The turbidity front locations obtained from the numerical model were compared to the ones from remote sensing presented above. The same algorithm for the turbidity front detection was applied to the modeled suspended sediment concentration in the upper 4 layers of the water column. This took into consideration that satellite images are able to characterize surface turbidity, hence we compared suspended sediment concentration near the surface with remote sensing turbidity. For this comparison, the study period was 2015-2016, as model results were readily available. With a similar procedure, the salinity front was identified in the model in order to analyze the role of salinity on the front position.

The results of the comparison are encouraging, showing that the numerical model is able to capture the complex dynamics of the turbidity front in several occasions (Figure 1). The combined analysis of the model results for the suspended sediment and salinity fronts, and the satellite images, showed that salinity may be playing a significant role on the turbidity front dynamics. This is a novel result, as previous studies where the model results were compared with point measurements, used to indicate that resuspension was the main process driving local turbidity; these new results emphasize the role of flocculation, particularly during mild conditions. The synoptic view provided via satellite imagery allowed for a better understanding of the model limitations, gaining insight into the processes that dominate larger temporal scales of sediment dynamics, and identifying potential improvements to the model.
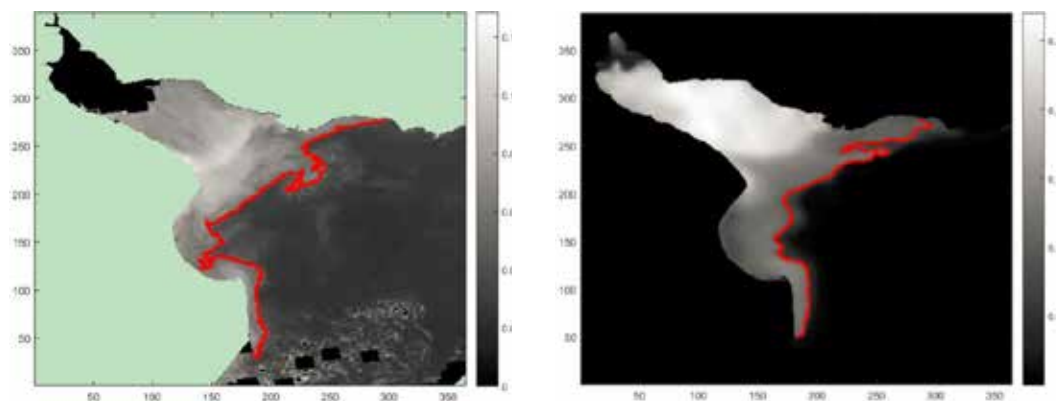

Figure 1: Synoptical comparison of the model results with satellite imagery. Left, satellite image. Right, model results. Axes units are relative distances in km.

INTERCOH - Suspended Matter and Flocculation

O1042 - FLOC DYNAMICS AT THE INTERFACE BETWEEN ESTUARIES AND COASTAL SEAS FROM THE TIDAL SCALE TO THE SEASONAL SCALE
Suspended Matter and Flocculation

Marion Chapalain [1], _Romaric Verney [1]_, Michael Fettweis [2], David Le Berre [1], Matthias Jacquet [1], Pierre Le Hir [1]
Ifremer, Dyneco/dhysed, Plouzané-France [1] Rbins, Odnature, Brussels-Belgium [2]

Context
Suspended particulate matter (SPM) dynamics in tidal systems is driven by cyclic processes: erosion, advection, flocculation and deposition. Flocculation processes have been extensively studied over the last three decades, mainly in laboratory or in estuaries, where strong hydrodynamic and sediment concentration gradients are observed. These investigations identified turbulence, concentration as the primary controlling factors of aggregation and fragmentation, secondary modulated by salinity and potentially by organic matter content. The influence of the latter was demonstrated mainly in laboratory, and punctually observed in situ. In the present study we focused on the influence of organic matter content on flocculation processes in a pivotal environment, at the interface between estuaries and coastal seas and based on an original 3-year in situ dataset.

Methods
14 field campaigns were conducted from 2016 to 2018 within the Seine river plume and the near Seine Bay in order to investigate flocculation dynamics and the potential relationship with the OM content. These campaigns consisted of ship-based monitoring and sampling through 12-h tidal cycle cruises carried out along the annual cycle (~ every 2/3 months, mainly spring tides) at two fixed stations: La Carosse (LC), at the mouth of the Seine estuary in the turbid plume, and BS1, located more offshore. During these surveys, we used a floating platform equipped with two downward looking RDI 1200kHz and 600kHz ADCP continuously recording along the 12-h tidal cycle. Every hour, samples at the sub-surface and 1m above the bed were collected from a horizontal Niskin bottle sampler for quantifying suspended sediment concentration (SSC), TEP, total OM (loss of ignition method) and chlorophyll a concentration. Finally, a frame equipped with a CTD profiler, an OBS3+, a turbidity meter (Wetlabs FLNTU) and a LISST100X was deployed at 15-min intervals during the tidal cycles. Dedicated post-processing methods were developed for LISST analysis, especially in the salinity gradient (flagging the Schlieren effect), but also in low SSC conditions.

Results
At the tidal scale, the turbulence is the main driver of flocculation processes, whatever the season. The usual cycle "low turbulence / large floc" to "high turbulence / small flocs" is well observed, as illustrated in fig. 1B. The influence of SPM concentration is not straightforward, as dynamically correlated with turbulence and settling.

At the seasonal scale, the organic content is shown to modulate the flocculation dynamic, using both the OM fraction and the Chla concentration as proxy: on average, the larger the OM

INTERCOH - Suspended Matter and Flocculation

content, the larger the flocs (Figure 2). The influence of the organic content was also observed at the tidal scale: during spring/summer periods when OM content is the largest, flocs are more resistant to breakup for similar hydrodynamic conditions, illustrating the increased cohesiveness of the particles forming flocs due to OM coating. Flocs formed in high OM conditions are also shown to be less dense, either due to the contribution of organic (low density) particles to flocs or to the modification of the floc structure (Fig. 1B).

TEP concentration was also measured from samples, however it was not possible to use this parameter as a proxy for characterizing the SPM dynamics, probably due to the various organic sources contributing to TEP.

Conclusions

This original dataset was used to examine the flocculation dynamics from the tidal scale to the seasonal scale, emphasizing the primary control of floc size by turbulence and the importance of the OM content, enhancing the formation of floc size of lower density but more resistant to shear break. These results will next be used to revisit the flocculation numerical models and evaluate the influence of these OM/sediment interactions on sediment fluxes.
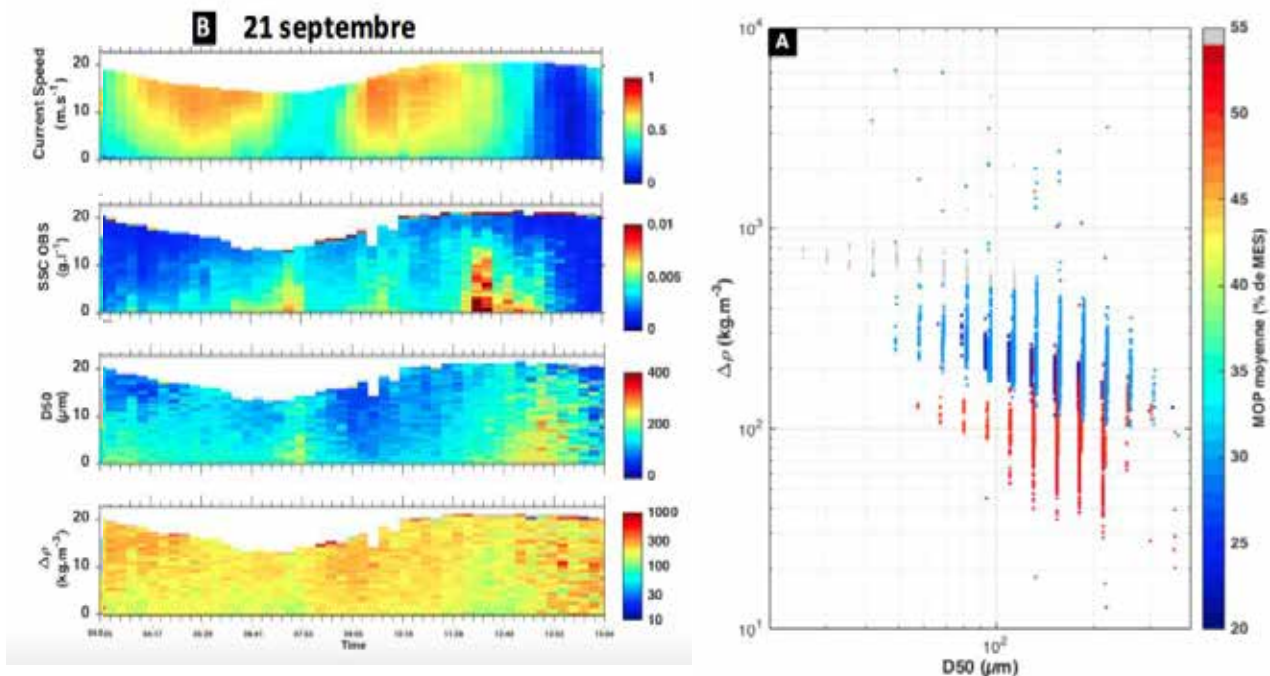
Fig. 1. Example of the SPM dynamics at the tidal scale (B) and seasonal floc population variability (A) at the interface between estuary and bay

INTERCOH - Suspended Matter and Flocculation
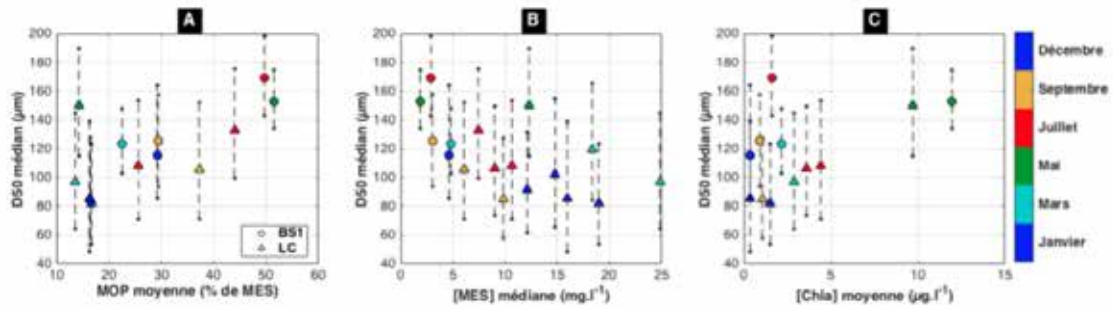
Fig. 2. Influence of organic content on floc size : average median flocs size versus chla concentration, SPM concentration and OM content (%)

INTERCOH - Suspended Matter and Flocculation

O1047 - FROM LASER DIFFRACTION TECHNIQUES TO PARTICLE SIZE DISTRIBUTION MEASUREMENTS AND INTERPRETATION OF DATA
Suspended Matter and Flocculation

Zeinab Safar [1], Claire Chassagne [1], Julie.d Pietrzak
Tu Delft, Environmental Fluid Mechanics, Delft-Netherlands Antilles [1]

Laser diffraction techniques such as LISST (Laser In Situ Scattering and Transmisometry) are usually used to determine the Particle Size Distribution (PSD) of Suspended Particulate Matter (SPM) and sediments in situ. The volume concentrations of particles are divided in 32 logarithmically spaced effective spherical diameter classes ranging for the 100X type from 2.7 to 460 um [2, 13]

However, sediment particles in natural waters are sometimes far from spherical and can have different shapes and orientations depending on their composition and settling mechanisms [6, 7]. For instance particles (flocs) that are composed of organic matter occulated with sediment can contain semi-transparent exo-polymers of low density [9,10]. Biological species such as different types of algae can have very elongated anisotropic shapes because they move through the water column in cell chains. These algae can also flocculate with sediment and form elongated flocs [3, 11]. Elongated flocs are also formed by differential settling when the water column turbulence is low specially by calm weather during the neap tides. These different types of particles impact the PSD measurement of the LISST (and other laser diffraction techniques used in the laboratory), as the software used to convert the raw data into sizes is based on the assumption of spherical particles.

Combining the LISST results with other in situ measurement techniques such as camera recording gives insight in the particle shape and its impact on the interpretation of the PSD measured by the LISST [8]. In our study LISST-HOLO (Submersible Digital Holographic Camera), LabSFLOC settling column camera system and underwater camera were used to define the relation between the shape of the particles and the measured PSD by LISST 100X.

LISST 100X and LISST-HOLO were deployed in Dutch coastal area 10 km from the Rhine river mouth and 12m depth mooring during the STRAIN II (Stratification Impact on Near-shore Sediment Transport) project from 17th September to 07th October 2014. The LISST 100X and the LISST-HOLO were placed at 1.65 mab and 1.40 mab respectively [5]. During a one day (13 h) boat survey, underwater camera and LabSFLOC settling column camera system were used to measure the settling velocity, density, size and shape of the particles and compare them with the LISST 100X and LISST-HOLO data from the mooring.

During the neap tide and calm weather conditions of that day, the measured PSD by the LISST 100X were mostly tri-modal distributed ranging from a peak at small particles (70 um), a medium peat (100 - 200 um) and higher sizes (300 - 400   m). The LISST-HOLO and underwater camera pictures showed presence of a lot of elongated particles that were most probably Skeletonema algae particles and organic matter occulated to some extend with sediment [1, 12]. Based on these photos and settling velocity measurements by the LabSFLOC settling column camera system, 3 types of particles could be distinguished:

1. High settling velocity, high density (close to 1600 kg.m3), composed of sediment and organic matter.

2. Moderate settling velocity, density (close to 160 kg.m3), open ocs composed of sediment and algae, with semi-transparent parts.

15th INTERNATIONAL CONFERENCE on COHESIVE SEDIMENT TRANSPORT PROCESSES
13 - 17 OCTOBER 2019 • ISTANBUL / TURKEY
YILDIZ TECHNICAL UNIVERSITY - YILDIZ CAMPUS

INTERCOH - Suspended Matter and Flocculation

3. Low settling velocity and low density (close to 16 kg.m3), highly anisotropic particles, algae alone or algae bound to little sediment.

It is the presence of anisotropic particles, which are mostly algae and biological species that cause the apparition of tri-modal PSD's as the extra peak in the range of 300 - 400 _m that appears is due to their random orientation during the laser diffraction measurement.

During the stormy weather conditions in the days that followed with high wave and wind activity re-suspended the bed material, and the measured PSD by LISST 100X turned from tri-modal to bi-modal and mono-modal with higher fraction of _ne sediment sizes. The LISST-HOLO displayed also mostly spherical _ne sediment particles.

High bed shear stresses, that exceeds threshold of _ne sediment and silt resuspention [4] confirmed that the measuredparticles are indeed resuspended fine sediment from the bed during the storm. At the beginning of the storm however, the PSD turned from tri-modal to bi-modal indicating the first material eroded from the bed(the u_ layer) is a combination of occulated organic matter and sediment. After depletion of this u_ layer, the PSD turned to mono-modal indicating the resuspension of _ne sediments from the bed.

During the spring tide, the PSD switched between multi-modal and mono-modal, as the water column switched from stratified to well mixed condition. When the water column was stratified by the river front arrival, the PSD was then mostly bi- or tri-modal. When the water column became well mixed by tidal forcing the PSD was mono-modal, indicating resuspension of _ne sediment from the bed.

The influence of the flood and ebb tidal cycles on the particles were also analyzed, it seems that the water column stratification and mixing condition due to frontal dynamics is the most influential on the shape, size and the composition of the SPM particles in the Rhine region of Fresh water Influence (ROFI) part of the Dutch coastal area.

The tri-modal PSD appeared to be an artifact, where elongated particles such as algae particles and organic debris are present. Therefore the tri-modal PSD's have to be treated with caution while interpreting the data and modeling flocculation by size classes. Appearance and shifting the large size classes peaks does not always indicate flocculation or break up of the particles, but highly anisotropic particles are disappearing from the water column or shadowed by smaller particles.

Bibliography
[1] A.L. Alldredge and C.C. Gotschalk. Direct observation of the mass flocculation of diatom blooms: Characteristics, settling velocities and formation of diatom aggregates.
[2] Y.C. Argrawal and P. Traykovski. Particles in the bottom boundary layer: Concentration and size dynamics through events. Journal of Geophysical research, 106:9533{9542, 2001.
[3] S. Balzando, Dianasarno, and W.H.C. Koostra. Effects of salinity on the growth rate and morphology of ten skeletonema strains. Journal of plankton Research, 33:937{945, 2011.
[4] Ra_ul P. Flores, Sabine Rijnsburger, Saulo Meirelles, Alexander R. Horner-Devine, Alejandro J. Souza, Julie D. Pietrzak, Martijn Henriquez, and Ad Reniers. Wave Generation of Gravity-Driven Sediment Flows on a Predominantly Sandy Seabed. Geophysical Research Letters, 45(15):7634{7645, 2018.
[5] R.P. Flores, S. Rijnsburger, A.R. Horner-Devine, and A.J. Souza. The impact of strom and strati_cation on sediment trasport in the rhine region of fresh water inuence. Journal of Geophysical Reseach: Oceans, 122, 2017.
[6] A.J. Manning and K.R. Dyer. The use of optics for the in situ determination of occulated mud characteristics. Journal of optics A: Pure and Applied optics, 4(4):S71, 2002.

[7] A.J. Manning, C. Martens, T. de Mulder, J. Vanlede, J. C. Winterwerp, P. Ganderton, and G.W. Graham. Mud floc observation in the tubidity maximum zone of the scheldt estuary during neap tides. Journal of coastal Research, Special Issue 50:832{836, 2007.

[8] O.A. Mikkelsen, T.G. Hill, P.S.and Milligan, and R.J. Chant. In situ particles size distribution and volume concentrations from lisst-100 laser particle sizer and digital oc camera. Continental Shelf Research, 25:1959{1978, 2005.

[9] R.F. Passow, U.and Shipe, A. Murray, M.A. Pak, D.K.and Brezezinski, and A.L. Alldredge. The origin of transparent exopolymer particles (tep) and their role in sedimentation of particulate matter. Continental Shelf Research, 21:327{346, 2001.

[10] U. Passow. Transparent exopolymer particles (tep) in aquatic environment. Progress in Oceanography, 55:287{ 333, 2002.

[11] J.L. Pavoni, M.W. Tenney, and W.F. Echelberger. Bacterial exocellular polymers and biological occulation. Journal WPCF, 41:414 { 431, 1972.

[12] l. Pepperzak, F. Colijin, R. Koeman, W.W.C. Gieskes, and C.A. Joordens. Phytoplankton sinking rates in the rhine region of freshwater inuence. Journal of Plankton Research, 25:365{383, 2003.

[13] Peter Traykovski, Rebecca J. Latter, and James D. Irish. A laboratory evaluation of the laser in situ scattering and transmissometery instrument using natural sediments. 159:355{367, 07 1999.

INTERCOH - Suspended Matter and Flocculation

O1056 - MODELING FINE GRAINED SEDIMENT TRANSPORT DUE TO VELOCITY SKEWNESS AND ASYMMETRY
Suspended Matter and Flocculation

Pham Thanh Nam [1], Joanna Staneva [1], Magnus Larson [2], Nguyen Thi Thao [1]
Centre for Materials and Coastal Research, Helmholtz-zentrumgeesthacht, Hydrodynamics and Data Assimilation, Geesthacht-Germany [1] Lund University, Water Resources Engineering, Lund-Sweden [2]

When waves propagate in shallow water, their shape is deformed and they become asymmetric, due to the decrease in water depth, eventually experiencing wave breaking. This wave shape produces a near-bed orbital velocity variation with similar asymmetric features. In deep water, the horizontal orbital velocity is identical during the onshore and offshore phase; however, in shallow water the onshore velocity component is typically larger than offshore component. The discrepancy between the onshore and offshore wave orbital velocities may lead to a net sediment transport that results in onshore- or offshore-directed transport, depending on the relationship between the wave properties and the sediment characteristics. In case of prevalent onshore transport, this mechanism is one of the main factors affecting the evolution of different morphological elements in the nearshore as well as the beach recovery after storms. The overall objective of this study is to determine the net sediment transport due to velocity skewness and asymmetry. Thus, a numerical model was developed to calculate nearshore random wave transformation, peak onshore and offshore orbital velocities, and net sediment transport. The bedload is determined based on the Lund-CIRP formula with several modifications applicable to very fine or cohesive sediment. The suspended load is calculated using the advection-diffusion equation in which the effects of velocity skewness and asymmetry are included. The sensitivity of the transport rate due to changes in the main input parameters were investigated for different semi-empirical formulas that were employed to describe the effects of wave asymmetry. The model was tested for selected hypothetical cases with different forcing and bathymetric conditions as well as qualitatively compared with relevant laboratory and field data. The long-term goal of the modeling is the robust and reliable predictions of sediment transport and morphological change in the nearshore, where wave breaking, wave-induced currents, and wave asymmetry are the main agents for sediment transport and bathymetric change.

POSTER
PRESENTATIONS

INTERCOH - Bottom Shear, Erosion and Bed Exchange

P1002 - CONCEPTUAL DESIGN FOR INVESTIGATIONS ON NATURAL COHESIVE SEDIMENTS FROM WESER ESTUARY
Bottom Shear Erosion and Bed Exchange

Justus Patzke [1], Roland Hesse [1], Edgar Nehlsen [1], Anna Zorndt [2], Peter Fröhle [1]
Tu Hamburg, Institute for River and Coastal Engineering (irce), Hamburg-Germany [1]
Federal Waterways Engineering and Research Institute, Hydraulic Engineering In Coastal Areas, Wedel-Germany [2]

Keywords: microcosm, bottom shear, erosion, Weser, Elbe

Due to the complexity of fine sediment dynamics in tidal estuaries a large number of parameters is necessary to describe the processes for the formation of temporally and spatially variable bottom conditions. By virtue of the Van-der-Waals forces, which dominate below a critical distance against repulsive forces, fine sediment mixtures with clay contents above ~5-10% tend to aggregate to flocs. The time- and location dependent physical, chemical and biological environmental conditions significantly influence the cohesiveness of the individual particles and thus also the transport dynamics of the particles. Furthermore, tidal asymmetries and estuarine circulation lead to the formation of an estuarine turbidity maximum zone (ETM). The location of ETMs is often linked with the mixing zone of salt and fresh water, where the environmental conditions change periodically (tidal cycles,...) and non-periodically (outflow, wind,...). As a result, high concentrations of suspended solids lead to the formation of stationary suspensions, resulting in near-bed lutoclines with partly non-newtonian behavior. The long-term accumulation of the sole is attributed to dynamic stratification and may rely on fresh water discharge when tidal energy is low during neap-tide cycles slack time.

In order to ensure the nautical depth, highly expensive regular maintenance dredging is necessary in estuaries where the ETM dynamics lead to accumulation of cohesive sediments. A previous study has shown improvements of modelling the dynamics of sediment transport for representing the Weser ETM by implementing a 2-Layer-concept for modelling sediment transport and bed exchange. Limitations in the model are due to missing crucial information on (fractious) insitu behavior of cohesive sediments in terms of consolidation, erosion and deposition fluxes. The main force leading to erosion is the flow, which contains turbulent and non-turbulent proportions. In contrast, critical bottom-shear-stress is seen as a key factor to model erosion resistance, which is naturally affected by various parameters like organic content, consolidation, stress history and ambient chemical conditions. Key factors to model consolidation are deposition and stress history. A sediments density is a cross-process parameter related to erosion resistance and the state of consolidation. The goal of the research started with hereby presented project FAUST (For An improved understanding of Sediment Transport) is filling gaps in knowledge by determining erosion, deposition and consolidation characteristics of natural soils from northern German estuaries (Weser) in laboratory experiments to improve the overall understanding of bed exchange of these sediments.

The methodology proposed is of a four-step schedule which consists of sediment sampling during slack water, onsite soil characterization (erosion tests, density measurements), lab sedimentation and erosion experiments and finally, the results lead to the development of an

updated bed exchange concept. Sediment samples from a site (Blexen) within the Weser ETM are drawn with a soil core sampler (cylindric core of 120cm height vs. 20 cm diameter) developed at IRCE in 2019 to cover the lower water body as well as upper soil layers. On board, a set of erosion and density measurements investigate the quasi-insitu natural sediments. Further on, a set of sediment cores are seperated into layerwise samples for further analysis, such as sieve/sedimentation analysis or TOC determination. The natural layer structure stays intact by a straight up transport of the sediment cores. They are stored at 6 °C.

In the lab, we perform two types of analysis. First of all, the aim is to reproduce the previously quasi insitu determined characteristics of the sediment stratification in settling experiments. Therefore, a settling column of 2.5 m height and 20 cm diameter was developed which is consistent to the sediment cores geometry. A set of settling experiments is carried out to analyse depth dependent density development. Subsequently, depth- and time-dependent critical erosion shear stresses as well as erosion rates will be determined by means of erosion tests. These tests are carried out by eroding the beforehand generated sediment samples. With this methodology, the effect of influencing parameters on erosion characteristics will be investigated (visually, density, sediment proposition). The erosion device used is a modified gust erosion chamber which is able to produce defined shear stresses on a soil samples surface to determine erosion rates at different flow states. To estimate erosion rates ultrasonic sounders measure the change in soil sediment height over time. For redundancy, the turbidity within the water column above soil is measured as well. The ultrasonic sounders are used beforehand to measure the generated flow field in the erosion chamber to estimate induced bottom shear stresses on the soil and to estimate mean measure settling velocities. For a combined analysis of erosion and settling experiments, the erosion chamber induces tidal flow field characteristics to investigate long-term sediment accumulation behaviors. Finally, the result will be further knowledge on how the natural sediment characteristics behave under certain conditions. An adapted bed exchange model specified for the examined estuary will be provided to improve existing numerical models.

Literature

GUST, G.; MÜLLER, V. (1997): Interfacial hydrodynamics and entrainment functions of currently used erosion devices. In: *Cohesive Sediments*, S. 149–174.

HESSE, R. F.; ZORNDT, A.; FRÖHLE, P. (2019): Modelling dynamics of the estuarine turbidity maximum and local net deposition. In: *Ocean Dynamics* 69 (4), S. 489–507. DOI: 10.1007/s10236-019-01250-w.

TORFS, H.; MITCHENER, H.; HUYSENTRUYT, H.; TOORMAN, E. A. (1996): Settling and consolidation of mud/sand mixtures. In: *Coastal Engineering* 29 (1-2), S. 27–45. DOI: 10.1016/S0378-3839(96)00013-0.

INTERCOH - Bottom Shear, Erosion and Bed Exchange

P1033 - CONTRASTING ERODIBILITY PATTERNS OF TWO DEEP SEA SEDIMENTS IN THE WESTERN PACIFIC OCEAN DEPENDING ON CALCIUM CARBONATE CONTENTS
Bottom Shear Erosion and Bed Exchange

Ho Kyung Ha [1], Jun Young Seo [1], Sun Min Choi [1], Kyung Eun Lee [2]
Inha University, Ocean Sciences, Incheon-Korea, South [1] Korea Maritime and Ocean University, Ocean Science, Busan-Korea, South [2]

Erodibility experiments using a Gust Erosion Microcosm System on deep-sea sediments (mainly clayey silt), which obtained in the western Pacific Ocean, have been conducted to estimate the erosion rate and controlling factors. The erosion rates of the deep-sea sediment, in general, were in the range of 10-7-10-5 kg m-2 s-1 indicating tight consolidation. Depending on the carbonate compensation depth (CCD) as a representative factor determining sediment properties (e.g., carbonate content), the erodibility exhibited two contrasting patterns. At one site (MC1) above the CCD, the bottom sediments (carbonate content: 18.32±1.00wt%) were easily resuspended, and resulted in an explosive increase in erosion rate by surface erosion. At another site (MC4) below the CCD, meanwhile, the bottom sediment (carbonate content: 0.06±0.04wt%) were less resuspended, resulting in a small increase in erosion rate by floc erosion. The erosion rate above the CCD was about 1-6 times greater than that below the CCD. The difference in carbonate content between two sites caused different variations in the bed resistance with depth. Enhancing the erodibility above the CCD was probably due to roughness and low bulk density of the particles. Once the bed shear stress exceeded about 0.39 Pa, the erosion type of MC1 sediments shifted from depth-limited to transitional erosion. However, the erosion type of MC4 sediment always remained depth-limited erosion over the entire range of bed shear stress. These results underline the effects of calcium carbonate on erodibility in the deep-sea environment.

INTERCOH - Measurement Techniques

P1006 - INFERRING SUSPENDED SEDIMENT ORGANIC AND MINERAL FRACTIONS AT HIGH FREQUENCY FROM THE OPTICAL RESPONSE OF A SUBMERGED SPECTROMETER
Measurement Techniques

Dhruv Sehgal [1], Núria Martínez-carreras [1], Christophe Hissler [1], Victor Bense [2], Ton Hoitink [2]
Luxembourg Institute of Science And Technology, Environmental Research and Innovation, Belvaux-Luxembourg [1] Wageningen University and Research, Hydrology and Quantitative Water Management Group, Wageningen-The Netherlands [2]

Traditionally, optical turbidity sensors (mainly side and backscattering) are used to quantify suspended sediment (SS) fluxes. Local calibrations are needed because site-specific factors, such as SS properties (composition, particle size distribution and concentration) and riverine conditions (flow strength, sediment input, salinity), are critical for converting turbidity into SS concentration (Soler et al., 2012; Sutherland et al., 2000). A major difficulty stems from the fact that not all sediment particles in suspension have the same characteristics and respond equally to elementary optical processes, like absorption and light scattering (Boss et al., 2018; Wozniak et al., 2018). The composition of SS in terms of organic and mineral fraction affects SS properties (e.g. particle size distribution and density) and, consequently, the relation between turbidity and SS concentration.

In many studies, variability in SS organic and mineral fractions is either approximated or not accounted for in data sets and analysis techniques (Maggi and Tang, 2015). This is partly due to the fact that a method to quantify SS fractions in-situ and at high frequency is still missing. In-situ and field-deployable sensors minimize sampling efforts and allow high frequency measurements. Moreover, any possible transformation or breaking of flocs during refrigeration and transportation to the laboratory for ex-situ analysis is also avoided (Gałuszka et al., 2015). Laboratory measurements are of course still required to crosscheck and detect unreliable field instrument readings. Previous investigations into marine environments have shown that the optical response of SS composition measured with a laboratory spectrometer can be used for the qualitative characterization of SS. These use ex-situ measurements made on particles in suspension contained in a 1 cm cuvette (Wozniak et al., 2010). Spectrometers make use of Lambert-Beer's law, which state that under certain conditions, such as no chemical scattering and a homogeneous medium, a linear relation exists between the concentration of specific chemical species and absorbance. Chemometric techniques are then used to infer the SS composition characteristics from the absorption spectrum, so as to estimate surrogate parameters like Total Organic Carbon (TOC) (Thomas and Burgess, 2017).

In this study, we investigate if absorption data from recently developed, portable and submersible spectrometers can be used to quantify SS organic and mineral fractions in river systems. These instruments have been developed, commercialized and used for drinking water providers and water treatment plants to measure absorption spectra (UV-VIS) at a temporal resolution as high as several minutes (e.g. Bass et al., 2011; Martínez-Carreras et al., 2016). An experimental laboratory setup (Size: 100 cm [h] * 38 cm [d]) is designed consisting of a cylindrical tank with an open top and a conical bottom and a horizontally installed UV-

spectrometer. A recirculation facility pumps water from the bottom drainage to the top of the tank. Along that, a stirrer facilitates the homogeneous mixing of SS and prevents the settling of heavy particles at the bottom. A submerged UV-Vis spectrometer measures the entire light absorption spectrum of water between 200 nm and 750 nm at sampling intervals as short as 2-minutes. We use chemometric techniques to estimate TOC and DOC (Dissolved Organic Carbon) from the absorbance readings of the spectrometer. The Particulate Organic Carbon (POC) is then calculated as the difference between TOC and DOC (Bass et al., 2011). The SS organic fraction is determined as the ratio of POC and SS concentration. SS concentration will be measured in the lab through the filtration of grab samples (1.2 μm Whatman filter papers).

We discuss the results obtained using distinct mineral particles, certified sediment references with high, medium and low organic content, and fresh SS with and without removal of organic matter with varying concentration. Results are verified through standard laboratory techniques.

INTERCOH - Measurement Techniques

P1007 - SALINITY ESTIMATION FROM ACOUSTIC DOPPLER VELOCIMETER MEASUREMENTSUSING AN ACOUSTIC DOPPLER VELOCIMETER TO ESTIMATE SALINITY IN ESTUARINE ENVIRONMENTS
Measurement Techniques

Rodrigo Mosquera [1], Francisco Pedocchi [1]
Universidad De La República - Fing, Imfia, Montevideo-Uruguay [1]

Introduction
Acoustic Doppler Velocimeters, usually referred to as ADVs, are commonly used to measure mean flow velocity associated with currents and waves, as well as turbulence statistics. ADVs have one piezoelectric transducer (transmitter) that generates an acoustic pulse, which travels through water while the echo is registered by other three or four piezoelectric transducers (receivers). The sound is scattered by particles present in the water and this echo is registered at the receivers. The recorded signal is then analysed using a covariance method to estimate the water velocity with high temporal resolution in a small sample volume (Rusello 2009, Vulgaris and Trowbridge 1998). To verify the instrument operation all ADVs run an alternative test, called Probe Check in Nortek's ADV. During this test, after the transmitter sends a pulse, all the receivers record the acoustic amplitude profile of the echo for a long period of time. In this work we show how the Probe Check data can be used to determine the sound speed, and with the aid of Del Grosso (1974) formulation, the salinity can be estimated.

Deployment site and set up
The data used in this work comes from a Vector ADV and a Seacat 19 plus V2 CTD deployed in the Río de la Plata estuary between May 25 and August 25 of 2018. Both instruments were positioned approximately 40 cm above the cohesive bed, attached to a tripod-like structure, 3.0 km south of Montevideo coast. During the deployment, water temperature varied between 10 and 18 ºC, salinity between 0 and 28 psu and water depth between 7 and 9 m. The ADV was configured to sample for 3 min. at 32 Hz, with 30-minute intervals. Probe Check profiles for all the receivers were recorded both at the beginning and at the end of each burst. The CTD data used in this work was the average of four instantaneous measurements taken at 2 Hz every 30 min., simultaneous with the beginning of each ADV burst.

Methodology and results
When the ADV is operating correctly, the Probe Check acoustic amplitude profile is composed by a first peak, near 13 μs, corresponding to the forward scattering between the transmitter and receiver, and a second peak near 100 μs associated with the return from the sampling volume. If a reflecting surface is present closer than 450 mm (around 300 μs) from the central transducer, a third peak could also be present. For a giving scattering scenario, the exact time to the second Probe Check peak can be related to the sound speed of the media. However, if just the maximum value of the profile was used, the coarse discretization of the Probe Check functionality would give sound speed estimations with errors of around 20 m/s.

To determine a theoretical curve for the acoustic profile, we utilized the integration of the beam pattern of both the transmitter and emitter transducers in a Rayleigh scattering regime with the fixed geometry of the ADV. Although the theoretical curve showed a good matching with the measured profiles, a simpler approach using a second order polynomial fit showed equivalent results for capturing the exact peak location. The polynomial fit provided us with subpixel resolution (Raffel et al. 2011), reducing the original error by a factor of at least four

when obtained by directly using the maximum value of the profile. As other ADV manufacturers also provide functionalities similar to Probe Check, this technique can be implemented not only with the Nortek Vector, but also other ADV brands. As the exact time to the second peak for fresh water is not usually provided by manufacturers, an initial measurement in fresh water should be made to calibrate each ADV. For this purpose, we recommend running the Probe Check routine under a mixture of tap water added with seeding particles in a large container, while simultaneously registering the water temperature. Once the time to the peak in fresh water is known, the time to the peak for brackish water can be easily converted to salinity using Del Grosso (1974) formulation.

Figure 1 shows the salinity result obtained with the proposed technique against the salinity estimations provided by the CTD during the previously described deployment in the Rio de la Plata. In Figure 1 a low-pass filter with a cut off frequency associated with the lunar semi-diurnal constituent (M2) of the tide was applied to the ADV data in other to facilitate the comparison.
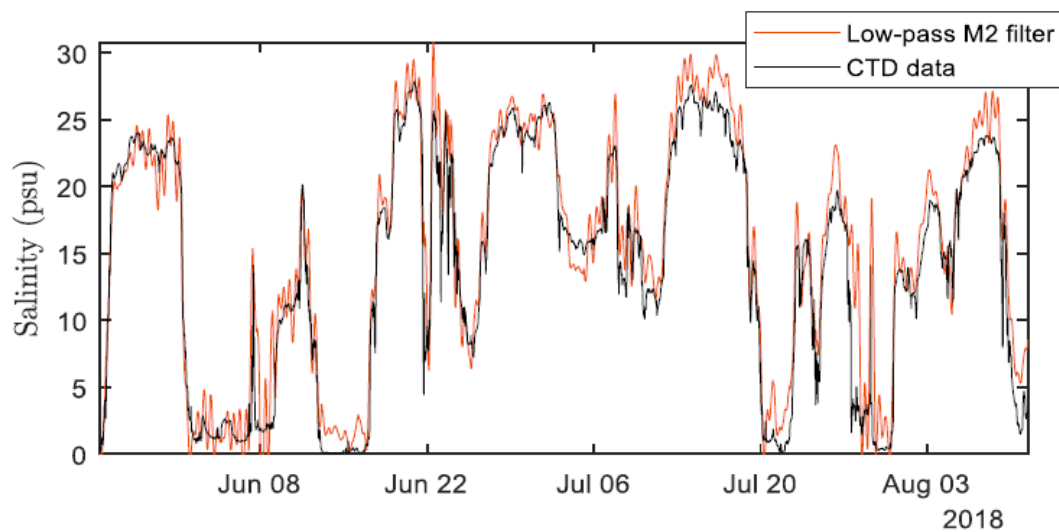
Fig. 1. Salinity computed by CTD (black line) and computed with the ADV data (orange line) and the proposed technique.

Conclusions

The results obtained with the proposed technique demonstrate that salinity can be estimated using the ADV Probe Check functionality under a wide range of conditions. The standard deviation of the difference between salinity estimations during deployment with both ADV and CTD measurements was 4 psu. . We consider that this methodology is particularly useful in estuarine environments, where cohesive sediment transport can be strongly affected by salinity. Finally, these results can be easily incorporated into the standard ADV post-processing software, allowing the regular user to record temperature, pressure, sound speed, and water velocity using a single ADV instrument.

Acknowledgments

References

Del Grosso, V.A., 1974. New equation for the speed of sound in natural waters (with comparisons to other equations). J. Acoust. Soc. Am. 56, 1084–1091. https://doi.org/10.1121/1.1903388

Raffel, M., Willert, C., Scarano, F., Kähler, C., Wereley, S., Kompenhans, J., 2011. Particle Image Velocimetry: A Practical Guide, vol. 30 Cambridge University Press.

Rusello, P.J., 2009. A Practical Primer for Pulse Coherent Instruments. TN-027. Nortek USA.

Voulgaris, G., Trowbridge, J.H., 1998. Evaluation of the Acoustic Doppler Velocimeter (ADV) for turbulence measurements. J. Atmos. Ocean. Technol. 15, 272–289.

INTERCOH - Measurement Techniques

P1024 - THE RELATIONSHIP BETWEEN PARTICLE SIZES OF SEDIMENT AND ECHO SPECTRUMS IRRADIATED BY ULTRASONIC
Measurement Techniques

Yoshitaka Matsumoto [1], Tomonari Ishikawa [5], Koki Nishimura [5], Shigeru Kato [2], Naohiro Hodzumi [3]
National Institute of Technology, Toyota College, Department of Civil Engineering, Toyota-Japan [1] Toyohashi University of Technology, Department of Architecture and Civil Engineering, Toyohashi-Japan [2] Toyohashi University of Technology, Department of Electrical and Electronic Information Engineering, Toyohashi-Japan [3]

Introduction

The sediment at the bottom of reservoirs, which is constituted by soil and fine organic particles provided from a terrestrial and aquatic ecosystem, causes the decline of water volume in a water body an d anoxic condition. As measuring the thickness and quality of the bottom sediment, the sampling method that divers get samples is the most useful and ordinary way. But this method requires a high cost and special skills, so we cannot obtain the sediment data throughout the reservoirs. The goal of our research is to develop the novel method of measuring the thickness and characteristics of sediment indirectly. Apart from the survey of the layer thickness at a sea bottom, they use the ultrasonic. Though the accuracy of measurement, there does not demand the centimeter order. The survey of thickness and characteristics of sediment in reservoirs needs to more certainty for accumulating thinner layer.

In this research, we examine the echo characteristics that reflected from the several glass beads sizes boundary for the first step of developing the new ultrasonic method to detect the quality of bottom sediment. And the sediment might accumulate on multiple layered structures at the bottom of reservoirs by the different depression time caused by the particle size. Therefore, we set the two types of experiment, single layer and double layers in this research.

Methods

The different diameter size of glass beads, 800, 400, 110, 70, 30 μm, set in single and multilayers for classifying the ability of detection. The different diameter size of glass beads stuffed in a tube and ethanol filled to the top in the column. In multilayer experience, 30μm glass beads set as the surface layer and other particle size beads settled in the bottom layer. The ultrasonic irradiated vertically to the glass beads from the liquid surface and received echos reflected from glass beads surface in the single layer experience and the boundary of different impedance in the multilayers experience. The centre frequency of the ultrasonic transducer is 800kHz. The signal of the echo was displayed on the digital oscilloscope. After collecting the echo data, we used the self-built Lab View program to convert them to a frequency spectrum by Fourier transformation algorism to verify the frequency characteristic.

Result and Discussion
Single Layer Experiment Result
The echo of each glass beads size showed different waveforms in each (Fig. 1). And the frequency spectrum of each bead's size represented the two peaks in approximately 60kHz and

160kHz, respectively. The power spectrum of low frequency is larger than high in all sizes (Fig. 2). As the ultrasonic irradiated larger size of glass beads, the echo was lower power spectrum. The irradia ted ultrasonic moves ahead at the boundary when the object size is larger than the wavelength and the ultrasonic reflects at the boundary when the object size is smaller than the wavelength in general. The relationship between the bead's size and the power spectrum is satisfied with the general characteristics of the ultrasonic echo.
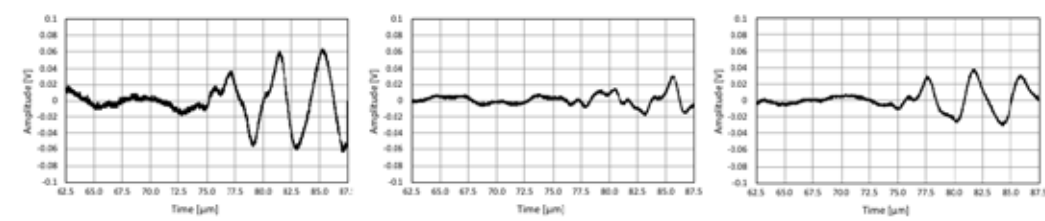
Fig. 1 Recorded echo wave forms in 30µm (left), 110µm (centre) and 1000µm (right) of glass beads size in the single layer experiment

Multilayers Experiment Result

The echo reflected from the second layer of each glass beads size also detected different waveforms in each. The echo peak band of the frequency of the second layer shifted to approximately under 100kHz in the lower frequency and under 250kHz in the higher frequency compared with the echo from the single layer experience (Fig. 3). On the other hands, the peak frequency under 70µm size experience appears the same band with the surface layer experiment. These results indicate the peak bands of the frequency of the power spectrum in the multila yer were altered by passing through in the surface layer relied on beads size.

The power spectrum of lower frequency is also larger than the spectrum of higher frequency except for 70 µm size (Fig. 4). This result shows the same trend between particle size and the power spectrum with a single layer experience. Then, the ultrasonic method to detect the sediment characteristics adapts even in the double layer.

Conclusion
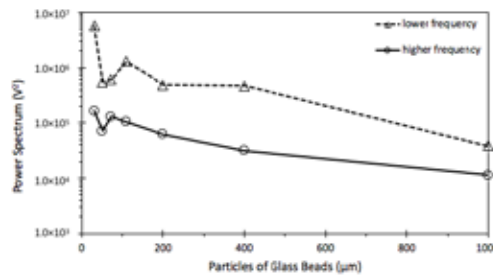
Fig. 2 The power spectrum of lower and higher peak frequency in each particle glass beads in the single layer experiment
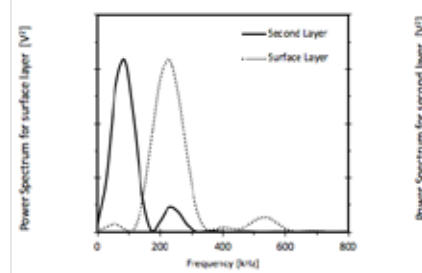
Fig. 3 The power spectrum of frequency transmitted by Furrier transmission algorism for the echo reflected from the surface and second layer
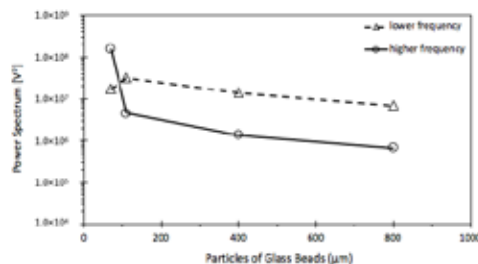

Fig. 4 The power spectrum of lower and higher peak frequency in each particle glass beads in the multilayer experiment

INTERCOH - Measurement Techniques

This research conducted the clarifying the echo characteristics of glass beads reflected from the bottom for the first step to develop a new measuring method using the ultrasonic. The echoes detected in the single and multilayer experiment, and each echo reversed from the different particle glass beads size represented the different wave pattern. The power spectrums of lower peak frequency were more significant than the higher frequency in both the single and multilayer experiments. The trends of the power spectrum of the lower and higher peak frequency were smaller with larger particle size in both tests. These results expressed that the echo analysis from the ultrasonic is practical to determine the characteristics of particles settled on the bottom of the reservoirs.

15th INTERNATIONAL CONFERENCE on
COHESIVE SEDIMENT TRANSPORT PROCESSES
13 - 17 OCTOBER 2019 • ISTANBUL / TURKEY
YILDIZ TECHNICAL UNIVERSITY - YILDIZ CAMPUS

YILDIZ TEKNİK ÜNİVERSİTESİ 1911

INTERCOH - Measurement Techniques

P1052 - HOW TO OBTAIN RELIABLE HIGH RESOLUTION PROFILES OF SUSPENDED SEDIMENT CONCENTRATION IN HIGHLY TURBID ENVIRONMENTS
Measurement Technique

Jianliang Lin [1], Qing He [1], Leicheng Guo [1], Bram C. Van Prooijen [2], Zhengbing Wang [2]
East China Normal University, State Key Laboratory Of Estuarine And Coastal Research, Shanghai-China [1] Delft University Of Technology, Faculty Of Civil Engineering And Geosciences, Delft-The Netherlands [2]

Abstract:
Concentrated suspension of cohesive sediment is one of the important contributors for harbor/channel siltation and transport of contaminant. However, a ccurate measurement of suspended sediment concentration (SSC) in highly turbid environments has been a problem due to the signal saturation and attenuation (H a et al., 2009; Kineke and Sternberg, 1992; Shao and Maa, 2017). The signal saturation causes a limited measurement range, while the signal attenuation raises the ambiguity problem of having a low optical/acoustic output could mean a low or high SSC Figure 1).

In this study, we propose a n integrated optic acoustic (IOA) approach Figure 2 to (i) overcome the ambiguity problem; (ii) increase the measurement range to high SSC values and (iii) measure high resolution SSC profiles. The IOA approach is a combination of an Argus Suspension Meter (ASM), an Optical Backscatter Sensor (OBS) and an Acoustic Doppler Velocimeter (ADV). With in low SSC (< ~ 10 g/L) where the ASM is not saturated the ASM derived SSC is preferred because it has the lowest relative error 26%26%)), follow ed by OBS 30%) and ADV 89%) The ASM also provides high resolution (1 cm) SSC profiles when it is un saturated Figure 3). The OBS derived SSC is used when the ASM derived SSC is missing due to the signal saturation. Both ASM and ADV help to identify the true SSC fr om the estimates given by OBS . Since the ambiguity problem is solved , the measurement range of OBS and ADV are extended to ~60 g/L and ~ 360 g/L , respectively The rather scatter of data and the low signal to noise ratio (SNR) suggest that the use of ADV to measure SSC is not reliable, but it can give a rough estimation. The IOA approach was tested in the Yangtze Estuary during two different campaigns. High SSCs were measured close to the bed, ranging up to 63 g/L.

Comparison between estimates given by IOA approach and the SSCs from in-situ water samples indicates that this approach is reliable, giving SSC estimates with an averaged relative error of 17—34%. To reduce the effects of particle size/composition, we suggest the usage of in--situ water samples or mixed bottom sediment for sensor calibration. Accurate calibrations with the particle size/composition correction are expected to access a higher accuracy in future research.

INTERCOH - Measurement Techniques
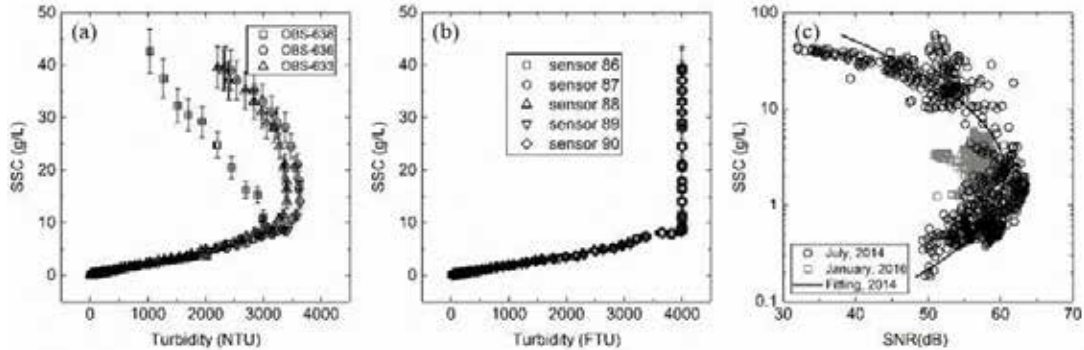

Figure 1.Calibrations of (a) OBS (turbidity in NTU), (b) ASM (turbidity in FTU) and (c) ADV (SNR in dB) against SSC (in g/L) with bottom sediment collected in the Yangtze River Estuary.
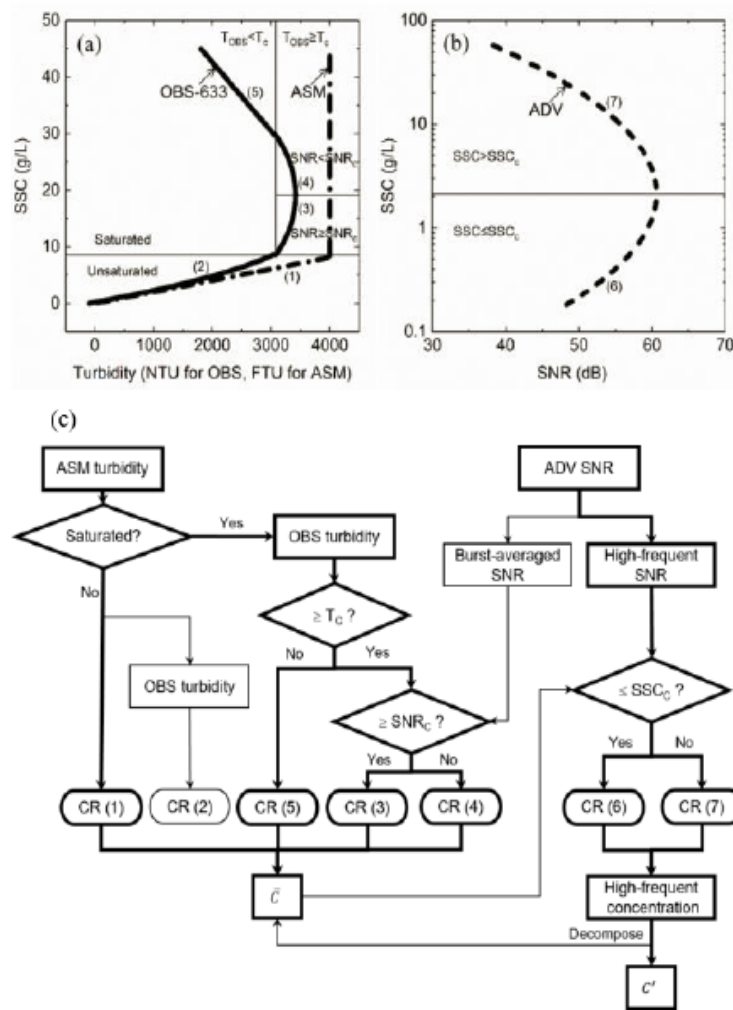

Figure 2 (a) (b) Example s of calibration curve (ASM, OBS 633 and ADV) for illustrating the conversion protocols of the IOA approach. T_c denotes the critical OBS turbidity (reading, i.e., T_c=3050 NTU, corresponding to SSC ~ 9 g/L) where ASM just saturates (with a reading around 4000 FTU), and SNR_c (~ 61 dB) indicates the critical SNR corresponding to

the max OBS turbidity (reading, i.e., 3400 NTU, corresponding to SSC = 20 g/L when using OBS. SSC_c indicates the critical SSC i.e., SSC_c= 2 g/ where the ADV returns the max SNR The numbers in parenthesis, e.g., (4), is a shorthan d of Calibration Relation (CR) 4. (c) Conversion protocols for ASM, OBS and ADV to estimate reliable SSC. Highlighted flowcharts show the optimal protocol of IOA approach according to the performance of each sensor.
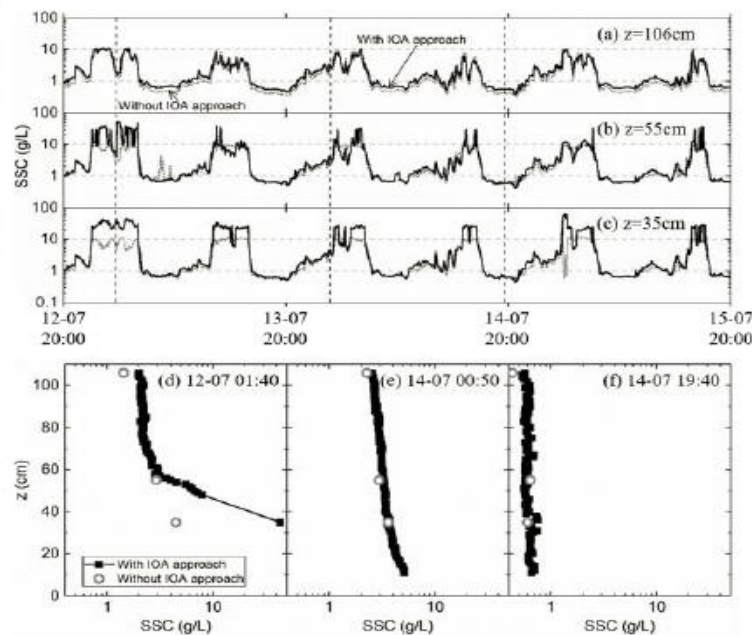
Figure 3. Time series of SSC from three tripod mou nted OBSs with (black solid) and without (grey dot) the IOA approach at 106 cm (a), 55 cm (b) and 35 cm (c) above bed , and three representative SSC profiles within high (d), mid (e) and low (f) SSC. The ASM readings below 50 cm from bed are saturated (d), and thus, removed, except the one at 35 cm above bed, which was recovered by the OBS reading at that time. A straight line between the SSCs from ASM at 35 and 50 cm is suggested as the possible SSC profile.

References:

Ha, H.K., Hsu, W.Y., Maa, J.P.Y., Shao, Y.Y., Holland, C.W., 2009. Using ADV backscatter strength for measuring suspended cohesive sediment concentration. Cont. Shelf Res. 29, 1310–1316. https://doi.org/10.1016/j.csr.2009.03.001

Kineke, G.C., Sternberg, R.W., 1992. Measurements of high concentration suspended sediments using the optical backscatterance sensor. Mar. Geol. 108, 253–258. https://doi.org/10.1016/0025-3227(92)90199-R

Shao, Y., Maa, J., 2017. Comparisons of Different Instruments for Measuring Suspended Cohesive Sediment Concentrations. Water 9, 968. https://doi.org/10.3390/w9120968

INTERCOH - Morphodynamics

P1046 - BEACH MORPHODYNAMICS POST HURRICANE HARVEY
Morphodynamics

Firat Y. Testik [1], Benjamin Lamm [1], Jin Ikeda [1], Murat C. Testik [2]
University of Texas at San Antonio, Civil and Environmental Engineering, San Antonio
United States [1] Hacettepe University, Industrial Engineering, Ankara-Turkey [2]

Hurricane Harvey made landfall east of Rockport, Texas, the United States in late August 2017. This study investigates morphodynamics of beach-dune systems at three selected beaches along the Mustang and North Padre islands in the Texas Gulf coast that were impacted by Hurricane Harvey. The selected beaches were monitored after Hurricane Harvey for beach topography and sediment characteristics at different times from August 2017 through March 2018. Topographical data using Real-time Kinematic Global Positioning System, sediment compaction data using a penetrometer, and cores of sediment samples were collected along cross-shore transects extending from the shoreline to the dune at each of the three selected beaches. The collected sediment samples were analyzed using the standard sieve analysis method for the sediment size distributions, and the relevant sediment statistics were calculated. Spatio-temporal topography data and sediment statistics led to various morphodynamics interpretations of the selected beaches. Our results and interpretations for individual beaches and intercomparisons among beaches will be discussed in the presentation. This material is based upon work supported by the National Science Foundation under Grant No. OCE-1760158 to the first author

INTERCOH - Suspended Matter and Flocculation

P1023 - APPLICATION OF A BAYESIAN METHOD FOR INVESTIGATING THE PROBABILITY AND UNCERTAINTY OF A TWO CLASS FLOCCULATION KINETIC MODEL
Suspended Matter and Flocculation

Byung Joon Lee [1], Qilong Bi [2], Erik Toorman [3], Michael Fettweis [4], Byeong Kwan Lee [5]
Kyungpook National University, School of Disaster Prevention and Environmental Engineering, Sangju-Korea, South [1] Flanders Hydraulics Laboratory, Sediment Transport Team, Antwerp-Belgium [2] Kul, Civil Engineering Department, Leuven-Belgium [3] Rbins, Od Nature, Brussels-Belgium [4] Korea National Park Service, Marine Research Center, Yeosu Korea, South [5]

Many cohesive sediment transport models adopt empirical flocculation equations based on the correlation between settling velocity (or floc size) and hydrodynamic and biochemical conditions of the water. Those empirical flocculation equations are robust in computation, but they disregard flocculation kinetics (i.e. time-dependent rate of floc growth and breakup). More realistic cohesive sediment transport model, with adoption of flocculation kinetics based on population balance equations have been developed (Winterwerp, 1998; Verney et al., 2011; Lee et al., 2014; Shen et al., 2018), and have been applied and validated in idealized 0 or 1 dimensional vertical test cases. Recently, Sherwood and coworkers applied and validated a flocculation kinetic and sediment transport model for an estuarine and coastal area (Sherwood et al., 2018). The drawback of flocculation kinetic models is the high complexity generated by the dozen of model parameters, which is the bottleneck for practical, realistic application, especially in large scale application. To the authors' opinion, the flocculation kinetic model parameters should be estimated with great attention, before being adopted to large-scale, multi-dimensional simulation. Various curve-fitting methods, such as linear, non-linear regression and genetic algorithm, are available for parameter estimation. Those curve-fitting methods find a specific set of the best-fit model parameters, but they can hardly estimate the probability and uncertainty of the model parameters. Bayesian methods instead have been applied not only to find the best-fit parameters but also to investigate the probability and uncertainty of and the correlation between model parameters. Throughout this research, we applied and tested a Bayesian method coupled with a flocculation kinetic model, and thus we could explore a highly complex flocculation kinetic model in a systematic manner.

A 1DV cohesive sediment transport model, with adoption of a two-class flocculation kinetic equation, was coupled with a Bayesian method (Vrugt, 2016). Experimental data measured in the Belgian coastal area were applied to parameter estimation of the flocculation kinetic and sediment transport model (Fettweis et al., 2014). The aggregation efficiency factor (*alpha*), breakup efficiency factor (*Eb*), breakup exponent constant (*q*), fractal dimension (*Df*), erosion rate constant (*M*), and critical shear stress (*tau,c*) were selected as the curve-fitting parameters. Four thousands numerical simulations were performed with different sets of the model parameters, based on the Markov chain Monte Carlo theory. Afterwards, the simulation results were statistically analyzed regarding their probability, uncertainty and correlation. As shown in Figure 1, each parameter composes a statistical distribution with their median and standard deviation, indicating the most probable value and the uncertainty of a parameter. The Bayesian

method also shows the correlation between the model parameters. For example, the correlation between the aggregation efficiency and breakup efficiency factors (*alpha* and *Eb*) and between erosion rate constant and critical shear stress (*M* and *tau,c*) could be identified by the Bayesian method. Therefore, the Bayesian method gives us better insight into the complex flocculation kinetic model, regarding the parameters' probability and uncertainty and the correlation between model parameters. The Bayesian method combined with the 1DV flocculation kinetic and cohesive sediment transport model will be further applied to various measured data sets in different seasonal and spatial conditions. The Bayesian method will eventually help us understand flocculation kinetics and set a realistic, rigorous cohesive sediment transport model.
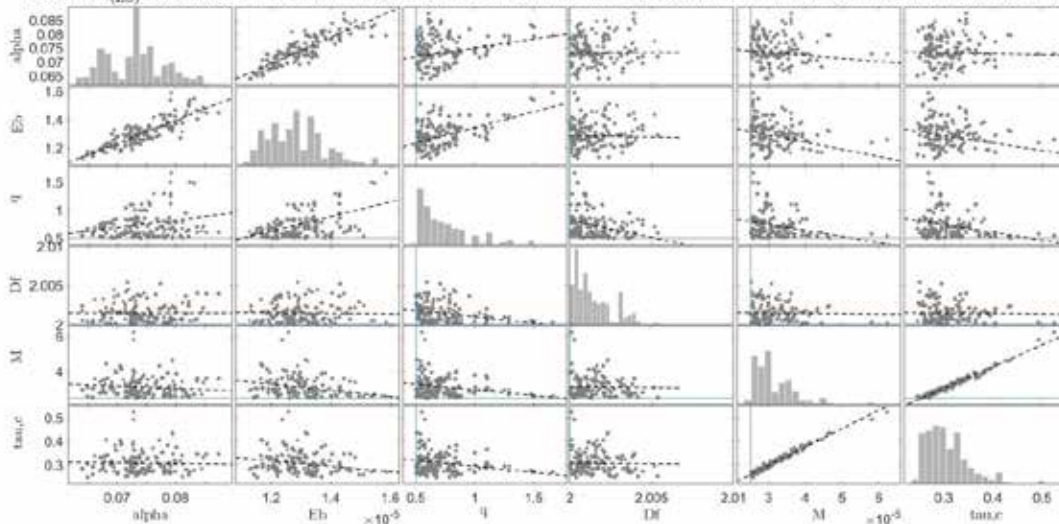
Fig. 1. Histograms of the marginal posterior distribution of the two-class flocculation kinetic model parameters, aggregation efficiency factor (*alpha*), breakup efficiency factor (*Eb*), breakup exponent constant (*q*), fractal dimension (*Df*), erosion rate constant (*M*), and critical shear stress (*tau,c*),
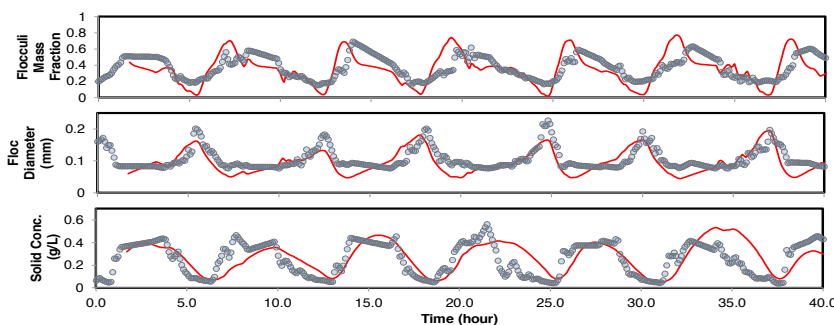
Fig. 2. Simulation result with the best-fit model parameters estimated by the Bayesian method with the 1DV flocculation kinetic and cohesive sediment transport model

INTERCOH - Suspended Matter and Flocculation

References

Fettweis M., Baeye M., Van der Zande D., Van den Eynde D., Lee B.J. (2014). Seasonality of floc strength in the southern North Sea. J. Geophys. Res. Oceans 119, 1911–1926.

Lee B., E. Toorman, and M. Fettweis (2014). Multimodal particle size distributions of fine grained sediments: mathematical modeling and field investigation. Ocean Dynamics 64(3), 429–441.

Shen, X., E. Toorman, B. Lee, and M. Fettweis (2018), Biophysical flocculation of suspended particulate matters in Belgian coastal zones. Journal of Hydrology, 567, 238 252.

Sherwood, C., A. Aretxabaleta, C. Harris, J. Rinehimer, R. Verney, and B. Ferre (2018). Cohesive and mixed sediment in the Regional Ocean Modeling System (ROMSv3.6) implemented in the Coupled Ocean–Atmosphere–Wave–Sediment Transport Modeling System (COAWSTr1234), Geosci. Model Dev. 11, 1849-1871.

Verney, R., R. Lafite, J. Claude Brun-Cottan, and P. Le Hir (2011), Behaviour of a floc population during a tidal cycle: Laboratory experiments and numerical modelling, Continental Shelf Research, 31(10), S64–S83.

Vrugt, J. (2016). Markov chain Monte Carlo simulation using the DREAM software package: Theory, concepts, and MATLAB implementation, Environmental Modelling & Software 75, 273–316.

Winterwerp, J. (1998), A simple model for turbulence induced flocculation of cohesive sediment, Journal of Hydraulic Engineering, 36(3), 309–326.

INTERCOH - Suspended Matter and Flocculation

P1066 - IMPLEMENTING MCPBE FLOCCULATION MODELS IN TELEMAC AND INVESTIGATING THE INFLUENCE OF FLOCCULATION ON LARGE SCALE SEDIMENT TRANSPORT
Suspended Matter and Flocculation

Qilong Bi [1], Byung Joon Lee [2], Xiaoteng Shen [3], Erik Toorman [3], Sven Smolders [1], Joris Vanlede [1]
Department of Mobility and Public Works of The Government of Flanders, Flanders Hydraulics Research, Antwerp-Belgium [1] Kyungpook National University, School of Construction and Environmental Engineering, Sangju-Korea, South [2] Katholieke Universiteit Leuven, Department of Civil Engineering, Leuven-Belgium [3]

The dynamically changing characteristics of cohesive sediment due to flocculation processes, i.e. aggregation of fine particles and breakup of aggregates that occur at microscopic scale, can affect large scale transport patterns. For instance, it can create a spatial and temporal dependent particle size, density and settling velocity. This is important for the advection-diffusion of particles, sediment mixing in the water column and interactions with the bed layer through erosion/deposition processes. Although some studies in the past have focused on the flocculation process, its influence on the large-scale sediment transport in the marine and estuarine environment is not yet fully understood. In order to gain better insights, this study aims to incorporate more sophisticated flocculation models into a schematic marine and estuarine modelling framework. The flocculation model considered is the multi-class population balance equation based (MCPBE) flocculation model proposed by Lee et al. (2011) and Shen et al. (2018).

Three versions of the MCPBE flocculation model have been implemented in the TELEMAC-MASCARET system, with additional optimizations for large-scale applications. The code development results in a customized modelling suite that allows complex 3D sediment transport modelling. In a typical scenario, mixed sediment with multiple classes can be introduced. Transport of cohesive sediment (with two or three floc size classes) can be modelled as suspended load with flocculation kinetics included, while transport of non-cohesive sediment is modelled as bedload. The bed layer model is also adapted to this multi-class mixed sediment system. Currently the implementation is under validation, eventually it will be integrated into the official release of the TELEMAC-MASCARET system.

Preliminary results already provide a better understanding of the influence of flocculation on large-scale sediment transport. A 3D sediment transport model (one class of sand and two classes of mud) has been created, in which the flocculation kinetics is modelled by the implemented MCPBE flocculation module. A simplified geometry of the Scheldt estuary, based on the observed widths and depths, is adopted (Dijkstra et al. 2019). A tidal signal containing only the M2 and M4 constituents is imposed at the downstream boundary, while a constant flow rate is imposed upstream.

The model predicts that larger flocs are more likely to occur in the region 60 to 80 km from the estuary mouth, where the width of estuary starts to increase drastically towards downstream (figure 1). Comparing to the case without flocculation (using a constant settling velocity averaged from previous flocculation model results), the flocculation process tends to increase

INTERCOH - Suspended Matter and Flocculation

SPM concentration in the upstream (figure 2). Therefore, higher settling fluxes can be found in these two areas although they are due to different reasons (figure 3). The spatial and temporal variations introduced by flocculation processes affect
the averaged horizontal sediment flux as well (figure 4). It tends to keep more sediment in the upstream, while it accumulates sediment towards the region in reality where the ETM zone is usually found.
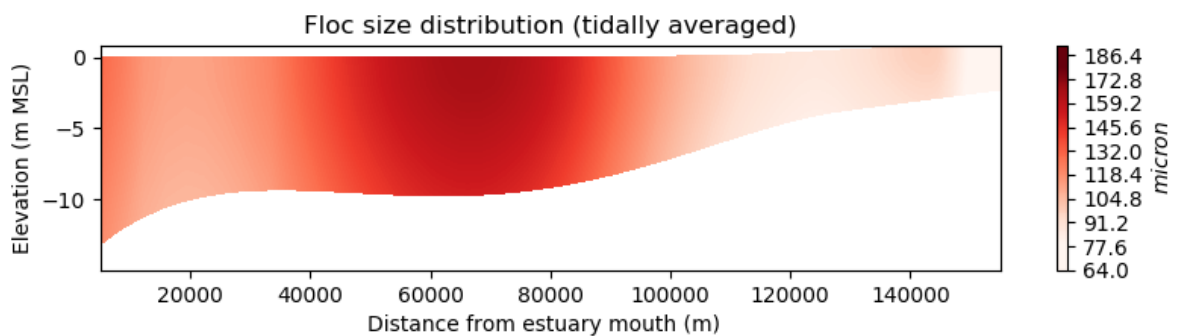

Figure 1 – Modelled size distribution of macroflocs averaged over a tidal cycle
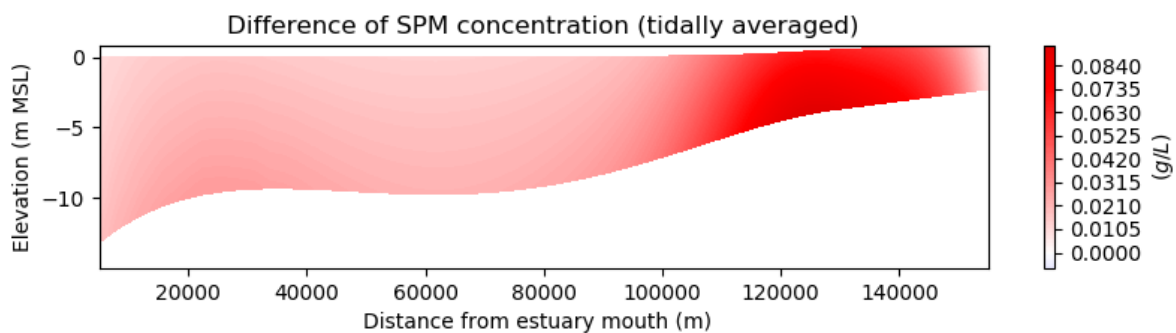
Figure 2 – Comparison of tidally averaged SPM concentration (model results with flocculation-model results without flocculation)
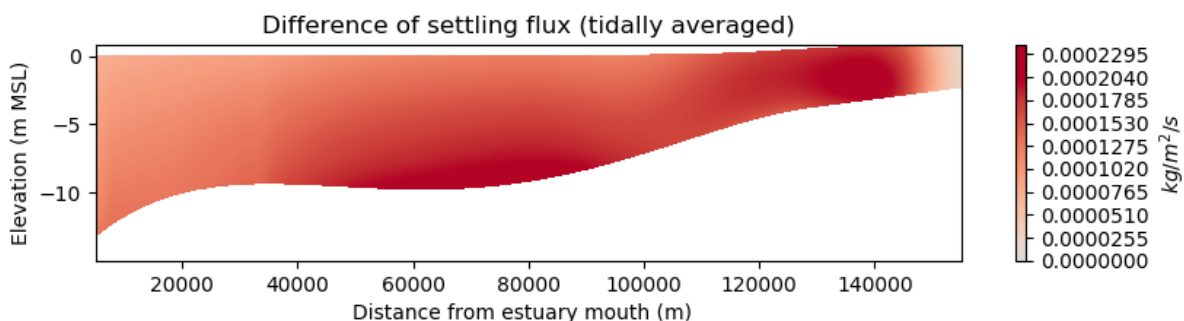

Figure 3 - Comparison of tidally averaged settling flux (model results with flocculation-model results without flocculation)
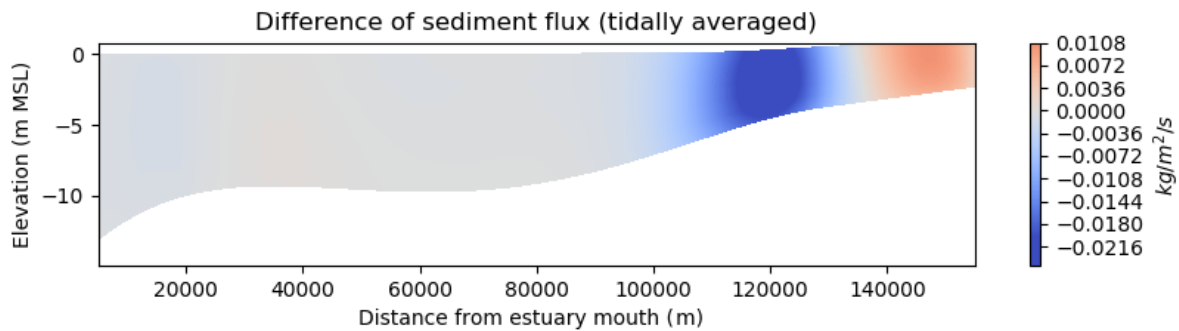
Figure 4 – Comparison of horizontal sediment flux averaged over a tidal cycle (model results with flocculation-model results without flocculation, positive value indicates more flux towards upstream, negative value means more flux towards downstream)

REFERENCES

Dijkstra, Y. M., Schuttelaars, H. M., & Schramkowski, G. P. (2019). Can the Scheldt River Estuary become hyperturbid? Ocean Dynamics, 69:809–827.

Lee, B. J., Toorman, E., Molz, F. J., & Wang, J. (2011). A two-class population balance equation yielding bimodal flocculation of marine or estuarine sediments. Water Research, 2131-2145.

Shen, X., Lee, B. J., Fettweis, M., & Toorman, E. A. (2018). A tri-modal flocculation model coupled with TELEMAC for estuarine muds both in the laboratory and in the field. Water research (145), 473-486.